

https://dspace.org/

Linear and non-linear resource estimation techniques applied in the Kanzi Phosphate project in the Democratic Republic of Congo

Mudau, Mpfariseni

2015-05-07
http://hdl.handle.net/10539/17666

Downloaded from a DSpace repository. https://dspace.org/

LINEAR AND NON-LINEAR RESOURCE ESTIMATION TECHNIQUES APPLIED IN THE KANZI PHOSPHATE PROJECT IN THE DEMOCRATIC REPUBLIC OF CONGO

Mpfariseni Mudau

A research report submitted to the Faculty of Engineering and the Built Environment, University of the Witwatersrand, Johannesburg, in partial fulfilment of the requirements for the degree of Master of Science in Engineering.

Johannesburg, 2014

DECLARATION

I declare that this research report is my own, unaided work. It is being submitted for the degree of Master of Science in Engineering to the University of the Witwatersrand, Johannesburg. It has not been submitted before for any degree or examination in any other University.



.....
(Signature of Candidate)

22nd July 2014
..... day of..... (year) .....

ABSTRACT

The main aim of this project was to conduct a comparative analysis of the linear and non-linear estimation techniques used for a Kanzi Phosphate Project in the Democratic Republic of Congo. Kanzi phosphate is an elongated sedimentary unit with a north-south strike direction and a fairly flat dip angle. It was deposited between two graben structures.

The Kanzi phosphate was divided into the North and South areas. The North and South areas were treated as different domains because they are far apart. The geology and assay results of the intersected phosphate mineralization were used in defining the layers. The layering was noted in South Geo-Zone. This led the South Geo-Zone to be sub-divided vertically into three layers namely Top, Middle and Bottom layers. The Top and Bottom layers had low P_2O_5 grades and higher SiO_2 than the Middle layer. The Middle layer was the most laterally extensive layer than other layers.

Drillholes were done by the Aircore drilling technique and the samples were taken at 1m intervals. No compositing was done as all samples contributed equal statistical weights in terms of length and density measurements. The declustering was not done because the drillholes were well-spread.

The statistical evaluation of the domains showed that P_2O_5 is correlated to all other major variables (CaO, Al_2O_3, TiO_2 and SiO_2). A decision was taken to conduct mineral resource estimation on P_2O_5 only. Other block variables were estimated from the P_2O_5 using a linear regression relationship.

A 3-dimensional geological model was constructed for each domain. A model was filled with the blocks. A definition of the block sizes were based on the neighbourhood analysis, drillhole spacing and mining requirements. Half the drillhole spacing was used for X (125m) and Y (125m) dimensions and 5m thickness was used for Z dimension.

The traditional variograms for all the domains were created. Downhole variograms were used to determine the nugget effect. All variograms were omni-directional and have spherical models. The variogram ranges were used to guide the search volumes for both Ordinary Kriging (OK) and Inverse Distance Weighting (IDW). The estimation results from the OK and IDW techniques were comparable.

The data was pre-processed for Indicator Kriging (IK). The median cut-offs were selected and median variograms were calculated. It was assumed that all other indicators have similar variograms to that of the median indicator variogram. For estimation purpose, the cut-offs selected were 7.5%, 12.5%, 17.5%, 22.5% and 27.5%. These cut-offs were guided by processing characteristics on the Kanzi phosphate.

The results of the three estimation techniques (IDW, OK and IK) were analysed. The OK and IDW methods produced smoothed estimates. The OK and IDW methods defined the global resources well. The measure of uncertainty for OK was not clearly defined, partly due to widely spaced data.

The Median Indicator Kriging produced more useful results than the results produced by the OK and IDW methods and smoothing was minimized. As a probabilistic method, the Median Indicator Kriging defined the proportion of tonnages above the defined processing cut-offs.

The estimation methods were compared and ranked. The Median Indicator Kriging was the preferred estimation technique and was ranked high. The OK and IDW produced identical results and they were ranked low. OK performed like IDW as there were moderately mixed sample populations that were spatially integrated.

The recommendations to conduct conditional simulation, drill additional boreholes, estimate other variables using co-kriging and perform further processing studies were given. This will help in reducing risks and increase the geostatistical understanding of the phosphate resources.

ACKNOWLEDGEMENTS

I would like to express thanks to Minbos Resource Limited, in particular Mr Robert McCrae (former Managing Director) and Mr Scott Sullivan (Managing Director/Executive Chairman) for giving me permission to use data. Prof Richard Minnitt is thanked for giving the technical guidance and overseeing the project. Coffey Mining, in particular Ms Kathleen Body is thanked for motivation, technical guidance and allowing me to use specialized softwares. I am grateful to Dr. Ina Dohm (of Anglo-American) who introduced me into mineral resource evaluation. My lovely wife Kone is thanked for giving me moral support, time and space to conduct the research project.

Above all I thank the Almighty for giving me wisdom, perseverance and passion to conduct the research. My colleagues at Coffey Mining and all my friends who tirelessly encouraged me are highly thanked and appreciated. The two anonymous reviewers are thanked for their invaluable constructive comments.

Table of Contents

DECLARATION ..... **i**

ABSTRACT ..... **ii**

ACKNOWLEDGEMENTS ..... **iv**

1 Introduction **1**

1.1 Background 1

1.2 Location of a Study Area 2

1.3 Problem Statement 2

1.4 Aim 3

1.5 Methodology 4

2 Geological Interpretation and Domaining **6**

2.1 Regional Geology 6

2.2 Project Geology and Analysis of different geo-zones 6

2.3 Summary of the Project Geology: Principal Findings 18

3 Statistical Analysis of the Data **20**

3.1 Introduction 20

3.2 Declustering and Compositing 20

3.3 Dealing with the outliers 21

3.4 Comments on the histograms, descriptive statistics and probability plots 21

3.4.1 South Geo-Zone (Bottom Layer) 23

3.4.2 South Geo-Zone (Middle Layer) 24

3.4.3 South Geo-Zone (Top Layer) 25

3.4.4 North Geo-Zone 31

3.5 Correlation Matrix 33

3.6 Scatter Plots and Estimation Strategies 39

3.7 Discussion on Density 44

3.8 Principal Findings on Statistics 45

4 Spatial Analysis (Variography) **46**

4.1 Introduction 46

4.2 Variogram Theoretical Reviews 47

4.3 Application of Variograms to Kanzi Phosphate Project 50

4.3.1 Varmaps 50

4.3.2 Nugget Effect Analysis 52

4.3.3 Variogram Models 55

5 Model Construction and neighborhood parametres **57**

5.1 Introduction 57

5.2 Assumptions 57

5.3 Block Size Test work 57

5.4 Search and Estimation Parameters 59

6 Linear Estimation Methods used in Mining 60
6.1 Introduction 60
6.2 The IDW method 60
6.3 The OK method 62
6.4 Comparison of IDW and OK Results 64
6.4.1 Statistics 64
6.4.2 Cross-Sections 68
6.4.3 Grade Tonnage Analysis 70
6.5 Summary Findings on Linear Estimation Methods 72
7 Non-linear Geostatistical Modelling 74
7.1 Introduction 74
7.2 Non-Linear Geostatistical Techniques 75
7.2.1 Indicator Estimation 75
7.2.2 Results of the IK 85
7.3 Summary Findings on the IK 97
8 Interpretation and Discussion of results 98
8.1 Introduction 98
8.2 Comparison of the estimated P_2O_5 grades 98
8.3 Risk Assessment 98
8.4 Grade Tonnage Curve Analyses 98
8.4.1 Traditional Grade Tonnage Curves 98
8.4.2 Grade Tonnage Curves from different cut-offs 99
8.5 Practical Application to Mining Projects 101
8.6 Ranking of the estimation techniques used 101
8.7 Estimation of other crucial variables 101
9 Conclusion and Recommendations 103
9.1 Introduction 103
9.2 Conclusion 103
9.2.1 Methods and their outcomes 103
9.2.2 Implications of applying IDW, OK or IK in Mineral Resources studies 105
9.3 Recommendations 105
9.3.1 Conduct Conditional Simulation Studies 105
9.3.2 Twining using diamond drilling technique 105
9.3.3 Variography 106
9.3.4 Estimation of other variables 106
9.3.5 The processing studies of the phosphate mineralization 106
10 References 107

List of Figures

Figure 1.2_1: Project Location 4

Figure 2.2_1: Drillhole locations and positions of the cross-sections 8

Figure 2.2_2: Cross-Sections 9

Figure 2.2_4: CaO versus P_2O_5 for North Geo-Zone 11

Figure 2.2_5: CaO versus P_2O_5 for BL 13

Figure 2.2_6: CaO versus P_2O_5 for BL with outliers removed 13

Figure 2.2_7: CaO versus P_2O_5 for ML 14

Figure 2.2_8: CaO versus P_2O_5 relationship for ML: Different Populations 15

Figure 2.2_9: CaO versus P_2O_5 for TL 16

Figure 2.2_10: CaO versus P_2O_5 for TL: Different Populations 17

Figure 3.4 _1: Normal probability distribution, mean μ, standard deviation σ 21

Figure 3.4.1_1: Histograms for the layers in the South Geo-Zone 26

Figure 3.4.1_2: Histograms for the layers in the South Geo-Zone 27

Figure 3.4.1_3: Histograms for the layers in the South Geo-Zone 28

Figure 3.4.1_4: Histograms for three major variables drawn in the same scale: BL and TL 29

Figure 3.4.1_5: Histograms for three major variables drawn in the same scale: TL and North Geo-Zone 30

Figure 3.4.4_1: Histograms for North Geo-Zone 32

Figure 3.6_1: Scatter Plots for the Bottom Layer 40

Figure 3.6_2: Scatter Plots for the Middle Layer 41

Figure 3.6_3: Scatter Plots for the Top Layer 42

Figure 3.6_4: Scatter Plots for the North Geo-Zone 43

Figure 3.7_1: A phosphate sample 44

Figure 4.2_1: Demonstration of lag distances 47

Figure 4.2_2: Demonstration of experimental variogram calculations 48

Figure 4.5.2_1: Variogram maps and experimental variograms for different domains 51

Figure 4.3.2_1: Downhole Variograms for different geo-zones using same scale 53

Figure 4.3.2_2: Detailed Downhole Variograms for different geo-zones 54

Figure 4.3.3_1: Traditional variogram models for P_2O_5 56

Figure 5.3_1: Simplified plan view of the block model 58

Figure 6.2_1: The illustration of how IDW works 61

Figure 6.4.1_1: Comparison of the raw and estimate data statistics for BL and ML 66

Figure 6.4.1_2: Comparison of the raw and estimate data statistics for TL and North Geo-Zone 67

Figure 6.4.2_1: Comparison of IDW(2) and OK 69

Figure 6.4.3_1: The Grade Tonnage Curves for the different domains 71

Figure 7.2.1_1: Median Indicator Downhole Variogram Models for P_2O_5 80

Figure 7.2.1_2: Median Indicator Variogram Models 82

Figure 7.2.1_1: Examples of cut-off determined 83

Figure 7.2.2_1: The maps of North Geo-Zone showing the average P_2O_5 grade and proportions of materials above the cut-off 87

Figure 7.2.2_2: The maps of BL showing the average P_2O_5 grade and proportions of materials above the cut-off87

Figure 7.2.2_3: The maps of ML showing the average P_2O_5 grade and proportions of materials above the cut-off89

Figure 7.2.2_4: The maps of TL showing the average P_2O_5 grade and proportions of materials above the cut-off90

Figure 7 2.2_5: The grade tonnage curves modelled from IK 93

Figure 7 2.2_6: The grade tonnage curves modelled from 7.5% P_2O_5 indicator cut-off 94

Figure 7 2.2_7: The grade tonnage curves modelled from 12.5% P_2O_5 indicator cut-off 95

Figure 7 2.2_8: Proportion and Tonnage above the cut-off curves 96

Figure 8.4.1_1: The Traditional Grade Tonnage Curves produced by the OK, IDW and IK methods 100

List of Tables

Table 3.5_1: Correlation Statistics – South Geo-Zone: BL 35

Table 3.5_2: Correlation Statistics – South Geo-Zone: ML 36

Table 3.5_3: Correlation Statistics – South Geo-Zone: TL 37

Table 3.5_4: Correlation Statistics – North Geo-Zone 38

Table 4.3.3_1: Traditional Variogram Model Parameters 55

Table 5.4_1: Model Construction Parameters 59

Table 6.4.1_1: Comparison of the means of the drillholes, IDW and OK estimates 65

Table 7.2.1_1: P_2O_5 Median Indicators for the different domains 79

Table 7.2.1_2: Median Indicator Variogram Model Parameters for P_2O_5 81

Table 8.7_1: The formulae used to estimate SiO_2, CaO, Al_2O_3 and TiO_2 102

Table 9.2_1: The performance measure of three techniques on Kanzi Phosphate Project 104

List of Appendices

Appendix A – Maps and Cross-Sections

Appendix B – Histograms, descriptive statistics and correlation matrix

Appendix C – Variography

Appendix D – Block Size Test-Work

1 INTRODUCTION

1.1 Background

Minbos Resource Limited (MRL) conducted exploration for a phosphate mineralization in Kanzi in the western part of the Democratic Republic of Congo in 2011 and 2012. The MRL reported 58.5 Mt at 14.2% P_2O_5 for Kanzi Phosphate Project in their 2013 annual report (Minbos, 2013). Phosphate is mined in different parts of the world for use in agriculture and industry.

Mineral resources or reserves form the critical assets of a mining company. Evaluation of mining or exploration projects is fundamentally based on the mineral resources and reserves. Technical evaluation of these critical assets has bearing on the financial image or performance of a project.

The integrity of the mineral resource estimates depends on various technical factors. The geological interpretation of mineral deposits forms the basis of almost all mineral estimation techniques and good understanding of geology helps in choosing the appropriate estimation techniques.

The Ordinary Kriging (OK) method is the commonly used technique in Mineral Resource estimation because it produces better estimates and it is simple to understand. Kriging is well known for being the best linear unbiased estimator for a global mean. It smooths the local variability. This is not good for mining as local variability affects production and processing.

The estimation of mineral content and its volumes is critical to any mineral resource company as biased estimation may lead to incorrect financial assessments. Uncertainty in grade and volume is caused by the differences between the estimates and the “reality”. Over and under-estimation of the Mineral Resources negatively affects the valuation and performance of the mining company.

The understanding of uncertainty in resource estimates is a vital requirement of mineral resource evaluation. The probability of realising the estimated resources can be achieved through the application of advanced non-linear geostatistical methods (Sama, 2011). Since their introduction in the 1980s, the non-linear estimators have gained acceptance in the mining industry.

Data is the most valuable asset of a mineral exploration or mining company and is expensive to acquire. The costs of drilling and labour have doubled since the commodity booms in 1990s; the probabilistic geostatistical techniques need to be evaluated and implemented so that costs of conducting exploration can be minimised by drilling fewer drillholes and produce better estimates.

Rarely risk analyses are performed in the mineral resource estimation techniques. This is due to 'black box mentality' used in estimation. Risk analysis in resource estimation is not a simple task and needs rigorous appreciation of geo-statistical methods.

The financial models of mineral projects are fundamentally based on the mineral resources. The financial models do not require geostatistical uncertainty parameters. The assumption is that mineral resources used in the financial models are risk-free and an accurate representation of the mineralization.

Rather than simply producing a single set of estimated values from the OK method, non-linear geostatistical estimation techniques produce possible detailed multiple sets of possible estimate values that can be re-blocked into units and shapes to represent expected estimates. Uncertainty based modelling includes both a spatial model of the variable of interest such as grade taking the form of a regular 2 or 3 dimensional grid and a quantification of uncertainty ranges around the model at a given scale (such as global, block or bench). Uncertainty estimate consists of ranges of the variable of interest at different confident levels.

1.2 Location of a Study Area

The Kanzi project is located on the Democratic Republic of the Congo (DRC) border with Angola in the Bas Congo province of the DRC (Figure 1.2_1). The town of Boma is situated some 35km southeast of the project area which is accessible via a series of well-maintained gravel roads.

1.3 Problem Statement

Detailed and practical comparative studies on the linear and non-linear geostatistical techniques have not been extensively and clearly conducted especially on the sedimentary phosphate deposits. The problem of uncertainty in the estimates continues to hinder the mining and exploration companies. The advanced geostatistical methods need to be applied so that the variability and risks in developing the projects can be assessed.

The linear geostatistical techniques are mostly used in the mineral resources evaluation due to their simplicity. These methods are known to have smoothing effects and are unable estimate recoverable resources at both local and global scale. These smoothing effects (including under and over-estimation) may have detrimental effects to mining and exploration projects.

The risks in the resource model should be quantified in terms of probability of getting the estimated quality (grade) and quantity (tonnage) at a given cut-off grade (Sama, 2011). Linear geostatistical methods cannot provide the answer to this problem; as such, linear estimation methods expose mining projects to unnecessary uncertainties and risks.

The non-linear geostatistical methods should be explored and the results should be evaluated. These methods use advanced mathematical algorithms and their applications

and robustness need to be tested. The non-linear estimation methods are not commonly used as they are advanced techniques. And there are not enough skilled estimators and application is difficult due to lack of understanding and training on the part of mining and process engineers and financial professionals

1.4 Aim

The main aim of this project is to conduct a comparative study of the linear and non-linear geostatistical techniques used in the Mineral Resource estimation of Kanzi Phosphate project. The two most used linear methods in the minerals industry are Ordinary Kriging (OK) and Inverse Distance Weighting (IDW). These two linear methods will be compared to the Indicator Kriging (IK) which uses the indicator intervals to conduct estimation and provides measures of local uncertainty.

The specific objectives of this study are to;

- Interpret the geology of the area and establish different geo-zones (domains);
- Study spatial relationships between variables;
- Produce and compare Mineral Resource estimates from OK and IDW;
- Estimate the Mineral Resources using IK
- Compare results from linear techniques and non-linear methods.

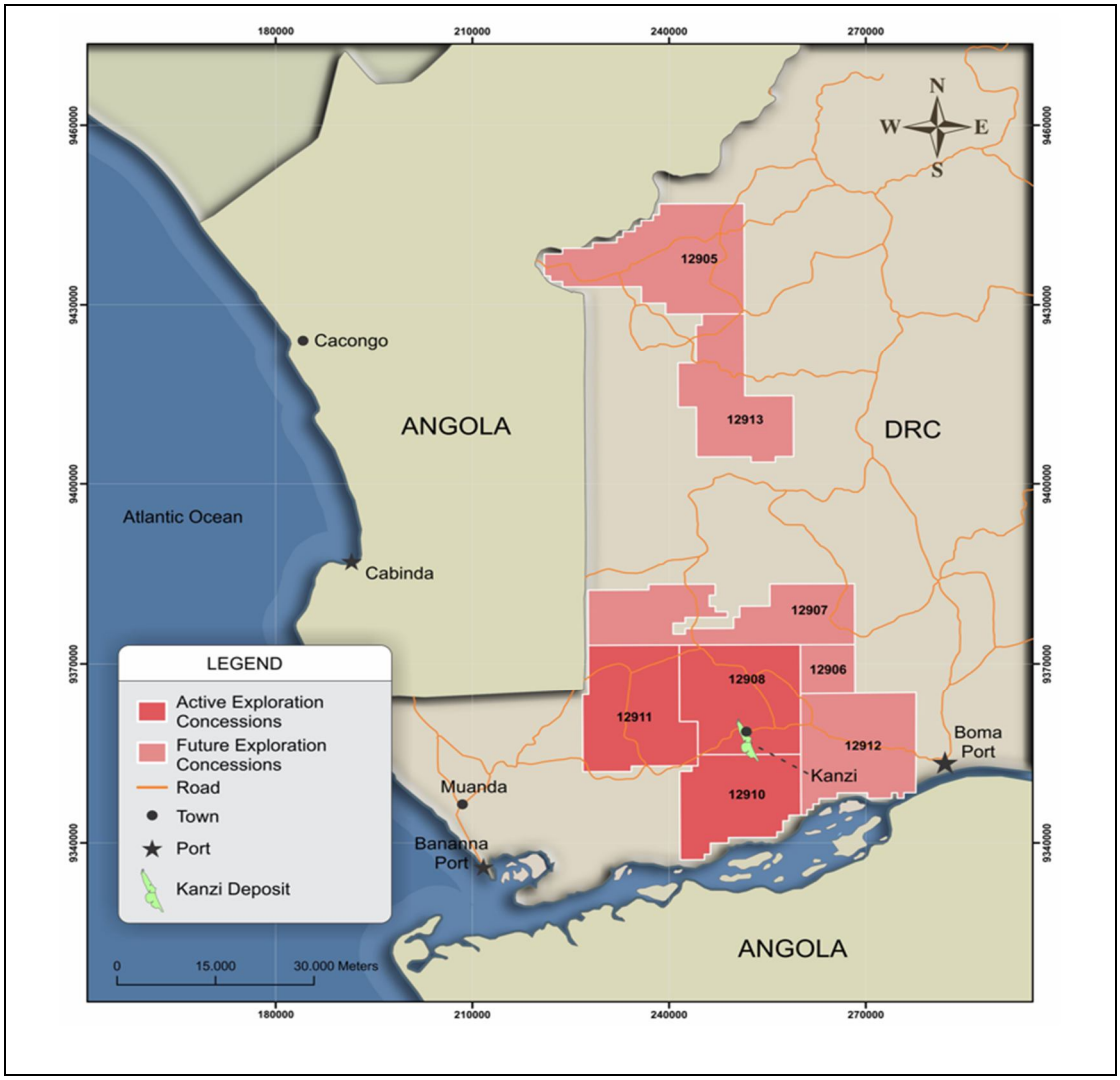


Figure 1.2_1: A base map of the western DRC showing the project location.

1.5 Methodology

The geostatistical techniques used in the Mineral Resource estimations should always follow geological interpretations. The understanding of the mineralization style is crucial in setting the appropriate estimation parameters and methods.

Chapter 2 summarizes the regional and project geology, mineralisation style, geochemistry and geo-zones of the Kanzi phosphate project. The basic statistics of the different geo-zones are explained and cross-sections through the geo-zones are presented and analysed.

Descriptive and spatial statistics are explained in Chapter 3. The theory and application of statistics per geo-zone are discussed. Major oxides are identified and commented on in detail. The analyses of scatter plots, histograms, correlation matrix and probability plots per geo-zone are presented. The estimation strategies based on the variable relationships are formulated on these results.

The spatial relationships were studied through the construction of three-dimensional variograms and visual inspection of grades and result are presented in Chapter 4. The variogram models for each geo-zone are presented and discussed.

Chapter 5 summarizes the model, estimation parameters and the search volumes used in the estimations. In this study only P_2O_5 was estimated.

The OK and IDW theory and applications are presented in Chapter 6. The estimation results are discussed. The IDW and OK are compared and their implications to the Mineral Resources are discussed.

The non-linear geostatistical method Median IK was applied to the deposit and is discussed in Chapter 7. The theory and applications are explored. The pre- and post-processing of the data that were performed are also discussed.

Chapter 8 discusses the Mineral Resource results from linear and non-linear estimation techniques. The results are compared and the ranking of the estimation methods are done.

The conclusion and recommendations are given in Chapter 9. Future studies are recommended based on the results found.

The specialized softwares that were used in the geological interpretation, statistical analyses and Mineral Resource estimation are Isatis (from Geovariances), Datamine Studio 3 (a trademark of CAE Mining) and Micromine.

2 GEOLOGICAL INTERPRETATION AND DOMAINING

2.1 Regional Geology

Phosphate deposits and phosphatic horizons are located in the coastal basin within the Cretaceous and Eocene sediments. Older Cretaceous sediments comprising redbeds, green-grey shales and sands are overlain by limestones of early Cretaceous and late Cretaceous age and form the footwall to the phosphate mineralisation which is hosted in late Cretaceous (Maastrichtian) sediments. This unit informally called the Lower Phosphate Member, (LPM), can be correlated across Cabinda and into the DRC and Congo-Brazzaville (ROC). The upper contact with the overlying Eocene, Upper Phosphate Member (UPM), is sharp and unconformable. The UPM is laterally extensive in Cabinda and extends into the DRC. The UPM is well developed and preserved in the grabens hosting the Cacata, Kanzi, Chivovo, Cambota and Mongo Tando Deposits (Body, 2013).

The UPM consists of medium to coarse grained pellets and nodules of phosphate and organic fragments and averages 10m in thickness at Kanzi. There is no outcrop of phosphate mineralization at Kanzi (Mudau, 2013). The UPM is well developed in Kanzi and has a north-south strike direction. It is fairly flat and has been affected by minor faulting in places. There are three sedimentary cycles that resulted in the phosphate concentration. These cycles are responsible for the upper, middle and lower layers of the UPM. The middle layer is the richest and has the lowest silica content.

Phosphate mineralisation in the DRC occurs within the Maastrichtian Vermelha Formation and the Eocene Ambrizete Formations and these are interpreted to be identical to the LPM and UPM, respectively, in Cabinda, Angola. The phosphorites are largely sandy silts and silty sands with subordinate grit or gravel beds. The phosphate occurs as pure phosphate (fluorapatite) grains, phosphatic coprolites, phosphatic organic debris and phosphatic nodules and concretions. Other constituents in varying proportions are; quartz, illite, smectite, calcite/dolomite, pyrite and organic matter. All of the phosphate deposits appear to be associated with a series of broad, gentle folds and grabens trending southeast-northwest, sub parallel to the coast. The phosphate deposits appear to be mostly preserved in the grabens. The phosphatic stratigraphy is overlain by Pliocene to Quaternary sands, clays and marine terrace deposits (Body, 2013).

Phosphate deposits in Kanzi are sedimentary in origin originally deposited in a marine environment. The deposits are similar to those found in Florida, USA and across North Africa/Arabia from Morocco to Saudi Arabia. General geological characteristics of the Florida-type phosphate deposits are summarized by Riggs (1960).

2.2 Project Geology and Analysis of different geo-zones

The single dominant feature is a graben with the eastern boundary fault having the major displacement. The displacement on the eastern fault is more than 70m and on the western is about 50m. Both faults strike approximately N25°W. The beds within the

graben have a general westward dip of 2 - 5°. The present known graben is 7km long and 1.2km wide. It is assumed to continue to the north and south some distance, possibly a few kilometres.

There are two mineralized layers intersected in Kanzi. These layers are Upper and Lower phosphatic layers. The separation distance between the layers is thought to be around 15m to 20m. No drillhole intersected all the layers as drillholes were stoped immediately after intersecting the first well-mineralized layer.

A full set of major oxides (Fe_2O_3, MnO, Cr_2O_3, V_2O_5, TiO_2, CaO, K_2O, P_2O_5, SiO_2, Al_2O_3, MgO, and Na_2O) and LOI were analysed for samples from the Kanzi Phosphate Project. This current study focused mostly on P_2O_5 content as it is what primarily determines the economics of the project. The deleterious elements SiO_2, Al_2O_3, TiO_2, and CaO were also studied as they determine the processing and environmental aspects of the project.

Upper Phosphatic Layer

The upper phosphatic layer is regionally termed Upper Phosphatic Member (UPM). The UPM consists of yellowish to greyish brown phosphorite or phosphatic siltstone with clay matrix. It has an average thickness of 10m. The phosphorite in the UPM comprised of coprolites, pellets and angular siltstone fragments. The bottom of the UPM is generally marked by a clay or silt. This layer has highest grades of P_2O_5 on the property.

The UPM is well developed elongated layer in centre of the Kanzi phosphate project. It is 4.5km long and 950m wide, on average.

The UPM is divided into North and South geo-zones. This division is done for modeling purposes as there are 10 drillholes that have not yet been assayed and Mineral Resource modeling could not be done passing through an area of un-assayed drillholes. These drillholes are situated on the border between the geo-zones. The division is based entirely on locality rather than spatial relationships between the variables as the continuity of UPM mineralization has not yet been established.

Figure 2_2_1 shows the location of the drillholes, the drillholes that intersected the mineralization and drillholes that didn't intersect mineralization. The drillholes that intersected mineralization and their samples are not yet assayed are also shown. Three cross-sections were drawn (A-B; C-D and E-F) as shown in Figure 2.2_1 and 2.2_2.

The longitudinal cross-section A-B shows the positions of North and South Geo-Zones. It shows that North Geo-Zone is the thickest and the South Geo-Zone is the most laterally extensive. The cross-section A-B illustrates that the South Geo-Zone is comprised of three different layers and the middle layer is the most continuous. The top and bottom layers of the South Geo-Zone are confined to the north and south respectively.

The cross-section C-D in Figure 2.2_2 shows that the North Geo-Zone is slightly dipping to the west and the mineralization is not disturbed by faulting. The North Geo-Zone is

single population and is not sub-divided. The South Geo-Zone as shown in cross-section E-F is slightly undulating but fairly flat. The basin-like structure is seen in the middle of the South Geo-Zone (Cross-section A-B) where the middle layer is thickest.

North Geo-Zone

The mineralized layer in the North Geo-Zone has an average thickness of 6.5m. The stratigraphy of the North Geo-Zone is simple as the top is covered by recent soil, then sand and clay in places overlies the phosphorite. The phosphorite in the North is sandy or clayey and consists of coprolites, pellets and fish teeth. The outline of the North Geo-Zone is shown on Figure 2.2_3.

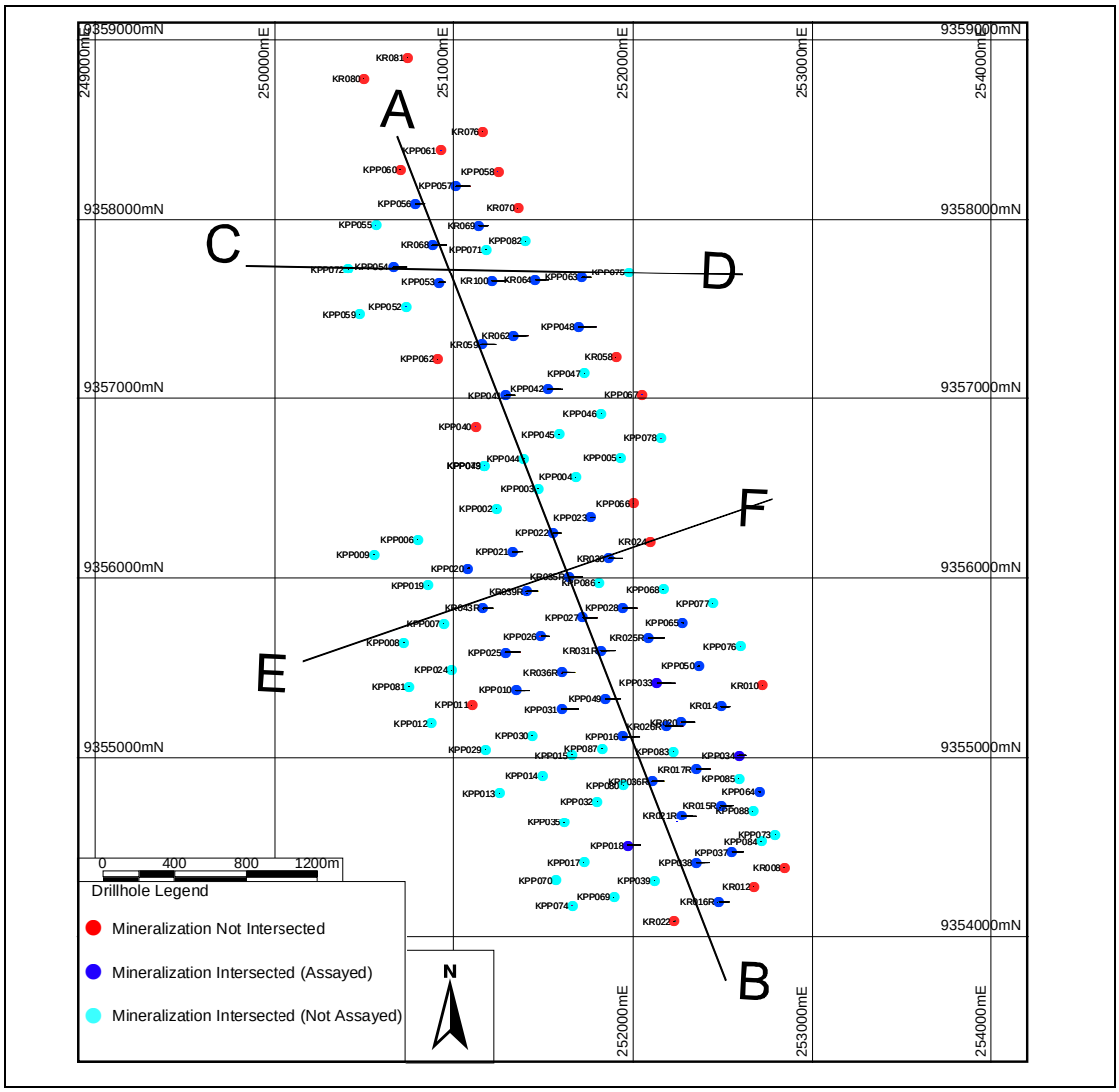


Figure 2.2_1: Drillhole locations and positions of the cross-sections.

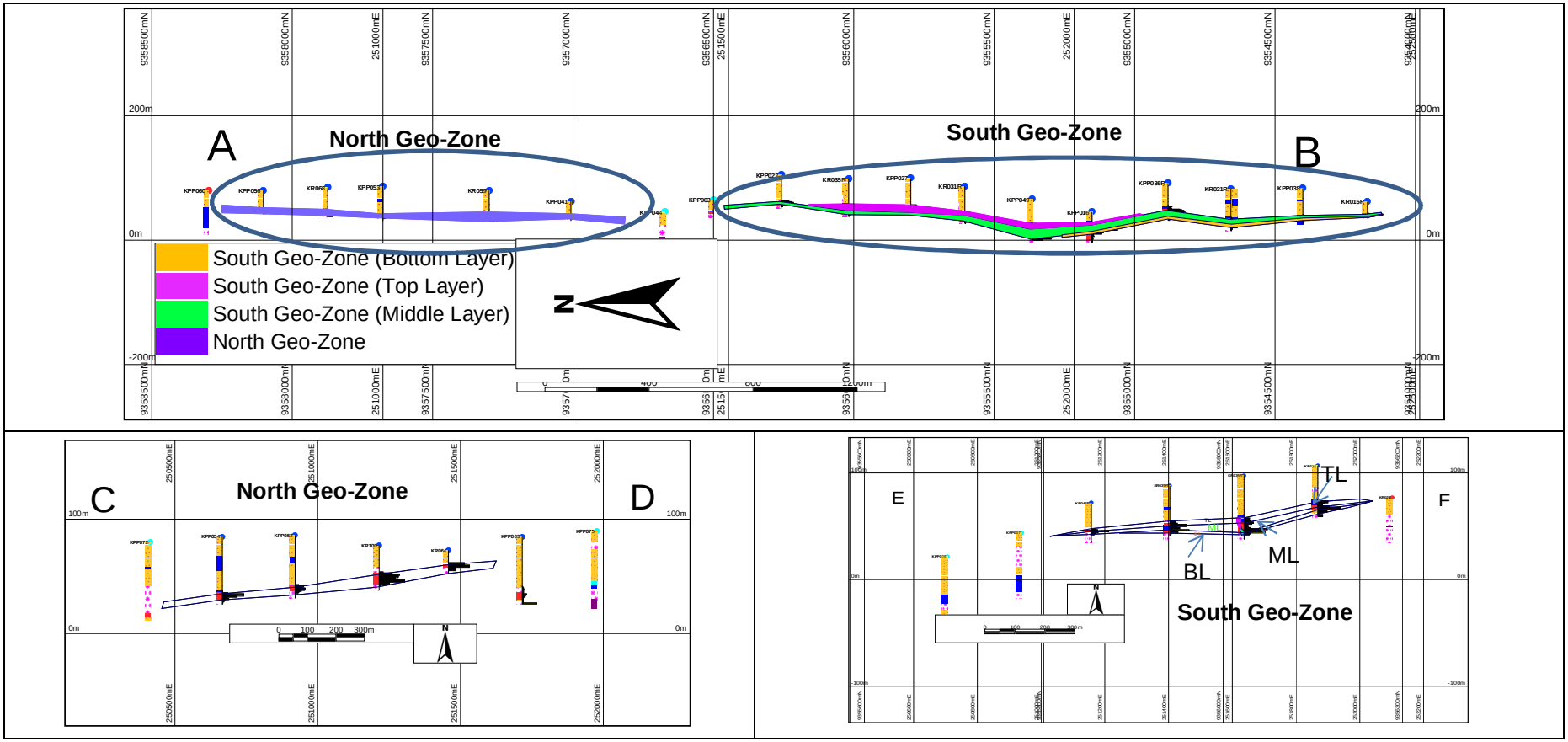


Figure 2.2_2: The cross-sections of the North and the South geo-zones.

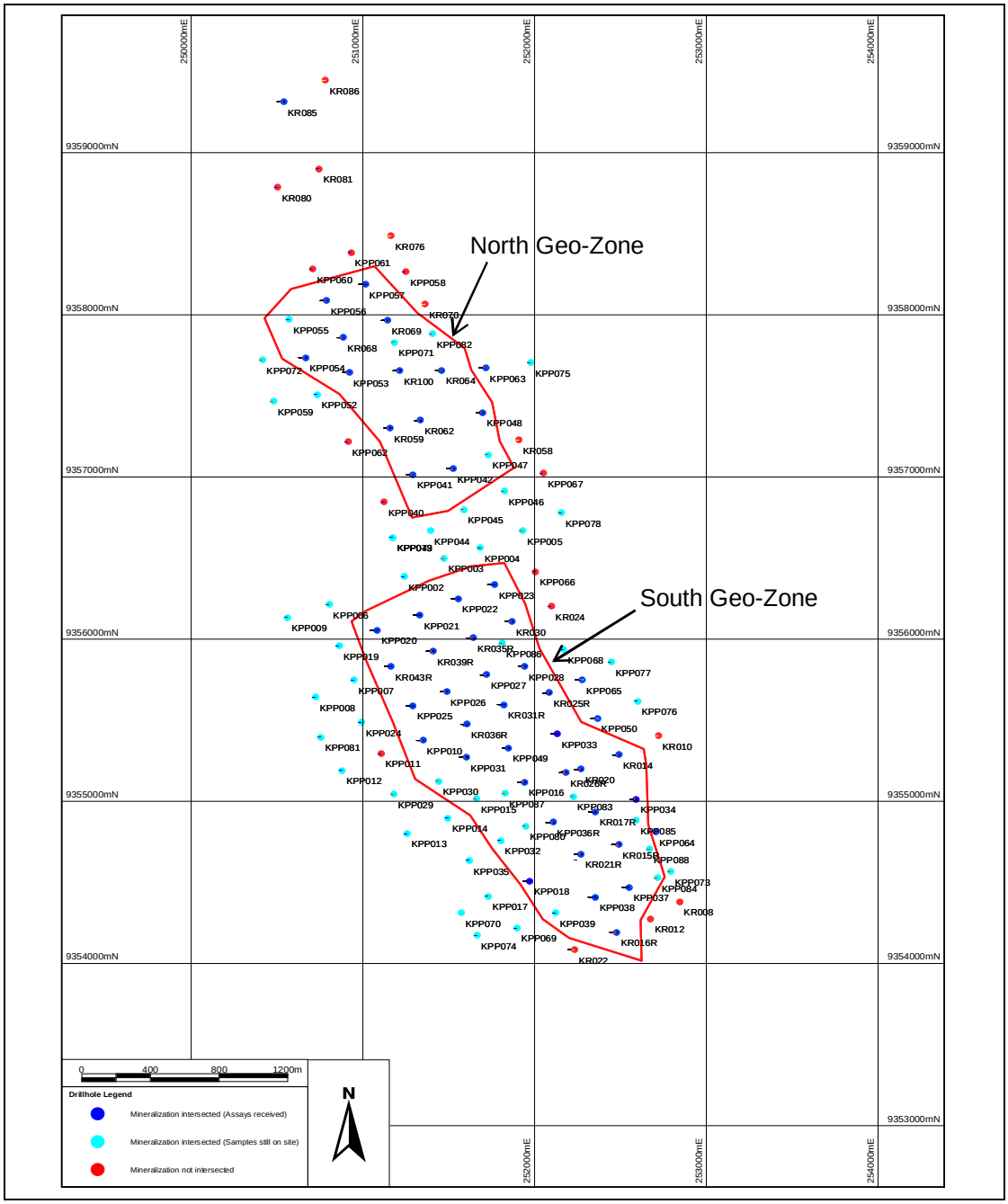


Figure 2.2_3: Outline of North and South Geo-Zones.

The statistical properties of the mineralized layer for North Geo-Zone are presented in Appendix B and Figure 3.4.1_5. The P_2O_5 has normal distribution and an average of 16.32% with a standard deviation of 6.46%. The co-efficient of variation (CoV) for P_2O_5 is low at 0.40 and the skewness is 0.32. The silica (SiO_2) has a mean of 44.62% with 15.95% standard deviation. The silica content has a normal distribution and a low CoV of 0.36. The CoV of the P_2O_5 and SiO_2 are as expected for the high grade phosphate deposit. The variability is low. CaO has a mean of 21.49% and a standard deviation of 9.96%. Al_2O_3 has a mean of 5.26% and positively skewed distribution. A low concentration of Fe_2O_3 is found in the mineralized layer.

The P_2O_5 has a strong correlation with SiO_2 (negative correlation of 88%) and CaO (positive correlation of 94%). The average CaO/P_2O_5 is 1.40 which indicates that the Calcium in the phosphate layer in the North Geo-Zone is primarily of apatite origin (Figure 2.2_4). The apatite has a theoretical ratio (CaO/P_2O_5) of 1.3. At low P_2O_5, the relationship suggests some dolomite in the matrix and minor clay layers.

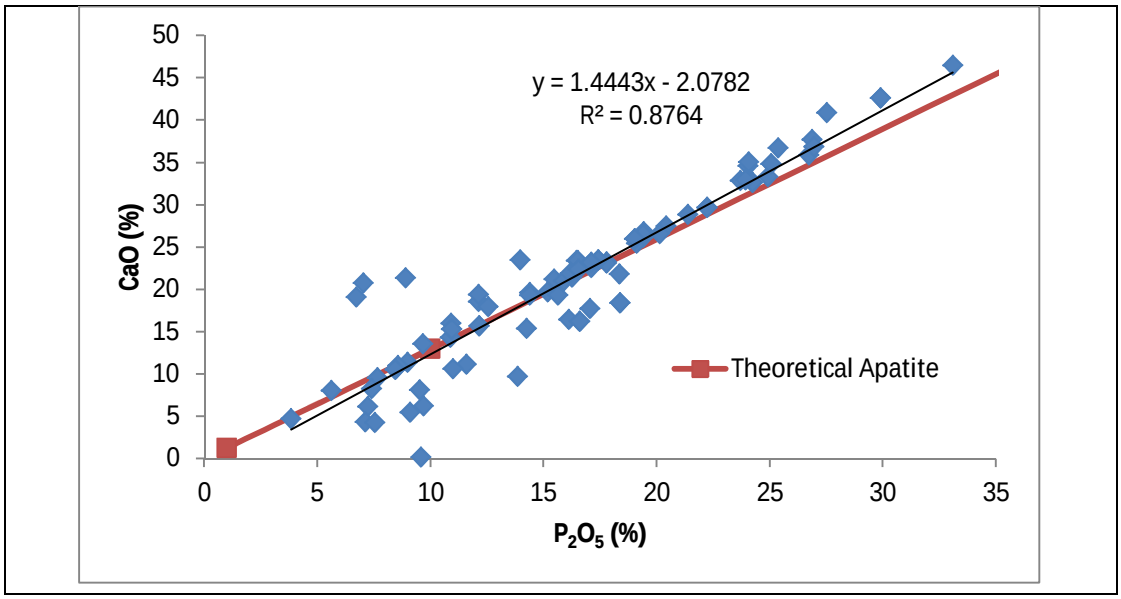


Figure 2.2_4: CaO versus P_2O_5 for North Geo-Zone.

South Geo-Zone

The area covered by the South Geo-Zone is bigger than the area covered by the North Geo-Zone as shown in (Figure 2.2_3). The South Geo-Zone is affected by minor sub-vertical faults.

The thickness of the mineralized layer in the South Geo-Zone varies from 5m to 20m. Based on the geo-chemical signatures of the mineralized layer, the South Geo-Zone is sub-divided into 3 layers; Top, Middle and Bottom layers.

Bottom Layer

The Bottom layer (BL) of the South Geo-Zone has an average thickness of 4.2m and its outline is shown on Figure A_1 in Appendix A. The BL is the thinnest layer and is located towards the most south.

The statistical properties of the BL are presented on Appendix B and Figures 3.4.1_1 to 3.4.1_4. The BL has an average P_2O_5 grade of 8.75%, a standard deviation of 3.04% and a skewness of -0.07. The P_2O_5 grade distribution is normal. Silica content in this layer is very high. The average SiO_2 content is 67.77% and the minimum and maximum SiO_2 contents are 51.89% and 91.29% respectively. The distribution of SiO_2 is symmetrical. The BL has an average CaO content of 11.16%, the lowest of all the layers. The P_2O_5 has a strong correlation with SiO_2 (at -89%) and CaO (at 73%).

The relationship between P_2O_5 and CaO is shown of Figure 2.3_8. The correlation between P_2O_5 and CaO is very strong and there are few outlier samples that have weak correlation. The low CaO and high P_2O_5 outliers (in Figure 2.2_4) are possibly due to contamination by footwall lithologies introduced during drilling as most of them are the bottom most samples. The footwall portions were taken with the mineralized portions to complete 1m samples. This is unavoidable with Aircore drilling technique. The high CaO and low P_2O_5 outlier is due to the clayey phosphorite intersected with low P_2O_5 grades and high CaO.

Figure 2.2_4 shows the CaO versus P_2O_5 with the outliers removed. The slope of CaO/P_2O_5 is around 1.3. The results indicate that the BL calcium is of apatite origin and has no dolomite footprint.

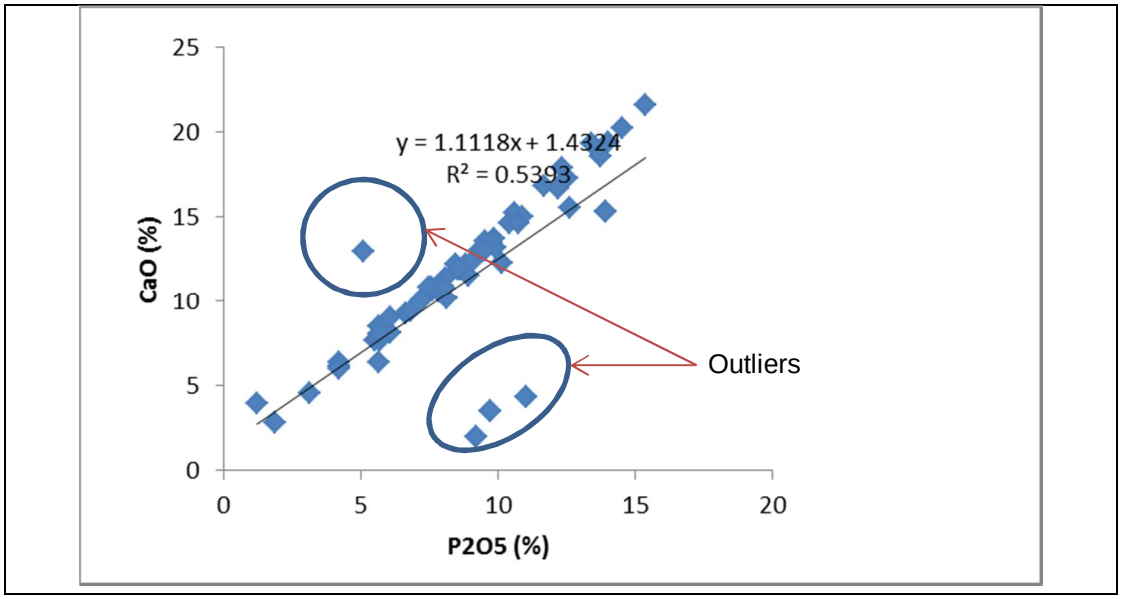


Figure 2.2_5: CaO versus P_2O_5 for BL.

Figure 2.2_6 shows the CaO versus P2O5 relationship with the outliers removed.

Figure 2.2_6
CaO versus P_2O_5 for BL without outliers

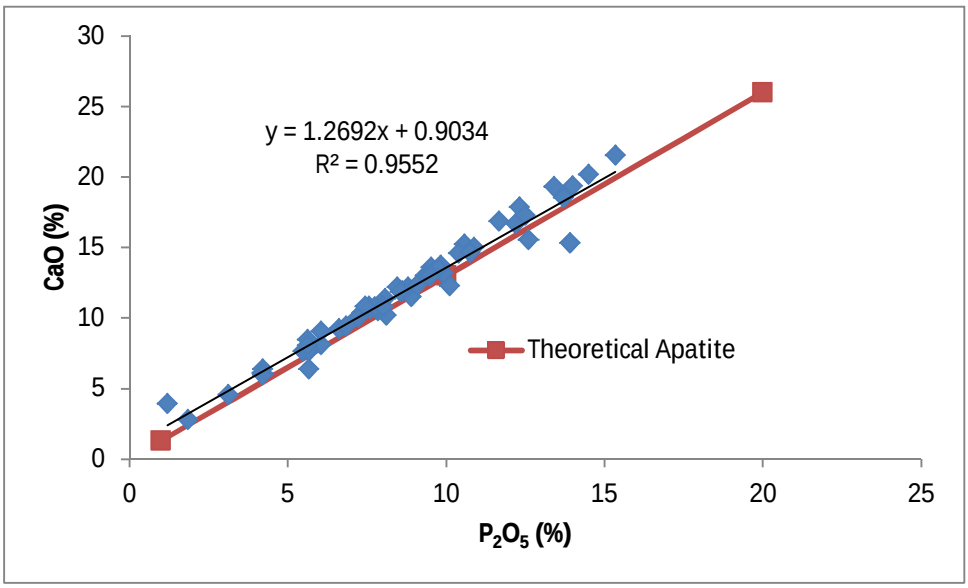


Figure 2.2_6: CaO versus P_2O_5 for BL with outliers removed.

Middle Layer

The Middle layer (ML) of the South Geo-Zone is the most laterally extensive domain. It is thickest towards the middle of the South Geo-Zone. The outline of the ML is shown in Figure A_2 in Appendix A.

The ML consists of silty phosphorite with coprolites, pellets and teeth. The average thickness of the ML is 6.4m. The geometry of the ML follows the paleo-topography. The statistical properties of the ML are presented on Appendix B and Figures 3.4.1_1 to 3.4.1_4. The ML has the highest P_2O_5 and lowest silica (SiO_2) grades 16.30% and 39.36%, respectively, of the three layers. The distributions of P_2O_5 and SiO_2 grades are symmetrical and have standard deviations of 6.87% and 15.42%, respectively. CaO has a normal distribution. Al_2O_3 has a positively skewed distribution. The average CaO content in the ML is the highest of all the layers at 23.39%.

There is a strong relationship between P_2O_5 and CaO as shown in Figure 2.2_6. The slope of 1.3 between CaO and P_2O_5 shows that the ML has apatite characteristics with a dolomitic matrix below 20% P_2O_5 as shown in Table 2.2_1. Two populations (A and B) are identified, though not well defined as shown in Figure 2.2_7 and 2.2_8. At low P_2O_5, the relationship between CaO and P_2O_5 is not well defined and at high P_2O_5, the relationship is clearly linear. Some of population B data are integrated in population A down to about 10% P_2O_5.

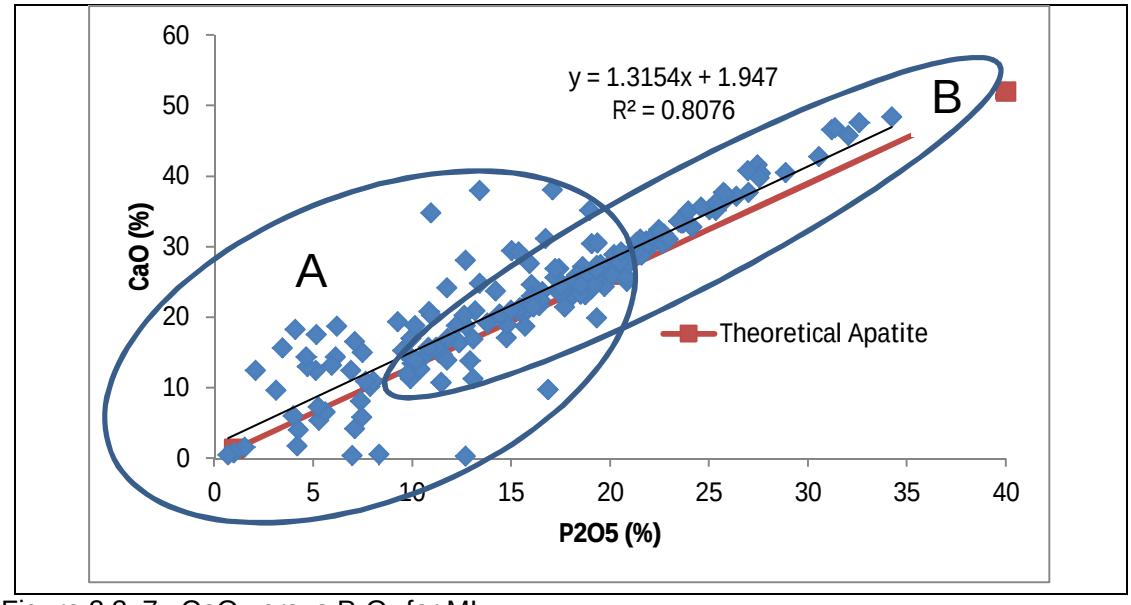


Figure 2.2_7: CaO versus P_2O_5 for ML.

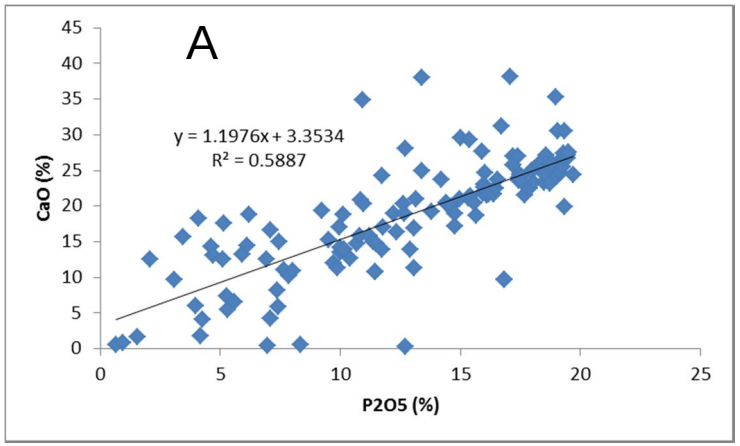
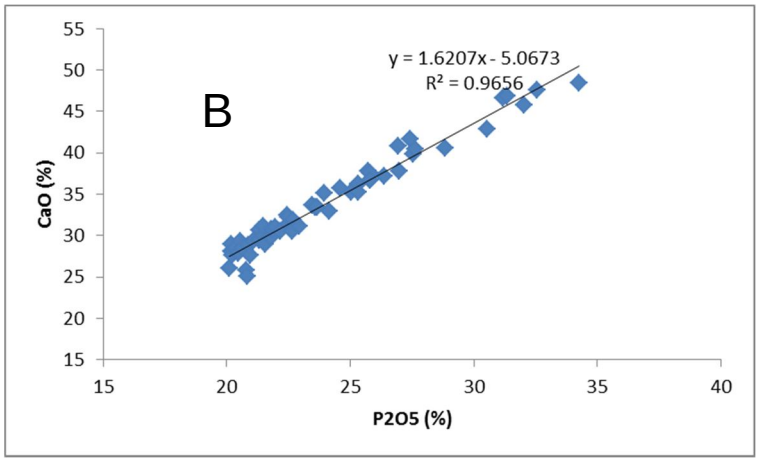
Lower P_2O_5	Higher P_2O_5
	

Figure 2.2_8: CaO versus P_2O_5 relationship for ML: Different Populations.

Top layer

The Top layer (TL) of the North Geo-Zone has an average thickness of 4.6m. The outline of the TL is shown in Figure A_3 in Appendix A. The TL is confined towards the north of the South Geo-Zone. The TL is comprised of phosphatic clay and argillaceous phosphorite with coprolites, teeth, bones and pellets.

The statistical properties of the TL are presented in Appendix B and Figures 3.4.1_1 to 3.4.1_5. The P_2O_5 in the TL has a positively skewed distribution of 1.43 and a high standard deviation of 4.73%. The P_2O_5 has a mean grade of 9.50%. Silica content is high with an average grade of 49.23% and a minimum and maximum of 27.98% and 71.64%, respectively. P_2O_5 has a strong correlation with Al_2O_3, Fe_2O_3, TiO_2 and CaO. The CaO versus P_2O_5 relationship is not well defined except at high grades as shown in Figure 2.2_9.

There are three populations (A, B and C) that are distinguished by P_2O_5 geochemistry. Population A is consists of un-mineralized clays within the sequence; Population B has a low grade portion with a CaO/P_2O_5 ratio of 1.73 and Population C has high grade portion with an average CaO/P_2O_5 of 1.37. Lower grade mineralization of population B (<13% P_2O_5) has a dolomite matrix indicated by the high CaO/P_2O_5 ratio. These populations are spatially integrated and are not well defined as there is not enough data to support.

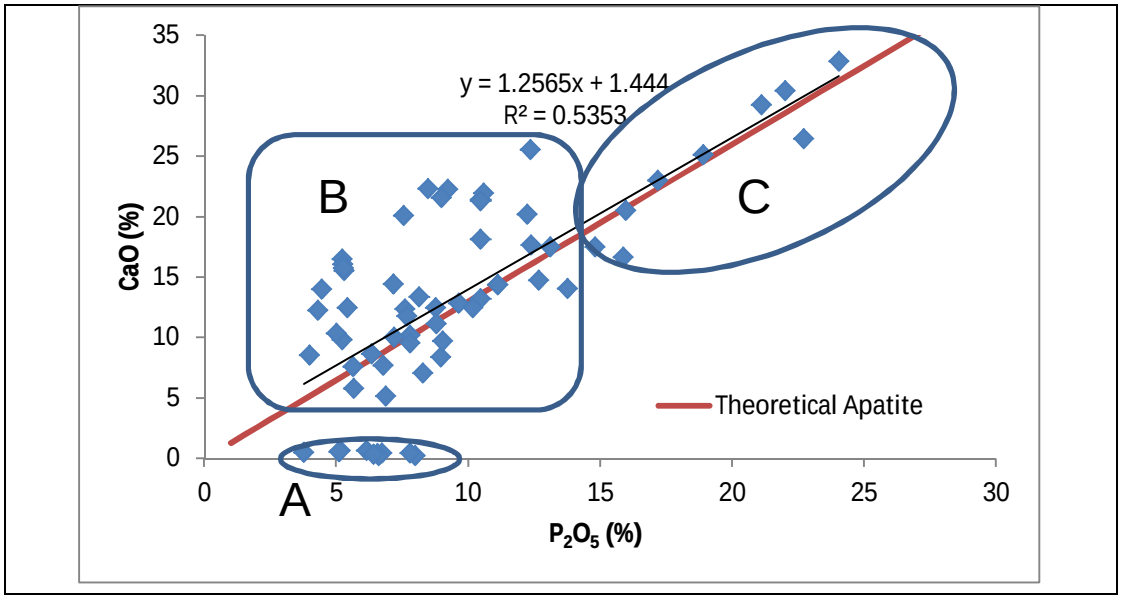


Figure 2.2_9: CaO versus P_2O_5 for TL.

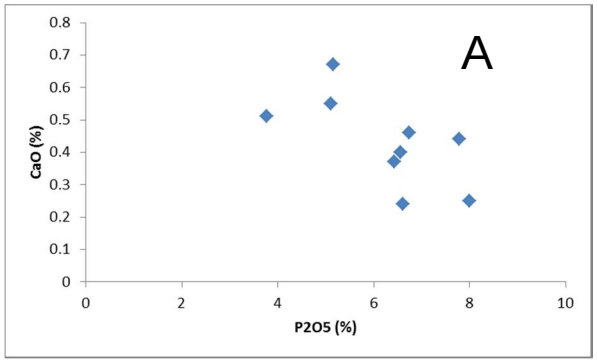
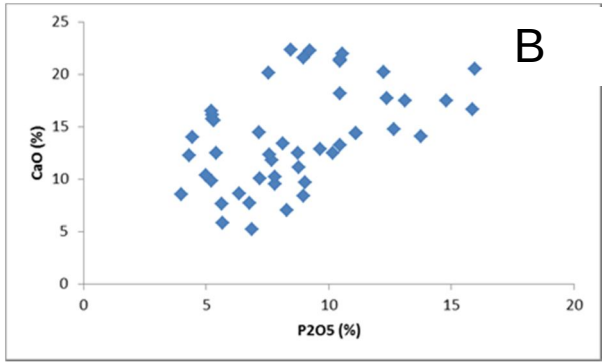
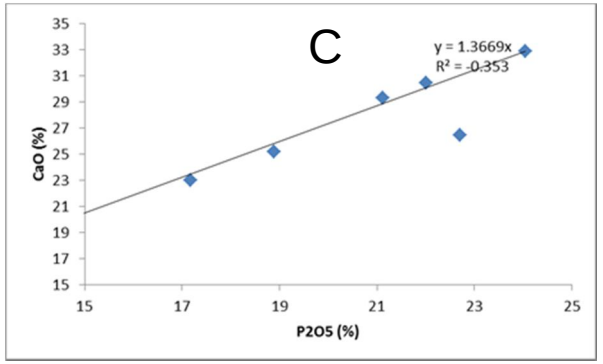
Lower CaO	Lower P_2O_5	High P_2O_5
		

Figure 2.2_10: CaO versus P_2O_5 for TL: Different Populations.

2.3 Summary of the Project Geology: Principal Findings

The Kanzi phosphate in the western part of the DRC is of sedimentary origin deposited through marine depositional mechanisms. The phosphate mineralization occurs in the Maastrichtian Vermelha and the Eocene Ambrizete Formations in the Upper Phosphate Member or layer (UPM). The mineralization is overlain by Pliocene to Quaternary sands, clays and marine terrace deposits. The UPM does not outcrop at Kanzi.

The drillhole data shows that the UPM has an elongated structure. It has a strike length of 4.5km and width of 950m and dips slightly to the west. The UPM is not affected by major structures.

The UPM is divided into North and South Geo-Zones based on location. The Geo-Zones are about 1km apart. The continuity of the UPM between the two geo-zones has not yet been established.

The North Geo-Zone is the thickest and dips slightly to the west. It has higher P_2O_5 grade and lower silica content than the South Geo-zone. A total of 13 drillholes, with 87 samples, have intersected the North Geo-Zone. The average thickness of this geo-zone is 6.5m. The P_2O_5 grade distribution is normal with a skewness of 0.06. The relationship between CaO and P_2O_5 shows that the calcium in the North Geo-Zone is of apatite origin as the ratio CaO/P_2O_5 is around 1.3.

The South Geo-Zone is sub-divided into three sub-zones based on geochemistry, statistics and stratigraphic position;

- Bottom Layer (BL)

  The Bottom Layer occurs in the southern part of the South Geo-Zone. A total of 16 drillholes intersected this layer. Number of samples taken from BL is 66. It is a thin layer at the bottom of the South Geo-zone and it has low P_2O_5 and high SiO_2. The BL has average thickness of 4.2m.

- Middle Layer (ML)

  The Middle Layer as the name suggests, occurs in the middle of the UPM in the South Geo-Zone. It is the most laterally extensive sub-zone. A total of 31 drillholes intersected the ML and samples taken are 196. The average thickness of the ML is 6.4m. It has higher P_2O_5 and lower silica than the other layers. The ML has a basin-like structure. At a low P_2O_5, the CaO/ P_2O_5 relationship is not well defined as a result of dolomite in the matrix and at higher P_2O_5, the relationship is clearly linear indicating that the phosphate is of apatite origin.

- Top Layer (TL)

  The TL occurs at the top most of the UPM. The P_2O_5 grade of the TL is very low and has high silica content. The TL occurs towards the northern side of the South Geo-Zone. The average thickness of this layer is 4.6m. Only 12 drillholes

intersected the TL and 65 samples were taken. Based on CaO/P_2O_5 relationship, three populations were identified. These populations are spatially integrated and cannot be separated.

3 STATISTICAL ANALYSIS OF THE DATA

3.1 Introduction

A good understanding of the underlying geology forms the basis of a proper statistical analysis. The study of statistical properties is crucial in understanding the grade distribution and behaviour of the mineral deposit. The quality of data is crucial in statistical studies and low quality data may produce inaccurate results even though sophisticated geostatistical techniques are applied. Kanzi phosphate data has been thoroughly assessed for quality and found to be acceptable for use in mineral resource estimation (Mudau, 2013).

The study of the statistical characteristics such as skewness, kurtosis, variance, standard deviation and co-efficient of variation forms a basis for understanding a mineral deposit. Capping is regarded as necessary if only a few values in the population are high enough (or low enough) to be considered outliers. Capping is done to minimize the impact of high or low values on the population mean and prevent local over or under-estimation.

3.2 Declustering and Compositing

Data used in a Mineral Resource Estimation is rarely taken uniformly over the area of interest. There are reasons for this which includes inaccessibility and under-sampling of lower grade zones.

Declustering

Declustering is crucial in performing statistics to avoid the negative effects of biased sampling. Over-sampling of high grades in one area may produce estimates that are biased to higher grades over much larger areas. Declustering can be solved by applying one of the following declustering techniques as defined by Coombes (1994):

- Certain holes or samples can be removed;
- Single drillhole or sample can be used per grid cell; or
- Use weighting techniques on the samples within the cell.

Declustering techniques are primarily based on geometrical configuration of the data and they generally don't consider data values (Leuangthong, et al., 2008).

The drillhole spacing followed at Kanzi has average grid of 250m X 250m and has a north-east to south-west orientation as shown in Appendix A. No declustering is needed as drillholes are well-spread. There was no bias in positioning drillhole spacing.

Kriging is a declustering technique so separate declustering is not crucial. The IDW has some declustering inherent but bias is common if one area is oversampled. However in IK or similar techniques clustering could be a serious problem as the grade distribution is skewed towards the more heavily sampled areas.

Compositing

The weights of sample grades may be related to the corresponding sample interval length in some mineral deposit. Compositing helps in making sure that the down-hole samples have comparable influence on statistics. Samples that are of different lengths do have different influences and produce biased statistics (Coombes, 1994). Compositing is sometimes weighted for density as lithologies may have different densities. There are warnings about deciding on the compositing sample interval length. Composited length should not be far from the original sampling interval length. Histograms are mostly used in deciding on a composite interval (Coombes, 1994).

Compositing should be done by considering the boundary of the domain. The boundary can be sharp or gradational; for sharp boundaries compositing must be done within the domain and for gradational contacts compositing should be done across the boundary, thus honouring the gradational changes (Coombes, 1994).

Sampling at Kanzi was done at one meter intervals as a Reverse Circulation (Aircore) drilling technique was used. No compositing is required as all samples have same length, same density and contribute equally to the statistics. A full 3D estimation will be conducted, thus no need to composite to a mineralized geo-zones. The other reason for not compositing into a geo-zone is that there are few drillholes and it may be problematic to get proper variograms with less data. The layers were treated as physically different and hard boundaries were used.

3.3 Dealing with the outliers

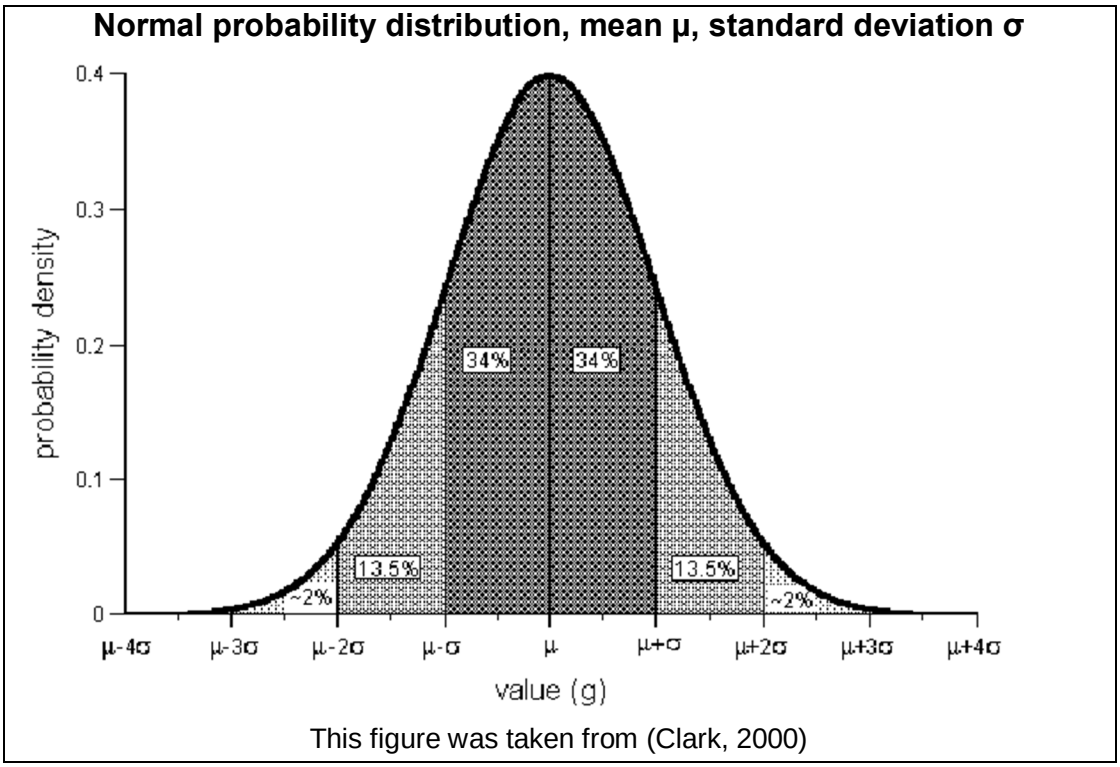
Effect of outlying values is significant in resource modelling and there is no single accepted method with theoretical justification for determining the treatment of these values. Capping is mostly applied and the choice of the upper value depends on the knowledge of the mineralization style.

3.4 Comments on the histograms, descriptive statistics and probability plots

Introduction

Histograms and descriptive statistics of the different domains as per the geological information and whole rock analysis are discussed in detail below. P_2O_5, SiO_2 CaO and Al_2O_3 have been studied in detail as they are they are crucial in understanding the grade and processing requirements of the mineralized layers.

Comments on histograms, descriptive statistics and probability plots are made per geo-zone. The basic statistical properties of the domains are described in terms of central tendencies, standard deviation, co-efficient of variation, range, skewness and kurtosis. Figure 3.4_1 shows the properties of a normal distribution.



This figure was taken from (Clark, 2000)

Figure 3.4 _1: Normal probability distribution, mean μ, standard deviation.

The normal distribution has a bell-shaped curve and the mean and median are the same. The negative and positive deviations balance each other as the distribution is symmetrical around the mean. For a normal distribution, the 68% of domain values should lie within the one standard deviation of the mean and 95% of the values should lie within two standard deviation (Clark, 2000; Dohm, 2010).

The kurtosis defines the “peakedness” of a population distribution. The skewness for a perfect normal distribution should be 0. For geological studies, the skewness for normal distribution does not perfectly meet the requirement as it is rarely if not impossible to have a perfect normal distribution. This may be due to sparse data.

Most of the variables have normal distribution. The IDW and OK methods performs well when the distribution is normal whereas the IK method is non-parametric.

Histograms of Major Variables

The histograms of major variables are presented on Figure 3.4.1_1 to 3.4.1_5. Figures 3.4.1_1 to 3.4.1_3 show the detail shapes of the histograms where Figures 3.4.1_4 to 3.4.1_5 show the histograms drawn on same scale. Histograms drawn on the same scale are easily compared and interpreted. The probability plots are shown in Appendix D (Figures D_10 to D_12).

3.4.1 South Geo-Zone (Bottom Layer)

P_2O_5

The Bottom Layer (BL) has a normal P_2O_5 distribution with a mean of 8.75% and standard deviation of 3.04%. A total of 66 samples were taken from this layer. The Co-efficient of variation (CoV) is 0.35. The skewness is low at -0.07. The median and mean are almost equal whereas the mode is low at 5.62%. The kurtosis is platykurtic. The grade range is wide at 14.15%. There are no outliers that can be visually determined from the histogram and probability plot.

SiO_2

This layer is characterized by higher silica content than the middle layer. The SiO_2 distribution is normal with a mean of 67.77 and a low standard deviation of 7.27%. The highest SiO_2 is 83.59% and the lowest is 51.89%. The range is wide. The CoV of the SiO_2 is 0.11. The mean and median are approximately equal. The skewness is 0 and kurtosis is -0.36. The distribution is symmetrical and there is no mixture of populations.

CaO

The CaO has a normal distribution with a mean of 11.16% and a standard deviation of 4.60%. The mean and median are equal and the skewness is 0. The distribution is symmetrical. The layer has minimum CaO of 2.0% and maximum of 21.56%. The range is wide. This might be due to discrete clay layers. The CoV is 0.42.

TiO_2

The TiO_2 has a mean of 0.36% and a standard deviation of 0.08%. The distribution of TiO_2 is narrow and symmetrical. The maximum TiO_2 is 0.59%. No capping is required as there are no major outliers.

Al_2O_3

The histogram of Al_2O_3 shows a normal distribution. The outliers are identified as shown in the histogram. With the outlier present the maximum Al_2O_3 is 8.90% and the mean is 4.11%. There are 6 samples that required capping. After capping is applied the maximum and the mean became 5.29% and 3.81% respectively. The standard deviation was reduced from 1.51% to 0.74%. The CoV was reduced from 0.37 to 0.19. The skewness

changed from 2.26 to 0.63. The range is reduced from 6.42% to 2.81%. The kurtosis is highly improved from 4.47 to -0.38. All statistics will be conducted on the capped data.

3.4.2 South Geo-Zone (Middle Layer)

The Middle Layer (ML) is the most laterally extensive layer. A total of 196 samples were taken from this layer.

P_2O_5

The P_2O_5 grade distribution is roughly a normal distribution with a mean of 16.30% and a high standard deviation of 6.87%. There are discrete internal waste layers in places contributing the lower P_2O_5 grade and this increased the grade range. The skewness is 0 and the kurtosis is -0.28. The median is slightly higher than the mean. The CoV is 0.42. No outliers are identified from the histogram and probability plot.

SiO_2

The ML has minor internal waste (silica) in places. This has contributed to higher SiO_2. The SiO_2 distribution is normal with a mean of 39.36%, a standard deviation of 15.42% and a skewness of 0.69. The CoV is 0.39 for phosphate deposits. The mean and median are almost identical. The outliers have not been identified.

CaO

CaO has a normal distribution with a mean of 23.39 and a standard deviation of 10.05%. The ML has the higher CaO than other layers. The skewness and kurtosis are 0. The mean, mode and median are almost equal showing that the distribution is symmetrical. CaO has CoV of 0.61. This shows the high variability in CaO. The clay layers contribute only small amounts of CaO and phosphorates have high CaO; thus wide range and high standard deviation.

TiO_2

The TiO2 for the middle layer has a normal distribution. The mean, median and the mode are 0.35%, 0.35% and 0.32% respectively. The range is high as the minimum is 0.01% and maximum is 0.85%. The CoV is 0.42. The standard deviation of 0.16% is moderate meaning that the variability is moderate.

Al_2O_3

Al_2O_3 is mostly introduced by clay minerals such as kaolinite. The clay internal waste and clayey phosphorite have high Al_2O_3. The Al_2O_3 has a mean of 5.55%, standard deviation of 2.98% and a skewness of 0.95. A high CoV of 0.54 is due to the presence of different lithologies. The distribution is slightly positively skewed and no outliers have been identified.

3.4.3 South Geo-Zone (Top Layer)

A total of 65 samples were taken from the Top Layer (TL).

P_2O_5

The P_2O_5 grade distribution is positively skewed with a mean of 9.50%, standard deviation of 4.69% and a skewness of 1.43. A high range of 20.28% is caused by the drilling technique wherein the portion of waste is included in the sample to make full 1m top samples. The probability plot shows that there are more than one population. Also contributing is the erosion of the upper parts of the deposit (Top layer) giving only a partial sampling of the population. The CoV is 0.50.

SiO_2

The SiO_2 content is high (a mean of 49.23%). The drilling technique used does not allow sampling only mineralized portion; inclusion of a small amount of un-mineralized material is always taken as samples are taken at 1m interval. The distribution is not well-defined due to lack of data. The CoV is 0.25 indicating that the domain is not contaminated. The mean, median and mode are almost equal suggesting that the distribution is symmetrical. The skewness is 0.23. A high range of 43.66% is caused by inclusion of waste portions.

CaO

A CaO has a mean of 13.39% and a standard deviation of 8.12%. A standard deviation is high. This introduces a large number of low values. The distribution is normal with almost equal mean, mode and median. The skewness is 0.13.

TiO_2

The distribution of the TiO_2 in the TL is not well defined. The mean is 0.49% and the CoV is 0.32. The minimum TiO_2 is 0.14% and the maximum is 0.76% meaning that the range is wide.

Al_2O_3

An Al_2O_3 has a mean 8.55% and a median of 8.90%. The skewness of -0.18 and equal mean and median suggest that the distribution is a normal distribution. The CoV is 0.29. A high Al_2O_3 is due to high concentration of clay matrix. The range of Al_2O_3 is wide.

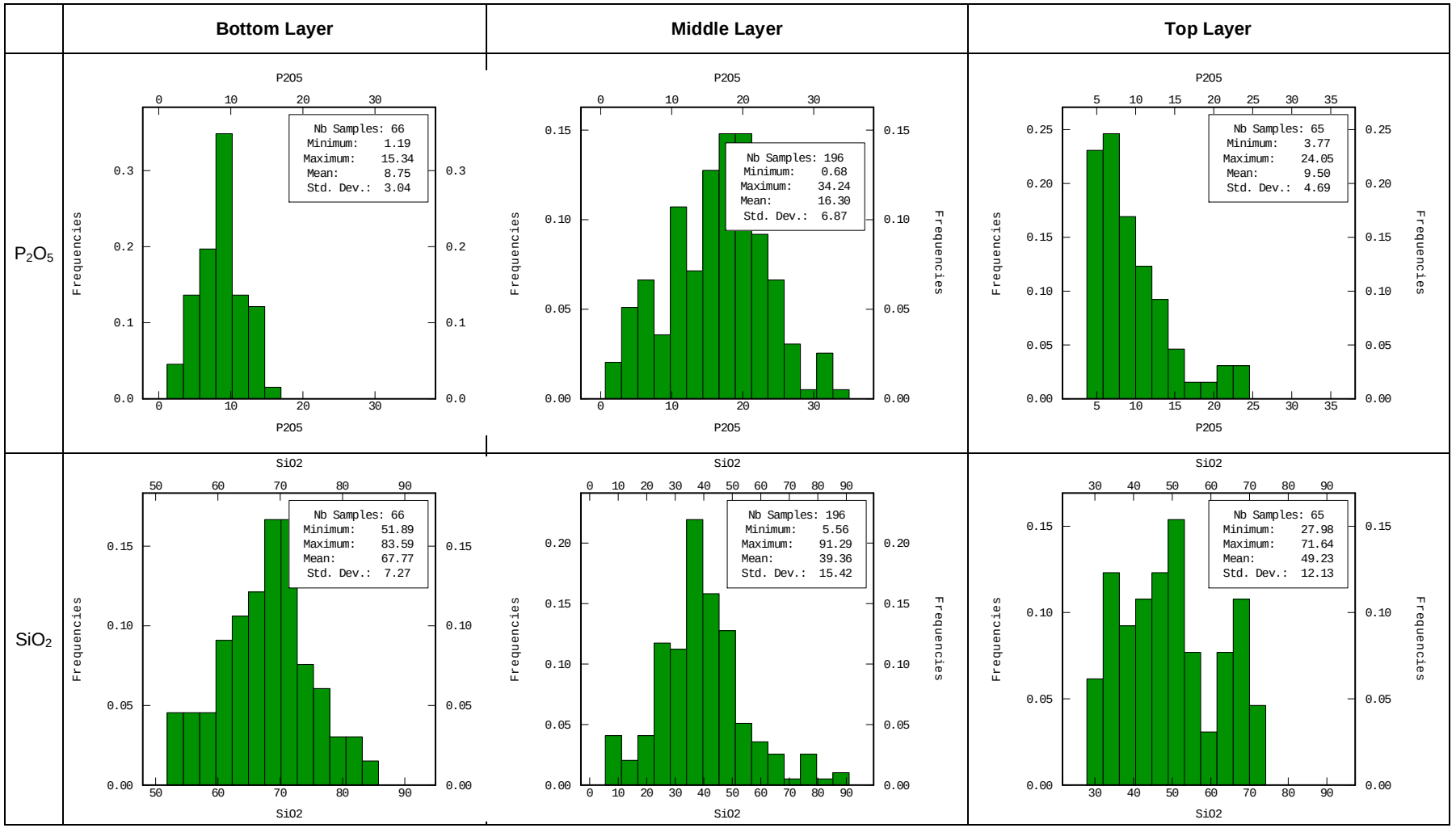


Figure 3.4.1_1: Histograms for the layers in the South Geo-Zone.

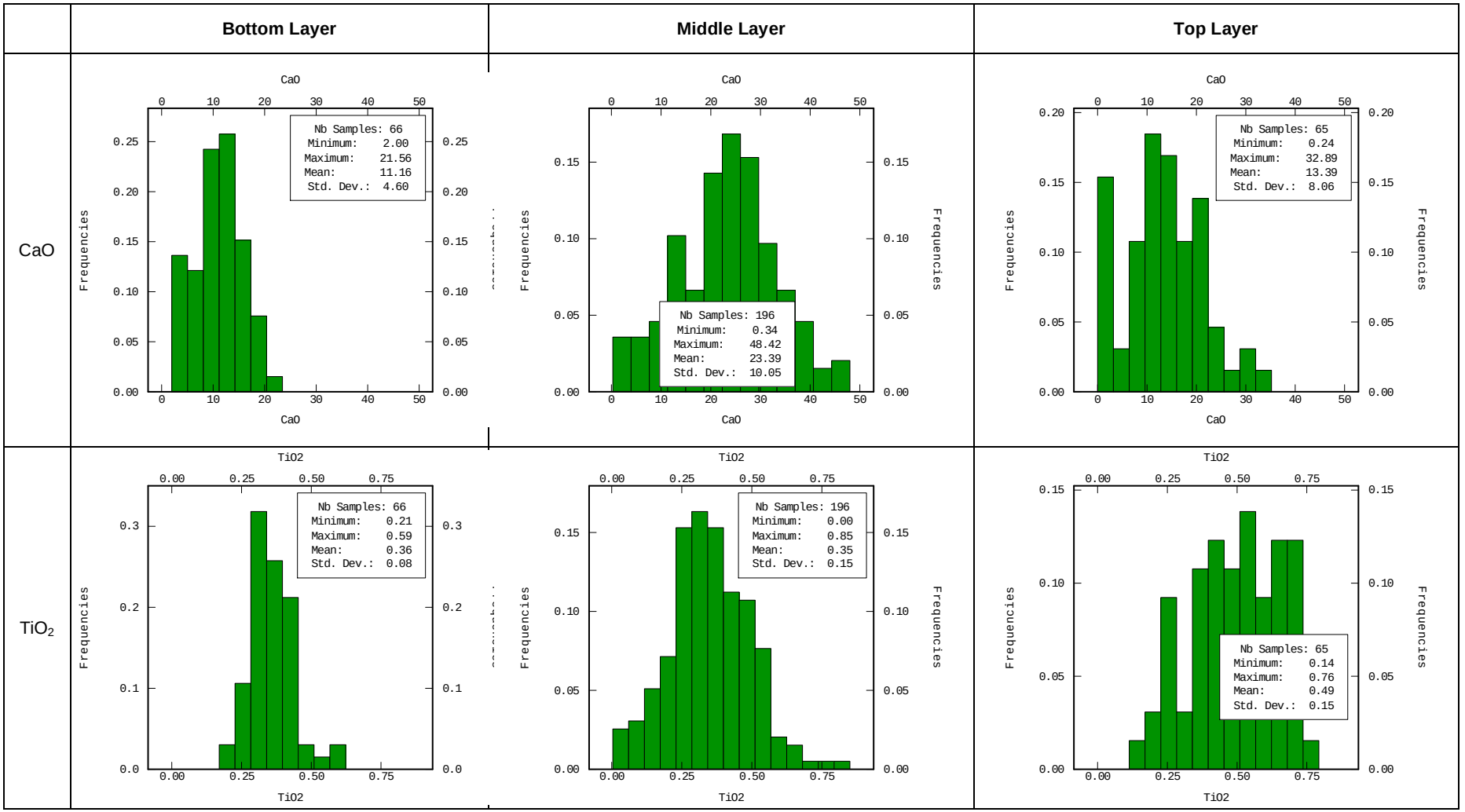


Figure 3.4.1_2: Histograms for the layers in the South Geo-Zone.

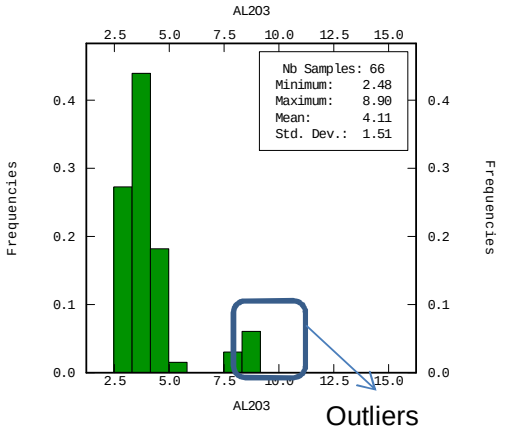
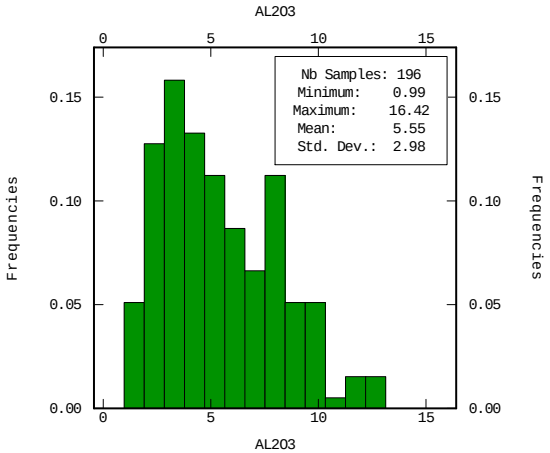
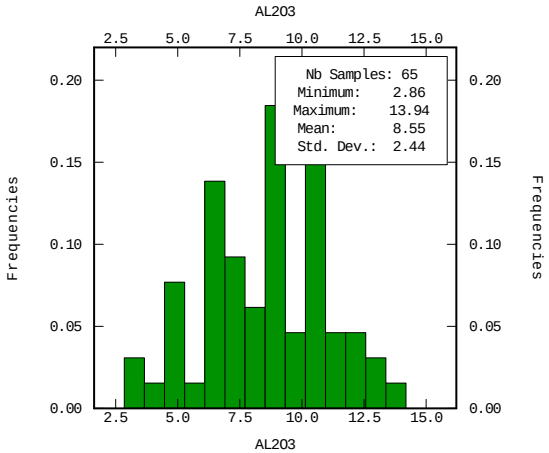
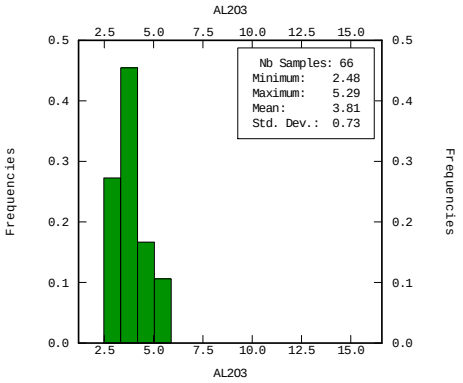
	Bottom Layer	Middle Layer	Top Layer
Al_2O_3	 Outliers		
Al_2O_3	Capped at 5.29% 		

Figure 3.4.1_3: Histograms for the layers in the South Geo-Zone.

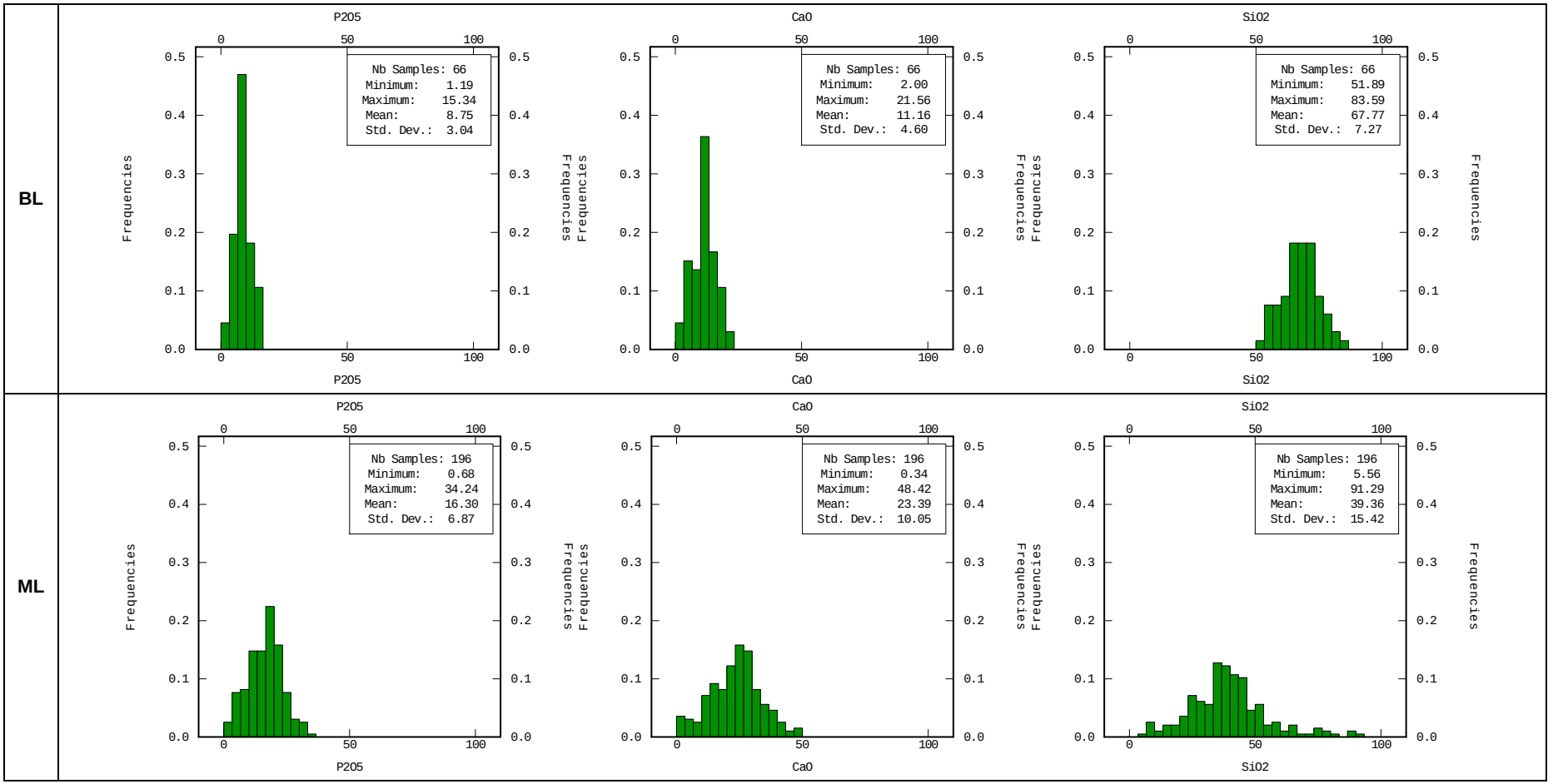


Figure 3.4.1_4: Histograms for three major variables drawn in the same scale: BL and ML.

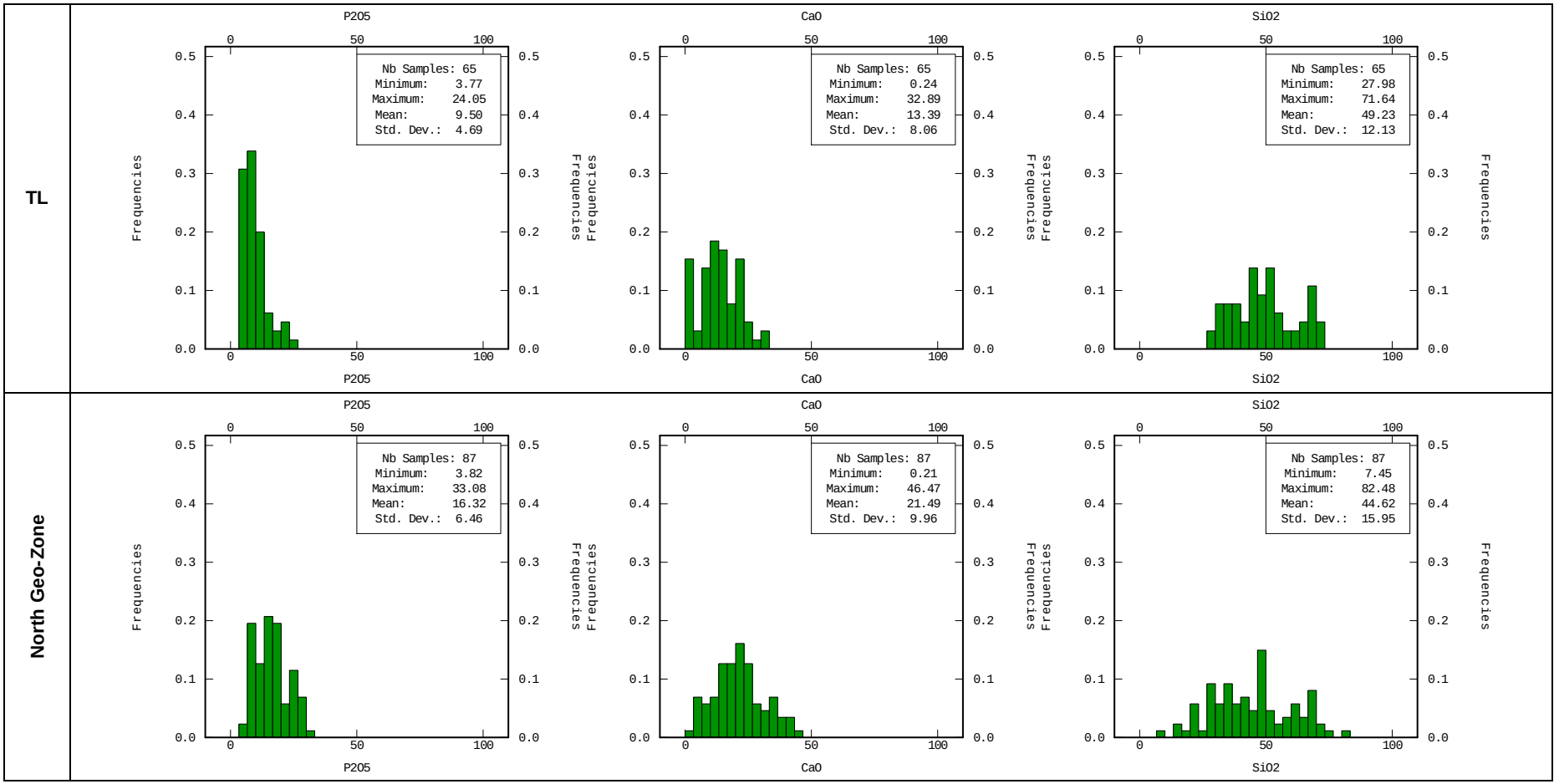


Figure 3.4.1_5: Histograms for three major variables drawn in the same scale: TL and North Geo-Zone.

3.4.4 North Geo-Zone

A total of 87 samples were taken in the North Geo-Zone. The histograms of different oxides show that North Geo-Zone is a single population domain (Figures 3.4.3_5 and 3.4.4_1).

P_2O_5

The P_2O_5 has a mean of 16.32% and standard deviation of 6.46%. The mean, median and mode are almost equal. The skewness is 0.32. The CoV is 0.40. The distribution is a normal distribution. The probability plot in Figure D_12 confirms that the North Geo-Zone has a normal distribution.

SiO_2

The distribution of SiO_2 is normal with a mean of 44.62 and standard deviation of 15.95%. The CoV is 0.36. The mean and median are almost equal. The wide range of 75.03% is due to minor internal waste in places.

TiO_2

The frequency distribution of the TiO_2 is normal with a mean, median and mode of 0.35%, 0.35% and 0.32%. More data is required to properly define the distribution. The wide range and a high standard deviation of 0.14% mean that the variability is high.

CaO

CaO has normal distribution with a mean of 21.49% and standard deviation of 9.96%. The mean and median are almost equal. The skewness is 0.24 and the CoV is 0.47. There are no outliers identified.

Al_2O_3

The Al_2O_3 has a mean of 5.26% and median of 4.77%. The standard deviation is 2.24%. The distribution of Al_2O_3 is positively skewed with skewness of 0.88 and CoV of 0.43. The high Al_2O_3 is due to clay matrix. No capping is necessary as no significant outliers are identified.

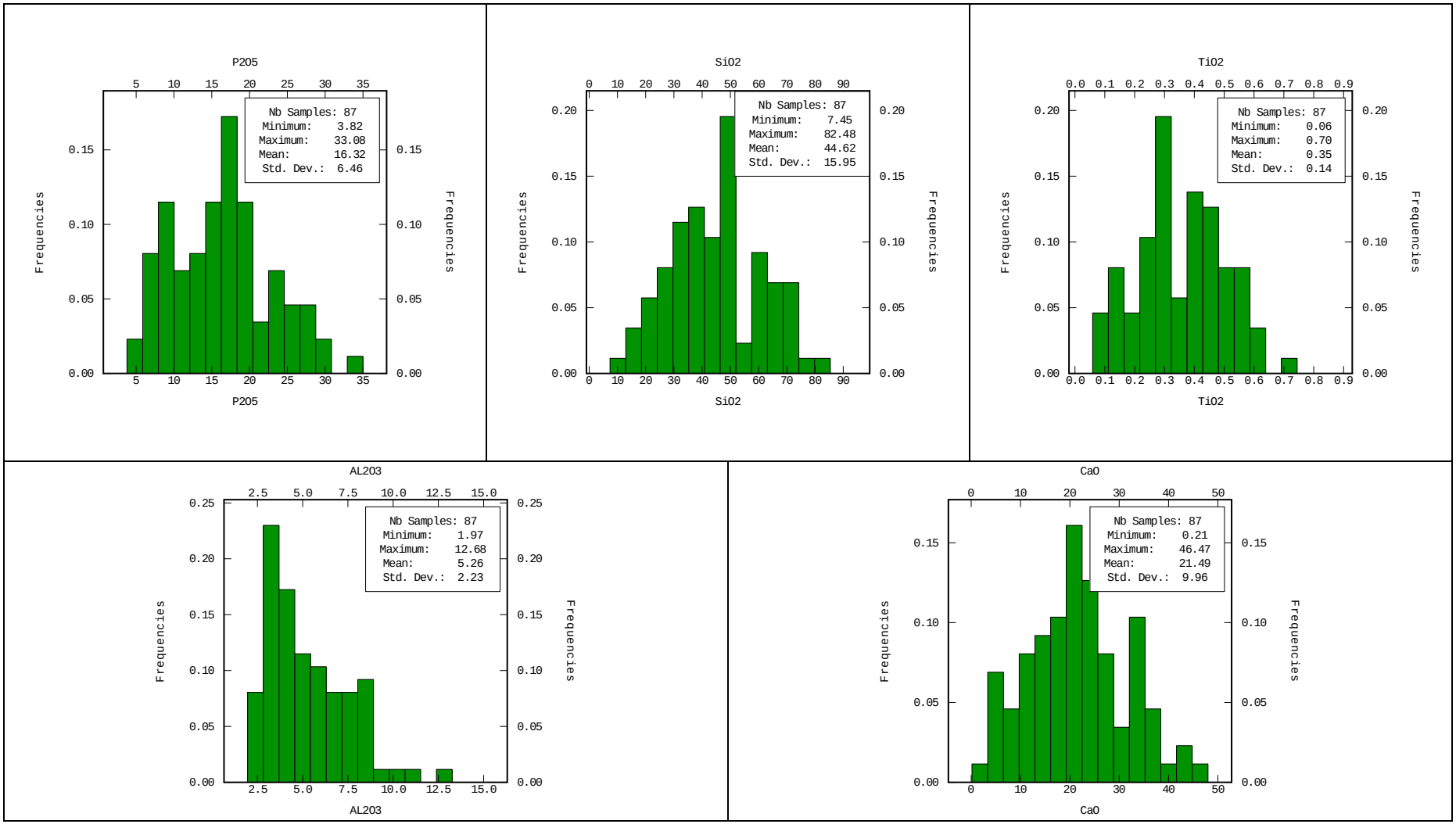


Figure 3.4.4_1: Histograms for North Geo-Zone.

3.5 Correlation Matrix

The correlation matrix (CM) refers to the matrix of the correlation all pairs of the datasets. The CM helps in understanding the nature of the mineralization. Figure 3.5_1 to 3.5_4 shows the CM of different variables. The CM can be used to confirm different domains by studying the relationships between elements in the domains. It can be further used to validate the Resource Models as the model and the data used for estimation should produce identical CM. Understanding of geochemistry is enhanced by studying CM.

The P_2O_5 versus others

The strong relationships between P_2O_5 & CaO and P_2O_5 & SiO_2 have been identified in both domains. The BL, ML, TL and North Geo-Zone have P_2O_5 versus CaO of 73%, 87%, 73% and 94% respectively. The ML and North Geo-Zone have higher P_2O_5/CaO correlation. This shows that the clays are minimal and P_2O_5 grades are higher in the ML and North Geo-Zone. The TL and BL have more clays and less P_2O_5 mineralization.

The relationship between P_2O_5 and SiO_2 is very strong and is inversely proportional in both domains. The BL, ML and the North Geo-Zone have the highest correlation values of 89%, 72% and 89% respectively. The higher correlations mean apatite phosphate mineralization without major contamination. The TL has the lowest correlation. This may be attributed to inclusion of the top recent silica sands.

The P_2O_5 and Al_2O_3 relationship for BL is non-existent as the correlation is 0%. For the ML and TL, the correlation factors are negative; -55% and -65% respectively. The North Geo-Zone has a weak negative correlation of 42%. The BL has no correlation because of the presence of high clay content.

The P_2O_5 versus TiO_2 shows significant information wherein the BL has a weak negative correlation of 13% and a ML has a negative correlation of 71%. The TL and North Geo-Zone have similar negative correlation of 66%.

A weak relationship between P_2O_5 versus Fe_2O_3 is seen on both the domains. The Fe_2O_3 is very low and it is towards the low detection limit. This further shows that the origin of phosphate is from the apatite.

SiO_2 and CaO

The SiO_2 and CaO have strong negative correlation of more than 80% in all the domains. This is anticipated for the phosphorite geochemistry. The relationship is identical to that of SiO_2 and P_2O_5.

Fe_2O_3 and Al_2O_3

All but the BL have a strong Fe_2O_3 and Al_2O_3 correlation of more than 80%. The BL has lowest Al_2O_3. This layer has less content of alumina minerals.

Table 3.5_1: Correlation Statistics – South Geo-Zone

Bottom Layer													
Element	Fe_2O_3	MnO	Cr_2O_3	V_2O_5	TiO_2	CaO	K_2O	P_2O_5	SiO_2	AL_2O_3	MgO	Na_2O	LOI
Fe_2O_3	100%												
MnO	19%	100%											
Cr_2O_3	26%	-38%	100%										
V_2O_5	54%	4%	22%	100%									
TiO_2	54%	61%	-3%	33%	100%								
CaO	19%	-27%	9%	23%	-27%	100%							
K2O	1%	-68%	29%	10%	-28%	14%	100%						
P_2O_5	6%	23%	-25%	7%	-13%	73%	-45%	100%					
SiO_2	-27%	-11%	8%	-26%	5%	-83%	24%	-89%	100%				
AL_2O_3	1%	62%	-32%	-15%	40%	-62%	-60%	0%	11%	100%			
MgO	23%	-14%	22%	26%	14%	10%	33%	-24%	-17%	-11%	100%		
Na_2O	14%	-30%	17%	1%	-25%	13%	28%	-6%	2%	-24%	5%	100%	
LOI	24%	47%	-11%	16%	37%	-15%	-47%	16%	-34%	64%	55%	-18%	100%

Table 3.5_2: Correlation Statistics – South Geo-Zone

Middle Layer													
Element	Fe_2O_3	MnO	Cr_2O_3	V_2O_5	TiO_2	CaO	K_2O	P_2O_5	SiO_2	AL_2O_3	MgO	Na_2O	LOI
Fe_2O_3	100%												
MnO	25%	100%											
Cr_2O_3	19%	-4%	100%										
V_2O_5	53%	20%	16%	100%									
TiO_2	76%	22%	12%	49%	100%								
CaO	-46%	-24%	-13%	-26%	-82%	100%							
K2O	58%	-2%	14%	52%	66%	-43%	100%						
P_2O_5	-38%	-9%	-15%	-32%	-71%	90%	-54%	100%					
SiO_2	11%	25%	5%	8%	57%	-87%	17%	-72%	100%				
AL_2O_3	87%	13%	16%	42%	89%	-67%	62%	-55%	29%	100%			
MgO	19%	-24%	10%	23%	10%	-7%	39%	-44%	-26%	21%	100%		
Na_2O	-23%	-31%	8%	-20%	-51%	60%	-16%	48%	-56%	-37%	9%	100%	
LOI	30%	-17%	15%	23%	14%	-6%	33%	-36%	-35%	32%	90%	5%	100%

Table 3.5_3: Correlation Statistics – South Geo-Zone

Top Layer													
Element	Fe_2O_3	MnO	Cr_2O_3	V_2O_5	TiO_2	CaO	K_2O	P_2O_5	SiO_2	AL_2O_3	MgO	Na_2O	LOI
Fe_2O_3	100%												
MnO	39%	100%											
Cr_2O_3	46%	9%	100%										
V_2O_5	72%	29%	50%	100%									
TiO_2	89%	44%	39%	76%	100%								
CaO	-64%	-52%	-23%	-37%	-72%	100%							
K2O	19%	-24%	30%	51%	35%	1%	100%						
P_2O_5	-52%	-19%	-30%	-52%	-66%	73%	-48%	100%					
SiO_2	36%	51%	3%	12%	46%	-89%	-20%	-46%	100%				
AL_2O_3	91%	38%	49%	65%	92%	-76%	30%	-65%	48%	100%			
MgO	-6%	-39%	13%	22%	-4%	33%	49%	-36%	-61%	-8%	100%		
Na_2O	-14%	-23%	40%	-5%	-22%	34%	7%	26%	-33%	-17%	9%	100%	
LOI	4%	-29%	17%	18%	4%	19%	39%	-39%	-55%	3%	84%	4%	100%

Table 3.5_4: Correlation Statistics – North Geo-Zone

North Geo-Zone													
Element	Fe_2O_3	MnO	Cr_2O_3	V_2O_5	TiO_2	CaO	K_2O	P_2O_5	SiO_2	AL_2O_3	MgO	Na_2O	LOI
Fe_2O_3	100%												
MnO	39%	100%											
Cr_2O_3	8%	24%	100%										
V_2O_5	25%	1%	2%	100%									
TiO_2	51%	30%	19%	18%	100%								
CaO	-23%	-42%	-34%	14%	-72%	100%							
K2O	33%	-19%	17%	32%	42%	-28%	100%						
P_2O_5	-12%	-28%	-28%	8%	-66%	94%	-45%	100%					
SiO_2	-10%	31%	28%	-19%	51%	-92%	13%	-88%	100%				
AL_2O_3	80%	36%	20%	12%	77%	-54%	42%	-42%	19%	100%			
MgO	18%	-11%	-8%	12%	14%	-1%	50%	-27%	-17%	25%	100%		
Na_2O	-19%	-18%	37%	-16%	-53%	45%	-10%	40%	-39%	-32%	-4%	100%	
LOI	44%	1%	3%	4%	21%	1%	40%	-9%	-34%	50%	68%	2%	100%

3.6 Scatter Plots and Estimation Strategies

Scatter plots are mathematical graphs that display the relationship between two variables. Mathematical formulae that describe the relationships are deduced. A line that best fit the correlation between two variables can be drawn. Correlation can also be inferred visually. The scatter plots are used to guide the estimation strategies as there are many variables to evaluate. Four major variables (P_2O_5, CaO, Al_2O_3 and SiO_2) are studied.

BL

There are some form of relationships between P_2O_5, CaO, Al_2O_3 and SiO_2. All variables are related. The scatter plots show the strong linear relationship between P_2O_5, CaO, and SiO_2. CaO and Al_2O_3 have strong relationship. Al_2O_3, P_2O_5 and SiO_2 have a relationship that is not well defined in terms of mathematics.

A strong linear relationship between P_2O_5, CaO, and SiO_2 is used in making a decision on estimation criteria. Only P_2O_5 should be estimated for BL. The results of the estimation will be used to produce CaO and SiO_2 estimates based on the linear regression with P_2O_5. To estimate Al_2O_3, the CaO results will be used as there is a strong correlation between CaO and Al_2O_3.

ML

A strong linear correlation is seen between P_2O_5 versus CaO and CaO versus SiO_2. There are also well defined correlations between P_2O_5 versus SiO_2, P_2O_5 versus Al_2O_3, Al_2O_3 versus SiO_2 and Al_2O_3 versus CaO.

Only P_2O_5 will be estimated and other variables will be calculated based on the relationship with P_2O_5. The best relationship will be chosen first. For example P_2O_5 versus CaO will be calculated first, and then followed by SiO_2 versus CaO.

TL

All four major variables show some correlation. All variables have a strong linear correlation with CaO. A decision is taken to estimate P_2O_5, then use regression line to calculate CaO. The SiO_2 and Al_2O_3 will be calculated from CaO values.

North Geo-Zone

The scatter plots show the strong linear relationships between P_2O_5 versus SiO_2, P_2O_5 versus CaO, and SiO_2 versus CaO. There is a good relationship between Al_2O_3 and CaO.

For estimation purpose P_2O_5 will be used. The SiO_2 and CaO will be derived from P_2O_5 values. Al_2O_3 will be calculated from CaO values.

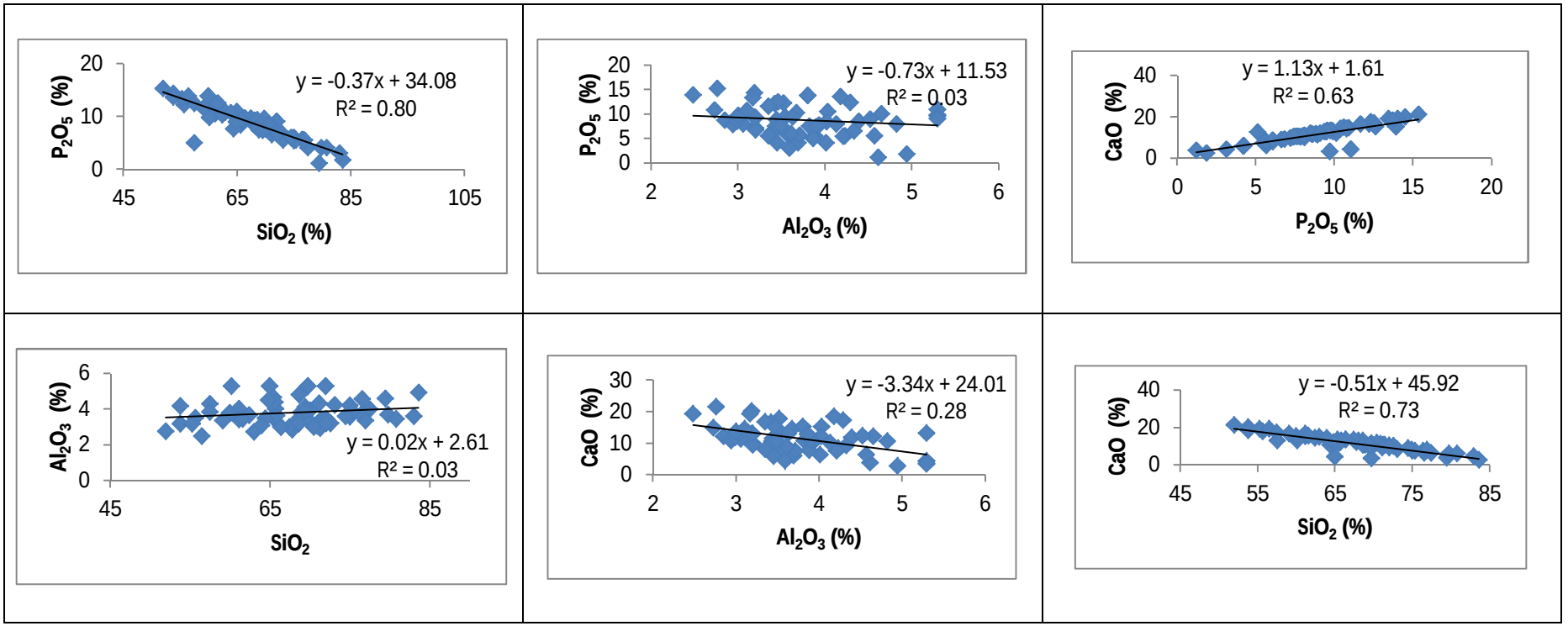


Figure 3.6_1: Scatter Plots for the Bottom Layer.

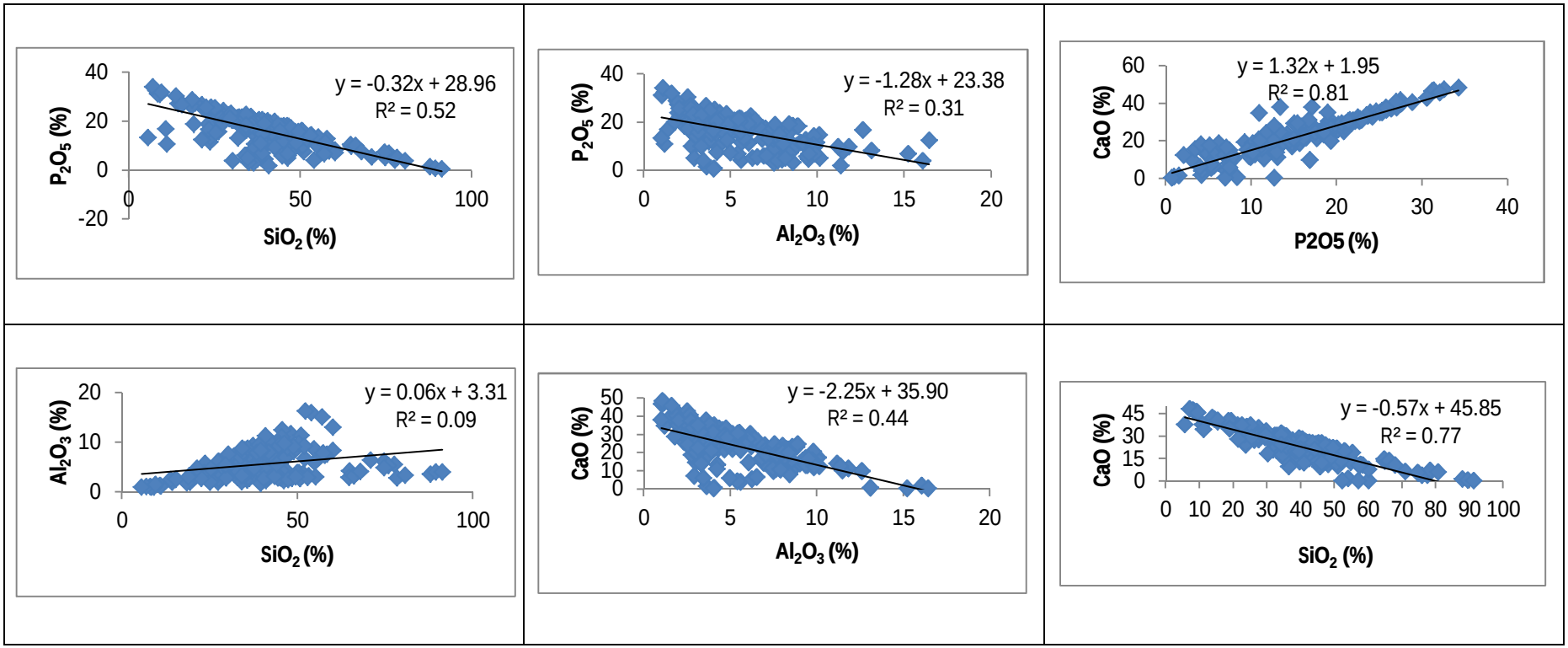


Figure 3.6_2: Scatter Plots for the Middle Layer.

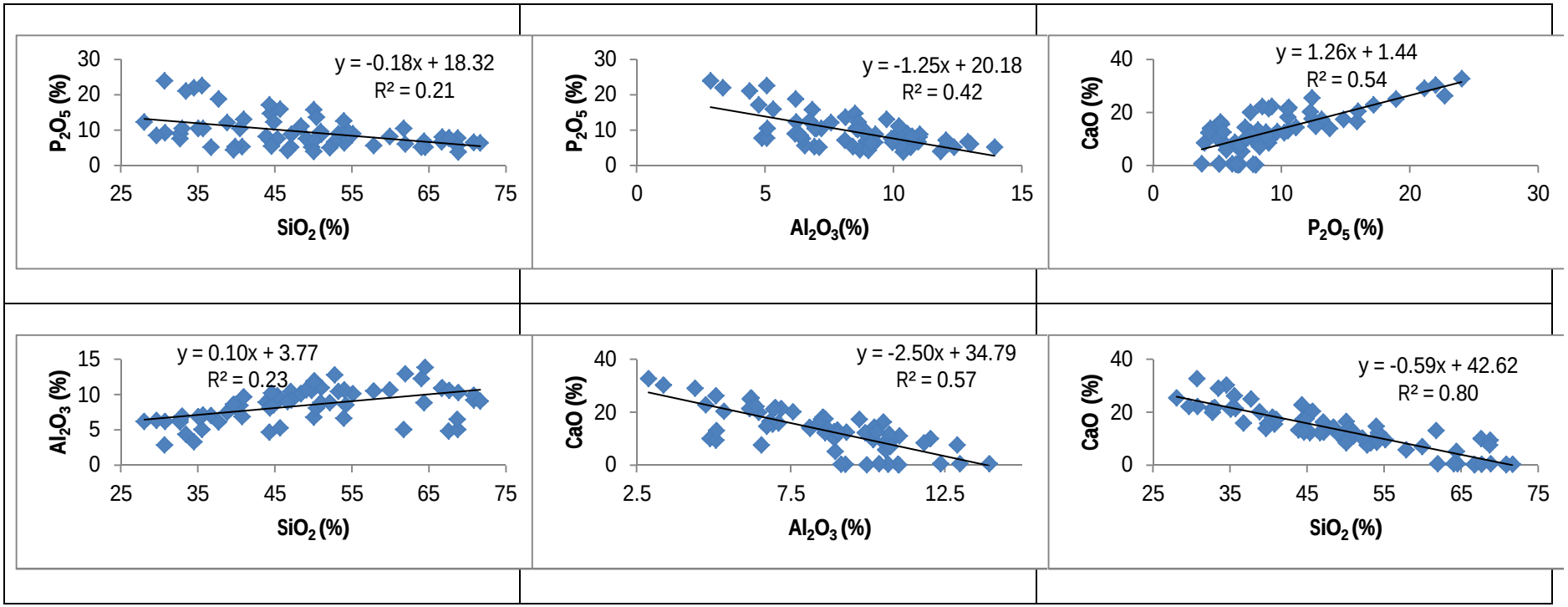


Figure 3.6_3: Scatter Plots for the Top Layer.

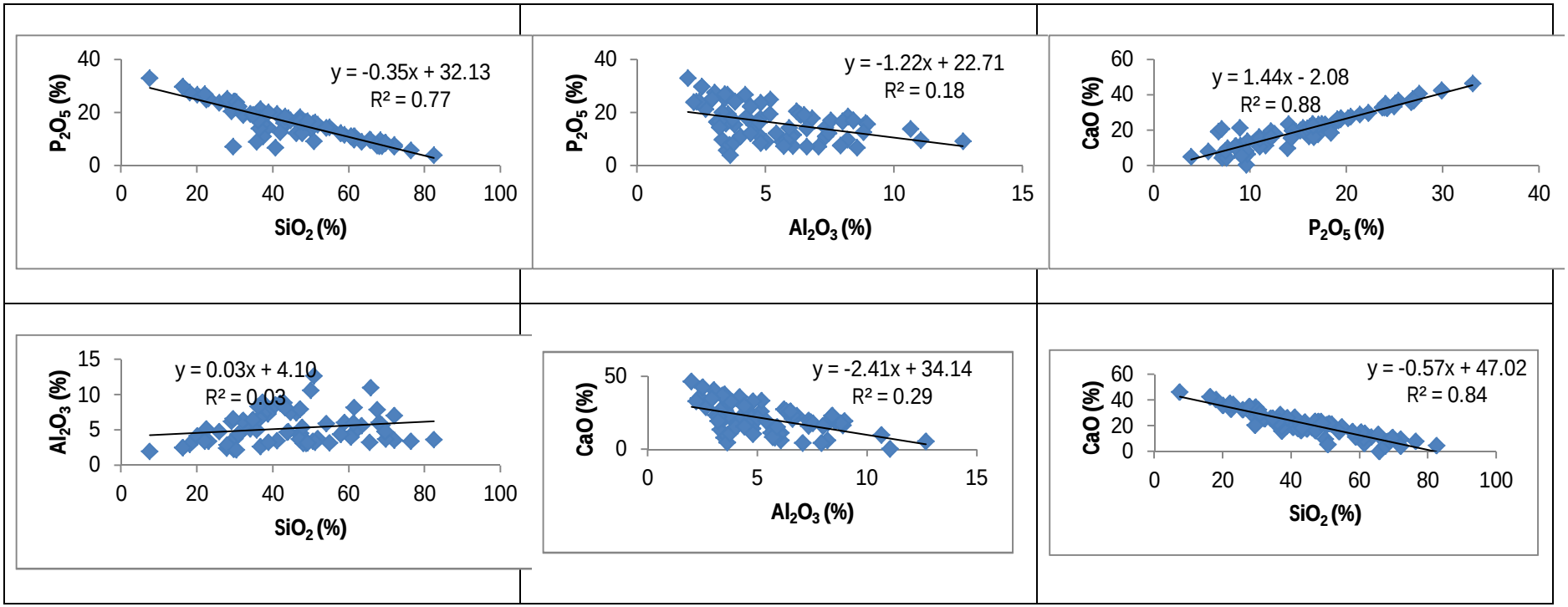


Figure 3.6_4: Scatter Plots for the North Geo-Zone.

3.7 Discussion on Density

Density measurements are critical to the estimation of the tonnage. At Kanzi, no bulk density measurements were taken. This is due to the drilling technique used. The Aircore drilling technique produced unconsolidated samples. Taking bulk density measurements on unconsolidated (sandy) samples introduce high uncertainty on tonnages due to voids. Only specific density could be taken in the laboratory and specific density is not suitable for tonnage estimation. The bulk density is needed for Mineral Resource Evaluation.

A phosphate sample shown in Figure 3.7_1 was recovered by the Aircore drilling technique at Kanzi. This sample shows that bulk density measurements could not be taken with confidence.

The neighbouring projects with the same geology (mineralization style) where diamond drilling took place were analysed (Body, 2013). The average bulk density measurement (1.9g/cm^3) from these neighbouring projects was used at Kanzi for all layers. A recommendation is made to drill diamond holes so that density could be determined at Kanzi.



Figure 3.7_1: A photo showing the blue bucket with a phosphate sample recovered by Aircore drilling technique. A yellow tag with sample identification number is also shown.

3.8 Principal Findings on Statistics

The following principle findings were made:

- Kanzi drillholes are well-spread and there is no need for declustering. Drilling was not biased to the high grades.
- Samples were taken at 1m intervals. All samples have equal weight in the statistics. The support is the same. There is no need for support correction.
- Minor contamination of the samples has been noted due to drilling technique used.
- Different populations identified in the geology section in Chapter 2 were confirmed by the statistical properties.
- Four major variables (P_2O_5, CaO, Al_2O_3, TiO_2 and SiO_2) were identified and explained per geo-zone. The distributions of the variables were studied in detail.
- Correlation matrices of the variables per domain were analysed and most of the variables have strong correlation with others
- Scatterplots revealed relationships between the variables. All major variables are somehow related.
- Because of its strong relationship with other major variables in all domains, P_2O_5 will be estimated and other block variables will be defined based on their relationships with P_2O_5.
- No outliers were identified on P_2O_5, thus no capping or top cutting will be implemented.

4 SPATIAL ANALYSIS (VARIOGRAPHY)

4.1 Introduction

The degree of spatial dependence of a variable is measured through a semi-variogram.

> *The semi-variogram is commonly referred to as variogram. In this project, the term variogram is used referring to a semi-variogram.*

The spatial variability of the variables separated by a distance h is defined as

$$E\{[Z(x+h) - Z^*(x)]^2\}$$

The variability is caused by number of factors:

- Measurement and sampling error,
- Petrographic factors such as changes in mineralogy,
- Variability due to alternation of the mineralised layer with the waste,
- Medium to large scale geological features

In Statistics, spatial variation is described by the semi-variogram,

$$\gamma(h) = \frac{1}{2N(h)} \sum_{(i;j)|h_{ij} \approx h} (v_i - v_j)^2$$

The variogram describes the spatial continuity of a dataset. This is done by averaging one half the difference of the square of a variable over all pairs of observation in a specified direction and separation distance (Barnes, 2013; Clark, 2000; Isaaks & Srivastava, 1989; Armstrong, 1998; Rendu, 1978; Goovaerts, 1997). A variogram is always positive since it is the expectation of a square. Variogram models are essential in geostatistical evaluation of mineral resources because they are typically used in:

- Kriging estimation
- Inverse distance estimation (ranges used for search volumes)
- Mineral resource classification
- Drilling space recommendations
- Block size selection and
- Conditional simulation.

It is critically important that variogram reflects the underlying mineralisation continuity. Therefore geological knowledge should guide and confirm the mathematical interpretation of variogram. The variogram on the other hand may increase the geological knowledge of

the mineralization by showing different structures and ranges which relate to the underlying geology.

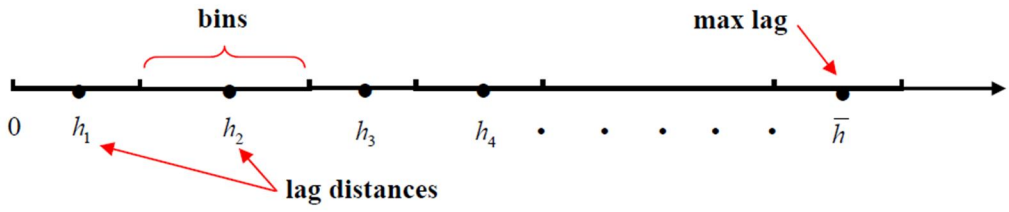
Variograms can also be used to describe the relationship between variables (Isaaks & Srivastava, 1989). This can be done through cross-variograms. The theory and application of cross-variogram will not be discussed in this study as cross-variograms were not used.

4.2 Variogram Theoretical Reviews

A variogram is a quantitative descriptive statistic that characterizes the autocorrelation or spatial continuity of a data set. Anisotropic and isotropic behaviour of the sample values is studied through variograms.

Non-directional variograms average the behaviours in all directions and do not imply that the spatial continuity or variability is the same in all directions (Isaaks & Srivastava, 1989; Journel & Huijbregts, 1978). With non-directional variograms the separation vector, $h_{ij,}$ is large enough such that directional tolerance becomes insignificant. Non-directional variograms help in understanding overall spatial continuity. The directional variograms are used to assess the spatial relationship in a defined direction. Figures 4.2_1 and 4.2_2 show how the experimental variograms are calculated.

Directional variograms depend on orientation and angle-dip and azimuth. Parameters used to calculate variograms including lag spacing, lag tolerance, lag numbers, azimuth definition, angle and angular tolerance (Coombes, 1997; Isaaks & Srivastava, 1989; Clark, 2000).



This figure was taken from (Penn, 2013)

Figure 4.2_1: Demonstration of lag distances.

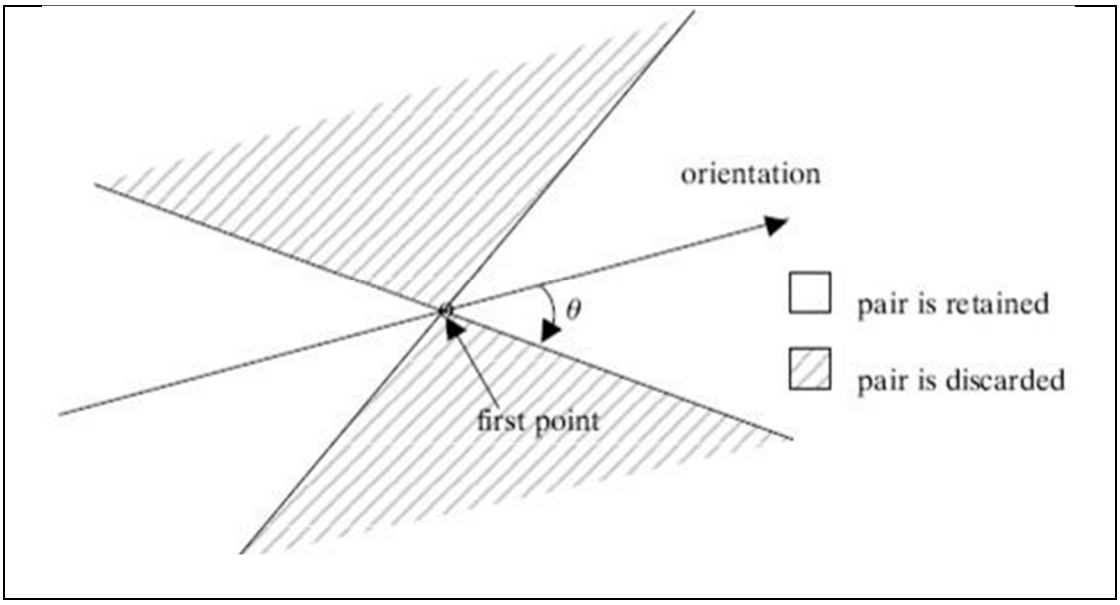


Figure 4.2_2: Demonstration of experimental variogram calculations. This figure was taken from (Deraisme, et al., 2004).

Variogram Modelling Theoretical Review

It is necessary to model the experimental variogram so that proper mathematical definition of spatial continuity can be described in the estimation. Bypassing this crucial step can lead to geostatistical disaster as kriging requires accurate numerical values for not just the distance between the points but also the data between the point and target grid nodes (Deraisme, et al., 2004).

The experimental variogram is fitted using a linear combination of basic functions that have different behaviours in the different directions of a space, to reproduce the anisotropic behaviour of the data. The fitting technique is usually manual and is a trial-and-error method until the right model is produced (Coombes, 1994).

The Spherical and Exponential variogram models (Appendix C) are mostly used in geostatistics according to Clark, 2000; Rendu, 1978; Journel & Huijbregts, 1978 and Isaaks & Srivastava, 1989). When the spatial relationship ceases to exist between variables, the average variance becomes equal to the population variance. This average variance is defined as a sill. The models are divided in terms of:

- Models with a sill or transition models
- Models without sill

Apart from the models described above, the hole-effect models and pure nugget effect do occur. The hole-effect appears on models with or without sills (Journel & Huijbregts, 1978). The hole-effect occurs when the growth of the sill is not monotonic but sinuous. A pure nugget effect indicates absence of spatial correlation and could be corresponding to measurement error, microstructures at a scale smaller than sampling interval or uniform variability in the deposit.

The sill from the non-directional variogram represents the total variance of the samples and can be used in modelling the total variance of the directional variograms. Theoretically total variance modelled from the directional variogram should be less or equal to total population variance (Clark, 2000; Coombes, 1997; Isaaks & Srivastava, 1989; Deraisme, et al., 2004; Journel & Huijbregts, 1978). This is true for a perfectly stationary population –which rarely exist in the real mining world. In reality the total variance of the experimental variograms can be more, less or equal to the sill over the ranges of interest.

Anisotropies

It is crucially important to study the spatial continuity in different direction so that regionalised variables in 2 or 3D can be defined. Two types of anisotropies that are well known are:

Geometric Anisotropy

This happens when the semi-variogram's range is a function of direction. Regionalised variables are not always isotropic. Some directions have greater continuity than others. A simple linear transformation is needed to restore isotropy (Clark, 2000; Isaaks & Srivastava, 1989; Deraisme, et al., 2004; Coombes, 1994; Olea, 1999).

Zonal Anisotropy

This is caused by the influence of mineral bedding or layering. Different layers will exhibit different spatial continuity. Different sills can also be calculated for different layers or beds (Coombes, 1994; Clark, 2000; Rendu, 1978).

When dealing with anisotropy cases, the following two are noticed in terms of the sill according to Rendu (1978) and Isaaks and Srivastava (1989):

- The range changes with directions but the sill remains the same; and
- Sill is lower in some directions.

Effects of Skewness in the Dataset

Most of mineral deposits are not defined by symmetrical distributions but by skewed distributions. To better define the spatial continuity, transformation of variables (to log-normalized or normalized variables) is important otherwise variogram will present proportional effects (Rendu, 1978; Coombes, 1994).

Range and Structures

Spatial autocorrelation between the variables varies with the distance and/or direction. As distance between data points increases the spatial relationship reduces. Beyond a certain range there is no longer spatial correlation and it is said that the total sill is reached. When a total sill is reached, variables loose the spatial relationship and the variability is constant.

There are number of variogram types; in the minerals industry the most used are traditional, normal score, indicator, lognormal and pairwise variograms. The correlogram and covariogram are also used to analyse continuity for symmetrical and negatively skewed distributions (Isaaks & Srivastava, 1989; Rendu, 1978) (see Appendix C for definitions).

Nugget Effect

A nugget effect appears on a variogram as discontinuity at the origin (Clark, 2000; Isaaks & Srivastava, 1989; Journel & Huijbregts, 1978; David, 1977; Verly, et al., 1984).

Nugget effect includes random errors incurred during sampling and geological variability of the deposit on a small scale (Journel & Huijbregts, 1978). The best way of estimating nugget effect is by analysing the down-hole contiguous samples' variability as the data points are closer enough to enable study of variability at shortest range.

The ratio of the nugget effect to the sill is critical in understanding the spatial variability. (Webster & Oliver, 2007). A higher nugget effect causes smoother kriging models. A high nugget effect may result in a low confidence in the local estimates due to inherent coarseness or randomness of mineralisation, poor sampling practices or insufficient data. The texture of conditional simulation models becomes more variable as nugget effect increases.

Variogram Maps

The variogram maps (varmaps) are used to analyse the spatial continuity in different directions. The varmaps are mostly drawn in 2D space to analyse the possible anisotropies in a plane. Experimental variograms are analysed for multiple direction and specific directions can be picked and displayed for further analysis. The varmaps are mostly displayed using the fan representation.

4.3 Application of Variograms to Kanzi Phosphate Project

4.3.1 Varmaps

The varmaps for different geo-zones are presented in Figure 4.5.2_1. The varmaps do not show clear definitions of anisotropy. The TL and North Geo-Zone varmaps show some anisotropy but further analysis shows that the direction of highest continuity is just the direction of drillhole positions and short range has virtually few drillholes. Anisotropy is due to the data configuration. When analysing the varmap, the orientation of the data points is crucial as the interpretation of the spatial continuity might be affected by the layout of the drillholes position.

The varmaps of the geo-zones show that there is no significant anisotropy and the variogram models should be isotropic. The isotropic nature of the variograms is supported by consistent geology in all directions.

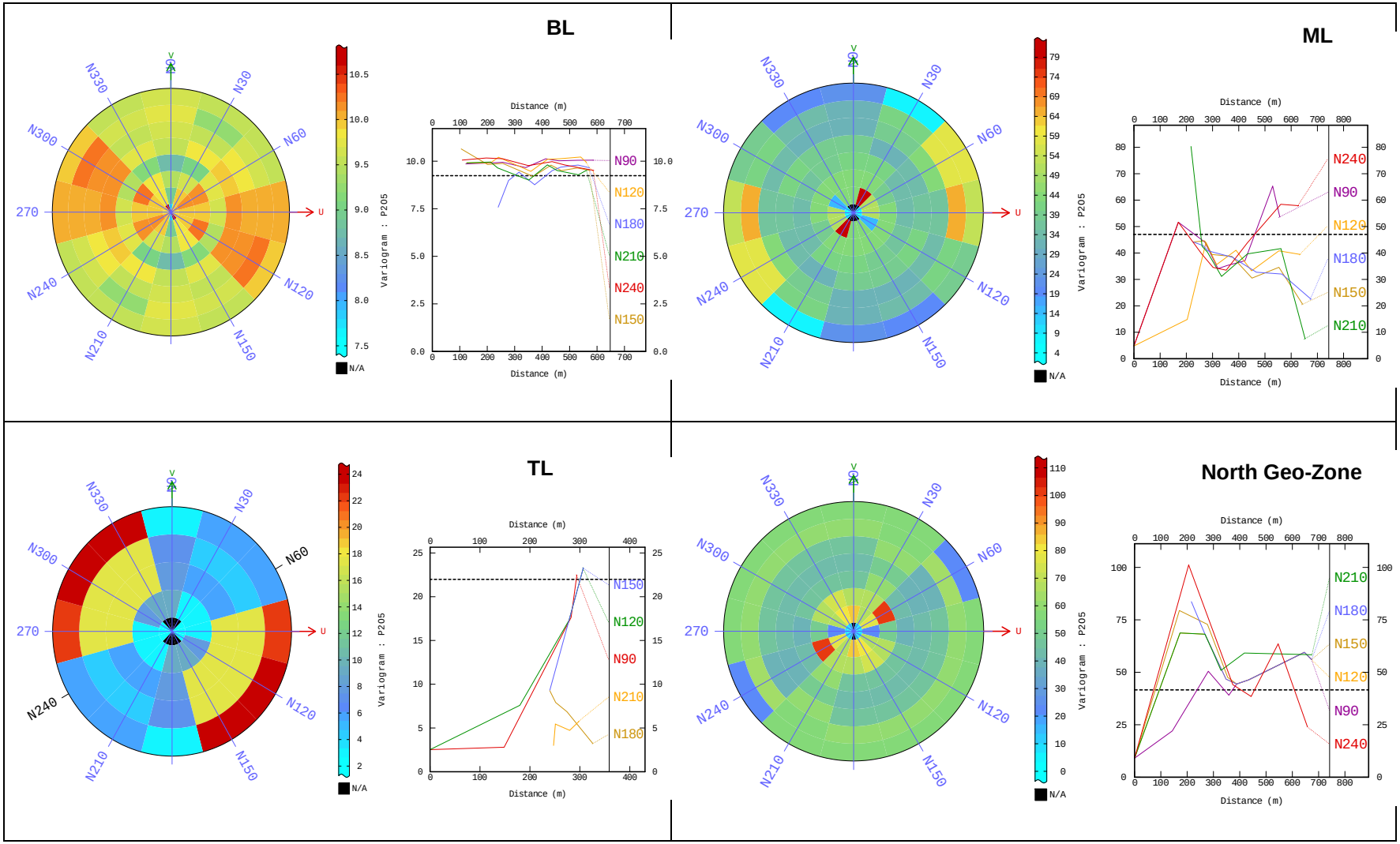


Figure 4.5.2_1: Variogram maps and experimental variograms for different domains.

4.3.2 Nugget Effect Analysis

The downhole variograms for different geo-zones are presented in Figure 4.5.3_1. These variograms are used in determining the nugget effects for the variogram models. The variograms are based on the downhole samples. The pairs on the variograms are used to guide the modeling of nugget effect. The first lag has the highest number of pairs and pairs decrease with the increase of lag distance.

BL

The downhole variogram shows a nugget effect of 5% P2O5. The nugget to sill ratio is 5.6%. The nugget effect is low showing that there is high continuity at a small scale. A phosphate deposit is mined in bulk and this low nugget effect is desirable. It implies that the P_2O_5 grades are easily predictable. The experimental variogram plots above the sill show that there may be more than one sedimentary unit. The variogram reaches the sill at about 4m. The average thickness of this layer is 4.2m. This shows that there is good continuity vertically.

ML

The ML has a nugget effect of 20% P_2O_5 and a nugget to sill ratio is 33.3%. There are many samples pairs for the first four lags; this gives confidence on the definition of nugget effect. This nugget is still very low and good for bulk mining. This layer has an average thickness of 6.4m and reaches the sill at 2m. At about 4m, the variogram shows that there may be extra sedimentary unit. This means that there is a population with multiple components that are spatially integrated.

TL

The nugget effect defined from the downhole variogram is 4% P_2O_5 and a nugget to sill ratio of 19%. The overall slope of the variogram is not steep. This layer has low nugget. The variogram reaches the sill at 3m. This is a high range as the average thickness of this layer is 4.6m and some holes have more than one sedimentary cycle.

North Geo-Zone

The North Geo-Zone has a low nugget effect of 4 % and a nugget to sill ratio of 9.7%. This layer has an average thickness of 6.5. The variogram reaches the sill at 2m. The slope is steep and this means there is low continuity at short range which might mean that the domain is uniform vertically at larger scale.

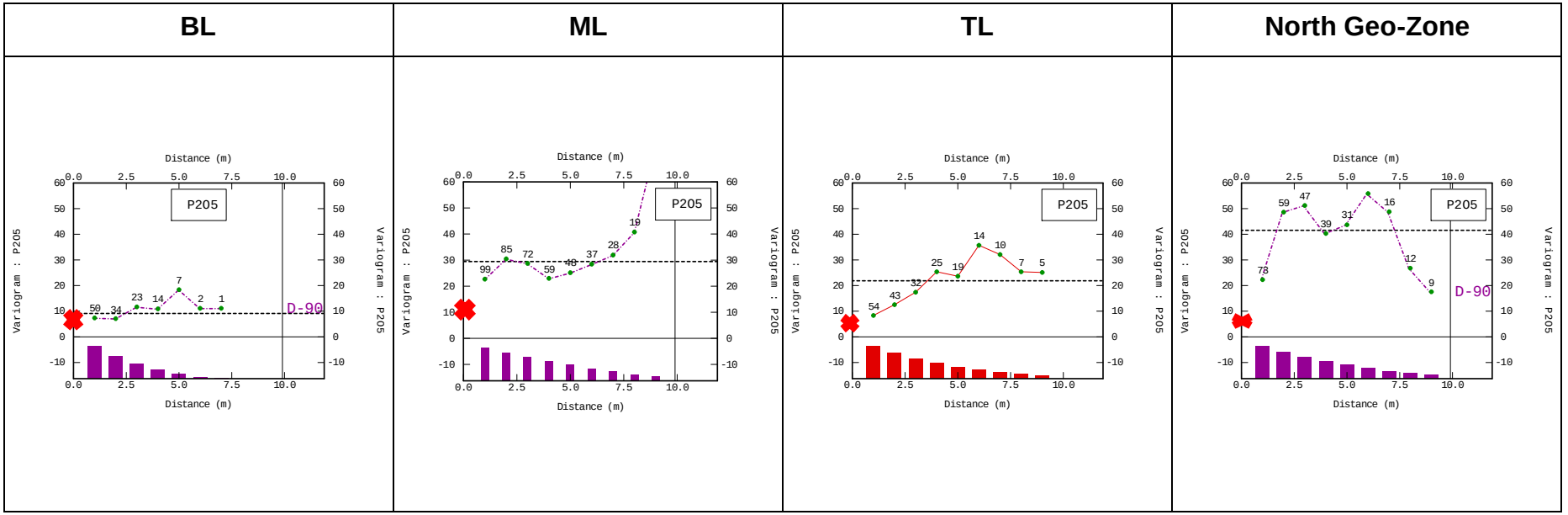


Figure 4.3.2_1: Downhole Variograms for different geo-zones using same scale. The modelled nugget effect is represented by a red star.

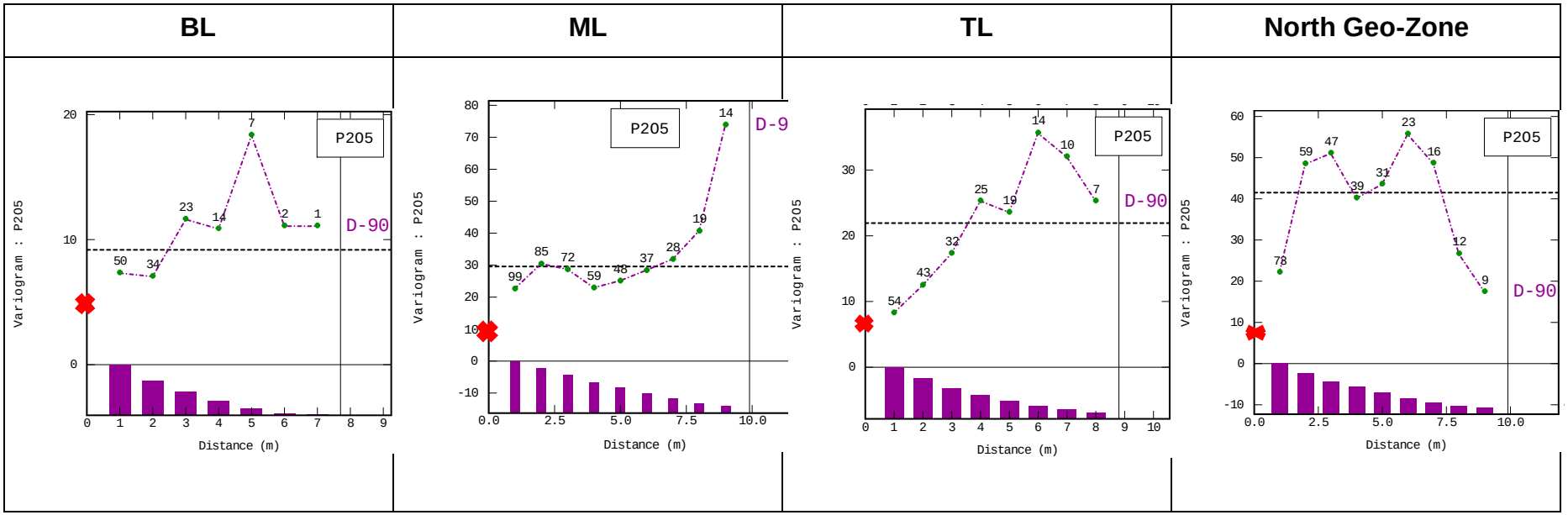


Figure 4.3.2_2: Detailed Downhole Variograms for different geo-zones. The modelled nugget effect is represented by a red star.

4.3.3 Variogram Models

Variogram models with modelled parameters for different domains are presented on Table 4.3.3_1 and Figure 4.3.3_1. The traditional variograms were calculated and modelled. The variogram models were not normalised. The models show that isotropic variograms can be used as the directional variograms are identical and because the geology is uniform over the scale of estimation. All the structures defined are spherical. The indicator variograms will be calculated in the non-linear section of this project.

Table 4.3.3_1: Traditional Variogram Model Parameters

Domain	Nugget	C1 Range (m)	C1 Sill	C1 Model type	C2 Range (m)	C2 Sill	C2 Model type
North Geo-Zone	4	430	42	Spherical	-	-	-
BL	5	350	9	Spherical	-	-	-
ML	10	250	17	Spherical	1000	10	Spherical
TL	4	500	23	Spherical	-	-	-

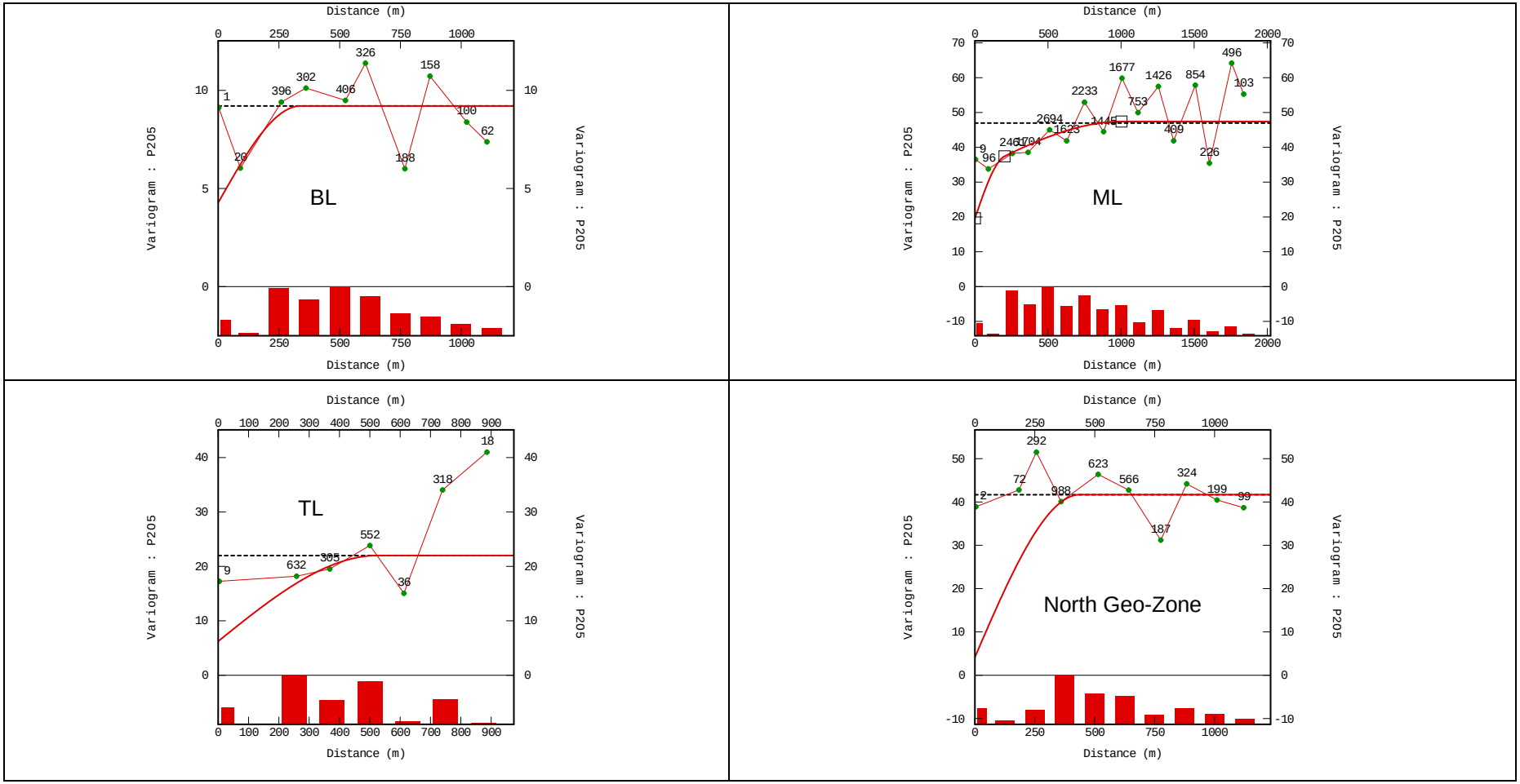


Figure 4.3.3_1: Traditional variogram models for P_2O_5.

5 MODEL CONSTRUCTION AND NEIGHBORHOOD PARAMETRES

5.1 Introduction

This chapter gives a brief summary on block model construction and parameters used in estimation.

5.2 Assumptions

The assumption made when constructing the block model is that the mineralization is continuous, homogeneous and isotropic within the defined zones. The drilling grid followed at the Kanzi Phosphate project is orientated in a south-west to north-east direction. The block model was rotated so that blocks are orthogonal to the drilling grid. This was done to minimize bias due to drillhole orientation.

5.3 Block Size Test work

A number of block sizes were tested. The sensitivity of block height was tested through the declustering technique. It was found that the mineralization is not sensitive to the height (Figure D_1). The 5m height was selected. This makes sense for mining purpose (the bench height can be designed in multiples of 5). A 3D model was rotated in Z direction at -18 degrees to be aligned with the drilling grid.

The block sizes tested were:

- 500mX x 500mY x 5mZ,
- 250mX x 250mY x 5mZ,
- 225mX x 225mY x 5mZ
- 200mX x 200mY x 5mZ
- 175mX x 175mY x 5mZ,
- 150mX x 150mY x 5mZ,
- 125mX x 125mY x 5mZ and
- 100mX x 100mY x 5mZ.

The kriging efficiency, slope of regression and discretization were determined (Figures D_2 to D_4) and used to determine “optimal” block size. The better results were from 100m to 150m block sizes in both X and Y directions. The 125mX x 125mY x 5mZ is selected. In relation to the nominal grid spacing, the 125mX x 125mY is half the drill spacing for Kanzi Phosphate Project.

The geological model shows that the mineralization is undulating. Sub-celling was allowed so that model volume could be filled accurately. A simplified plan view of the block model is presented in Figure 5.3_1.

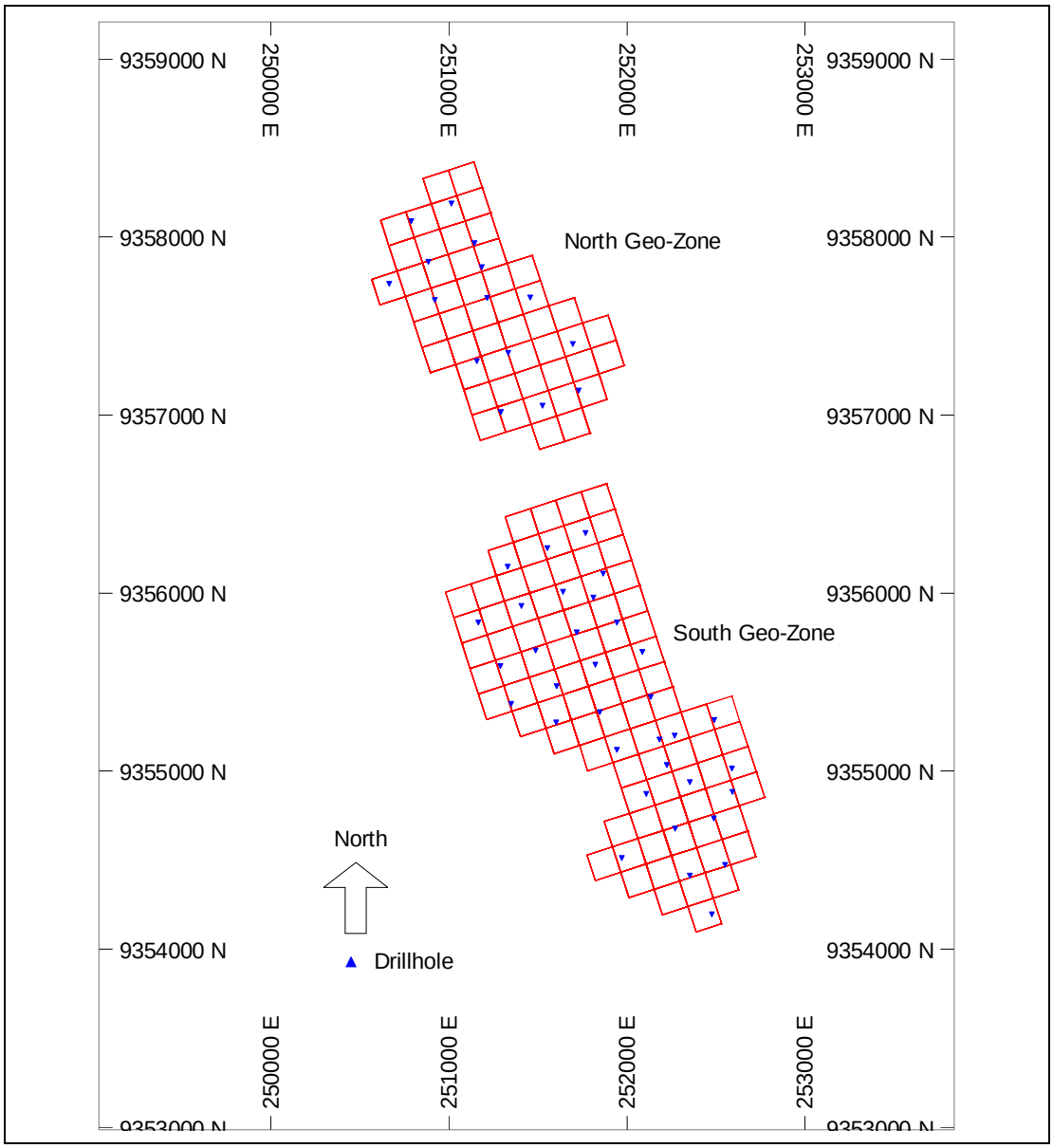


Figure 5.3_1: Simplified plan-view of the block model.

5.4 Search and Estimation Parameters

The search and estimation parameters were based on mineralization style, number of drillholes and samples, variography and orientation of the drillholes.

There are widely spaced drillholes at Kanzi. At least two holes are required to estimate grade for each block. The expansion of the search volume was allowed should the first pass not meet the requirements (Table 5.4_1). A discretization of 3X x 3Y x 3Z was allowed in order to better define the blocks (Appendix D). The block grade will be an average of the discretized points within the block.

The search volume was allowed to increase into first, second and third passes should it not find the required number of samples. A maximum of five samples per drillholes were allowed to estimate a block. This implies that a minimum of two drillholes is used in the estimation.

Table 5.4_1: Model Construction Parameters

ESTIMATION PARAMETER	SOUTH GEO-ZONE			NORTH GEO-ZONE
	Top	Middle	Bottom	
X Distance	500	500	500	500
Y Distance	500	500	500	500
Z Distance	10	10	10	10
Rotation	NO	NO	NO	NO
1st Expansion	2	2	2	2
2nd Expansion	3	3	3	3
Estimation Method	IDW/OK/IK	IDW/OK/IK	IDW/OK/IK	IDW/OK/IK
Min No of samples (1st Pass)	6	6	6	6
Max No of samples (1st Pass)	25	25	25	25
Min No of samples (2nd Pass)	5	5	5	5
Max No of samples (2nd Pass)	30	30	30	30
Min No of samples (3rd Pass)	3	3	3	3
Max No of samples (3rd Pass)	50	50	50	50
Discretization	3X3X3	3X3X3	3X3X3	3X3X3

6 LINEAR ESTIMATION METHODS USED IN MINING

6.1 Introduction

The mining industry has evolved overtime and the Mineral Resource Evaluation techniques improved and streamlined. The linear estimation techniques are mostly used due to their simplicity and fewer mathematical complications. The linear methods are grouped into geo-statistical and non-geostatistical methods. This study explores one method from each group, Ordinary Kriging (OK) from geostatistical methods and the Inverse Distance Weighting (IDW) from non-geostatistical methods.. The OK and IDW methods are the most commonly used methods in Mineral Resource Evaluation.

The theory of linear resource estimation methods is extensively discussed by (Isaaks & Srivastava, 1989; Clark, 2000; Rendu, 1978; Armstrong, 1998; Matheron, 1963) in detail and this chapter will deal with a brief discussion on theory and application applied to the Kanzi deposit.

The drawbacks of linear estimators defined by Vann and Guibal (1998) are:

a) Most of the mineral deposits have a mineral content that is highly positively skewed and the use of linear methods provides a wrong estimation because of smoothing effect.

b) The use of the arithmetic mean from the highly skewed distribution does not provide an appropriate mean.

c) Some deposits exhibit an inseparably bimodal distribution with two means. This phenomenon can only be solved by non-linear methods.

d) Linear methods can not estimate the distribution of the population but do estimate the expected value at certain position. Estimating the distribution of the deposit is very crucial to define the areas with the above cut off grades.

e) Estimation of recoverable (mineable) resources and reserves using linear methods gives unreliable estimates and non-linear methods provide solution to this.

OK and SK provide biased estimates of recoverable resources (both tonnage and metal content). This places mining projects in unnecessary risks especially if selective mining is the preferred method and the selected blocks are smaller than the borehole spacing (Vann & Guibal, 1998; Journel & Huijbregts, 1978).

6.2 The IDW method

The weighted linear combination of nearby samples is used to estimate the grade. The weighting factor is determined using the following formula

$$Z = \frac{1/d^{\alpha}}{\Sigma\frac{1}{d^{\alpha}}}.$$

Where *d* represents the distance of the sample to the point being estimated and α is the chosen power.

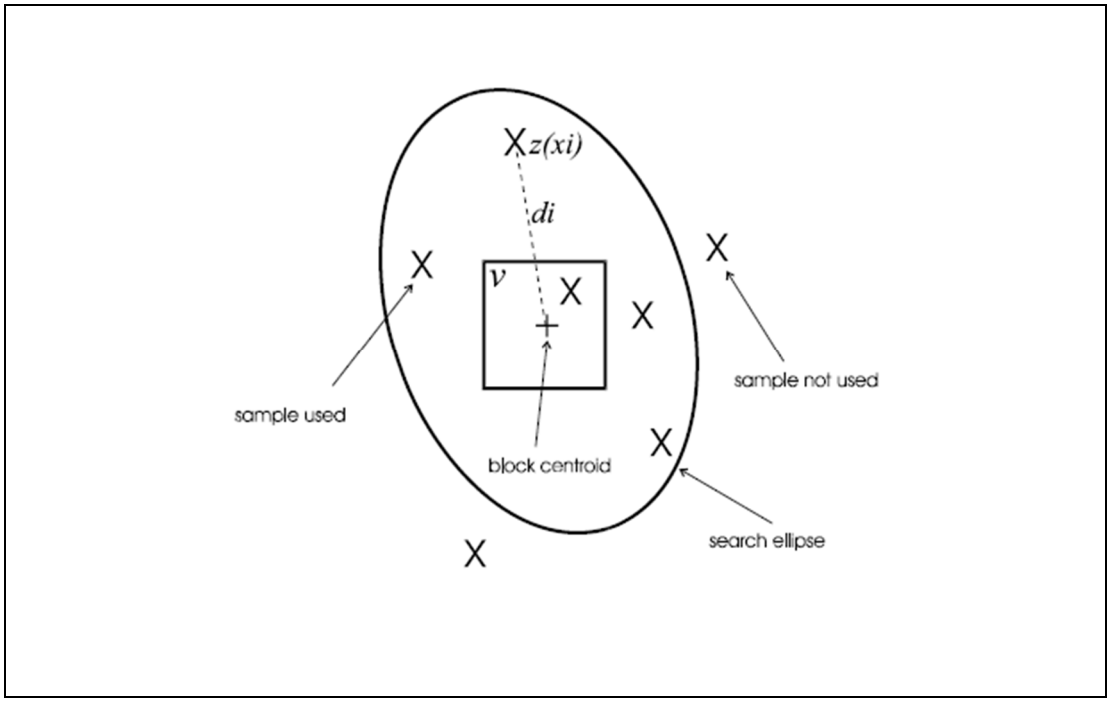


Figure 6.2_1: The illustration of how IDW works (modified from Vann, 2007).

The choice of power α is somehow subjective and this is the drawback of IDW. IDW does not fully honour the spatial relationship between the variables. The choice of power may be guided by cross validation, production data, comparing estimates to the kriging, etc. (Vann, 2007).

The IDW to the power of 2 commonly referred to IDW (2) is mostly used in the mining industry. The more the power is increased, the more the estimation resembles the nearest neighbour estimation techniques. The power of 2 or 3 provides better linear estimates in relation to the surrounding data point. IDW (2) is used in this project as other powers were tested and could give satisfactory results.

Some of the drawbacks of IDW are:

- There is no measure of when the relationship stops
- There is no measure of anisotropy

However, the IDW is known to perform better than kriging when there are fewer boreholes drilled. The IDW is the preferred method at the initial stages of exploration.

The validation of IDW estimates is commonly done through section analysis, mean–to-mean comparison and cross validation.

6.3 The OK method

Kriging was developed in the 1960s by Georges Matheron. In honour of the pioneering contribution by Danie Krige (mining engineer in the South African's Witwatersrand Gold Basin); Matheron named the new technique "kriging" (Vann, 2007).

Kriging is mostly known for being the best linear unbiased estimator (B.L.U.E.) of a random variable. Kriging depends on the spatial variability of the variables so emphasis is placed on:

- Variograms
- Continuity
- Trend analysis

Kriging assumes that the domains are "perfect" and the variogram model used is correct and trends are accounted for. For projects with sparse data, kriging does not perform well.

With OK, the sum of weights equals to one and the mean is estimated at each point making use of moving search neighbourhood. The OK estimator is represented by

$$Z^*(x) = \sum_{\propto=1}^{n} \lambda_\alpha Z_\propto,$$

Wherein λ_α is the kriging weight and α = 1 to n. The OK is a linear estimator so the λ_α is determined such that

Var(Z(x) –Z*(x)) is minimum and

the estimator is unbiased

$$E[Z(x) - Z*(x)] = m\left[1 - \sum_{\alpha}^{n} \lambda_\alpha\right]$$

In order to meet the OK requirements, the

$$\sum_{\propto=1}^{n} \lambda_\alpha = 1$$

$$or$$

$$m = 0$$

The kriging system can be summarized as

$$\begin{cases} \lambda^{\beta} C_{\propto\beta} + \mu = C_{\alpha 0} \\ \sum_{\propto=1}^{n} \lambda_{\alpha} = 1 \\ \sigma 2 = C_{00} - \lambda^{\propto} C_{\alpha 0} - \mu \end{cases}$$

The OK kriging matrix can be written as $\begin{bmatrix} C_{\propto\beta} & 1 \\ 1 & 0 \end{bmatrix} \begin{pmatrix} \lambda^{\beta} \\ \mu \end{pmatrix} = \begin{bmatrix} C_{\propto\beta} \\ 1 \end{bmatrix}$

Kriging has as an advantage a measure of uncertainty through the kriging variance. The problem with the kriging variance is that it is more dependent on the configuration of data than the actual values (Goovaerts, 1997). The kriging variance does not solve the issue of uncertainty in the accuracy of estimates.

Estimation Error

The difference between the estimated value and the "true" value is referred to as estimation error (Wackernagel, 1998). The estimation error is represented as

$$Error = Z^{*}(x) - Z(x)$$

The error of zero may mean that the estimation is unbiased.

$$Error[Z^{*}(x) - Z(x)] = 0$$

The variance of the errors is commonly referred to as estimation variance. The analysis of estimation variance is important in defining errors produced in performing estimation. (Journel & Huijbregts, 1978). The variance estimation can be defined by

$$E\{[Z_V - Z_v]^2\} = 2\bar{\gamma}(V, v) - \bar{\gamma}(V, V) - \bar{\gamma}(v, v)$$

Estimation variance is influenced by the following four factors:

- The relative distance between the block and the information used to estimate this block;
- The block size and geometry;
- The quantity and spatial arrangement of the information and
- The degree of continuity of the mineralisation (Clark, 2000; Isaaks & Srivastava, 1989; Journel & Huijbregts, 1978).

The distribution of errors is used in establishing confidence interval for the proposed estimates. Mostly $\pm 2\sigma_E$ (95% Gaussian confidence interval) is used in mining industry in estimation variance, σ_E^2 (Journel & Huijbregts, 1978).

The variance of the estimator is used to determine the variation of the estimated value around the population mean as shown below (Wackernagel, 1998).

$$\delta^2 = var(M^*)$$

$$= \frac{1}{n^2}(\sum_{\propto=1}^{n} var(Z_x)$$

$$= \frac{\sigma^2}{n}$$

6.4 Comparison of IDW and OK Results

The performance of IDW (2) and OK is compared in terms of general statistics, grade tonnage curves and cross-sections of the model versus the drillhole data. The best estimates are the one that are not far from the “reality”. The “reality” in this case is the drillhole data. The assumptions are the drillhole data is representative of the ore-body and the domains are homogeneous.

6.4.1 Statistics

The IDW (2) and OK estimates are compared to the drillhole data in Table 6.4.1_1. The percentage difference in terms of the means was analysed. The means of the drillhole data are comparable to means of the estimates from the IDW and OK methods. If a sparse dataset is used, checking the difference in the means is a good tool to validate the estimates.

The histograms in Figure 6.4.1_1 showed that the linear methods used over-smoothed the P_2O_5 grade. Smoothing spatially integrated population results in bad estimation; as seen in OK and IDW (2) estimates. The histograms show narrow range and low standard deviation. The change of support also played a role but the estimation by linear methods made the smoothing worse.

The change of support was considered when analysing the histograms. The graph shows that IDW (2) provides estimates identical to those produced by the OK method.

There are number of populations spatially integrated and the second order of stationarity is not honoured; that is the weaknesses of OK over the IDW (2) as the variograms are not robust. OK performs better where there is single and normally distributed population. Because the variograms are not so “robust”, the estimates are either over or under-estimated as shown in the graph. When using the search volume guided by the variograms, IDW (2) provided the better estimates. This phenomenon works to the advantage of IDW as it performs better in spatially integrated populations. This is because the IDW (2) does not use variogram model to define the relationship; it uses the inverse distance relationship and averages the sub-populations without short-scale weighting but uses the true proportions of the population.

Table 6.4.1_1 Comparison of the means of the drillholes, IDW and OK estimates

Domain	Drillhole Mean	IDW Mean	% Difference (IDW)	OK Mean	% Difference (OK)
BL	8.75	8.88	1.49	8.82	0.80
ML	16.30	15.75	-3.37	15.72	-3.56
TL	9.50	9.12	-4.00	9.60	1.05
North Geo-Zone	16.32	16.09	-1.41	15.96	-2.21

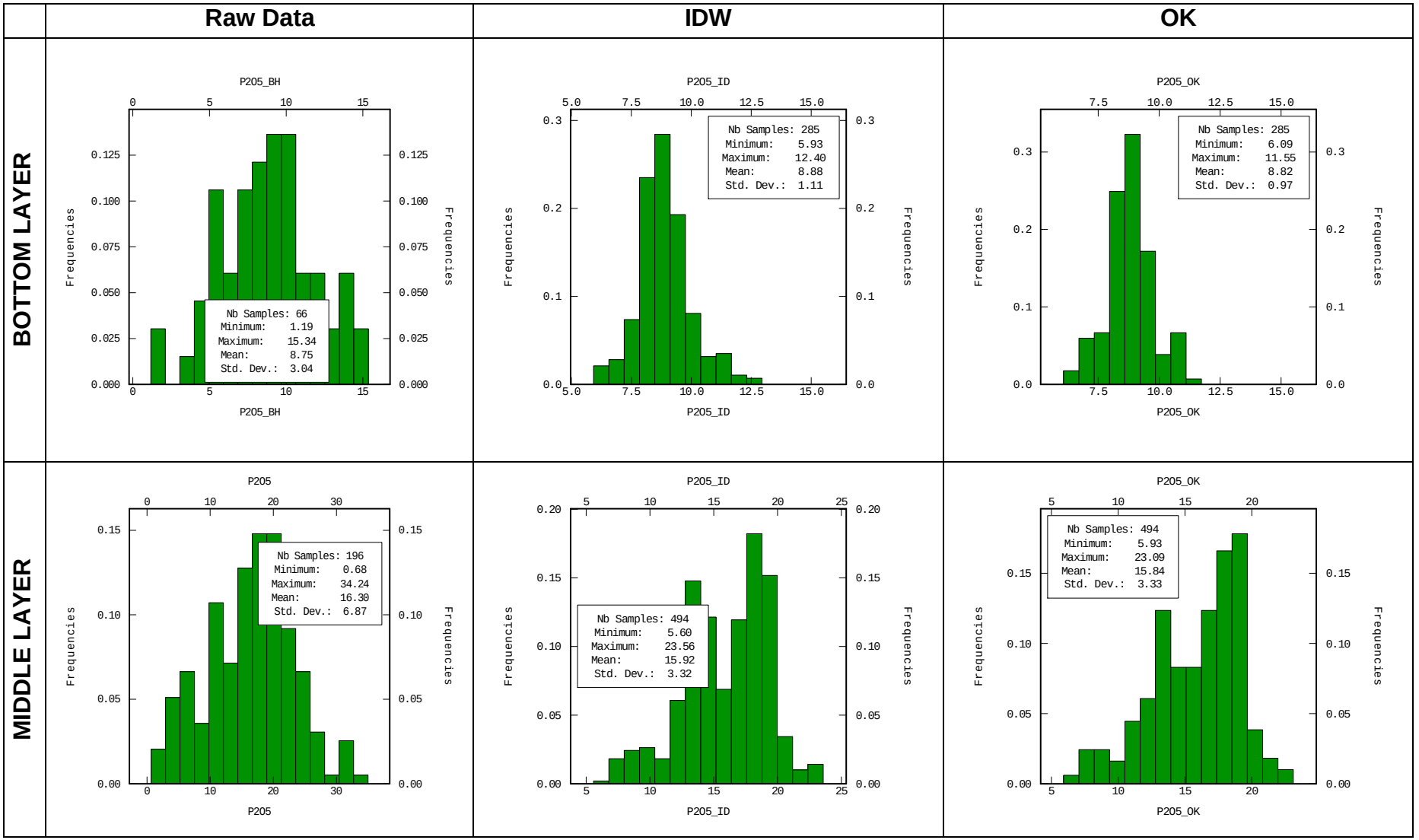


Figure 6.4.1_1: Comparison of the raw and estimate data statistics for BL and ML.

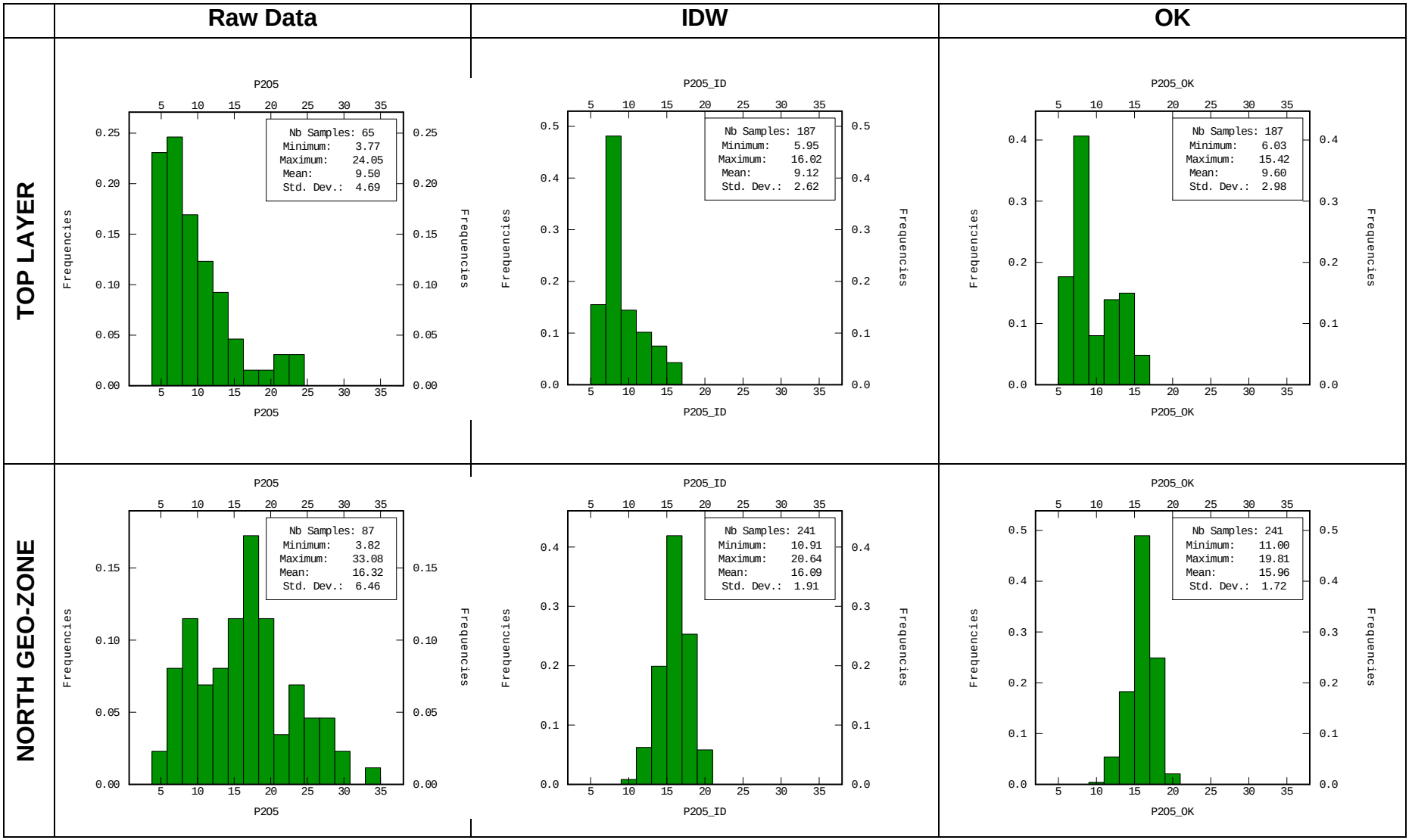


Figure 6.4.1_2: Comparison of the raw and estimate data statistics for TL and North Geo-Zone.

6.4.2 Cross-Sections

The cross-sections in Figure 6.4.2_1 show the IDW (2) and OK provided acceptable results though there is smoothing effect. There is a good correlation between the estimates and drillhole grades. The IDW provided better estimates for the North Geo-Zone. The OK over-smoothed the domain. For South Geo-Zone, the IDW and OK produced the identical results.

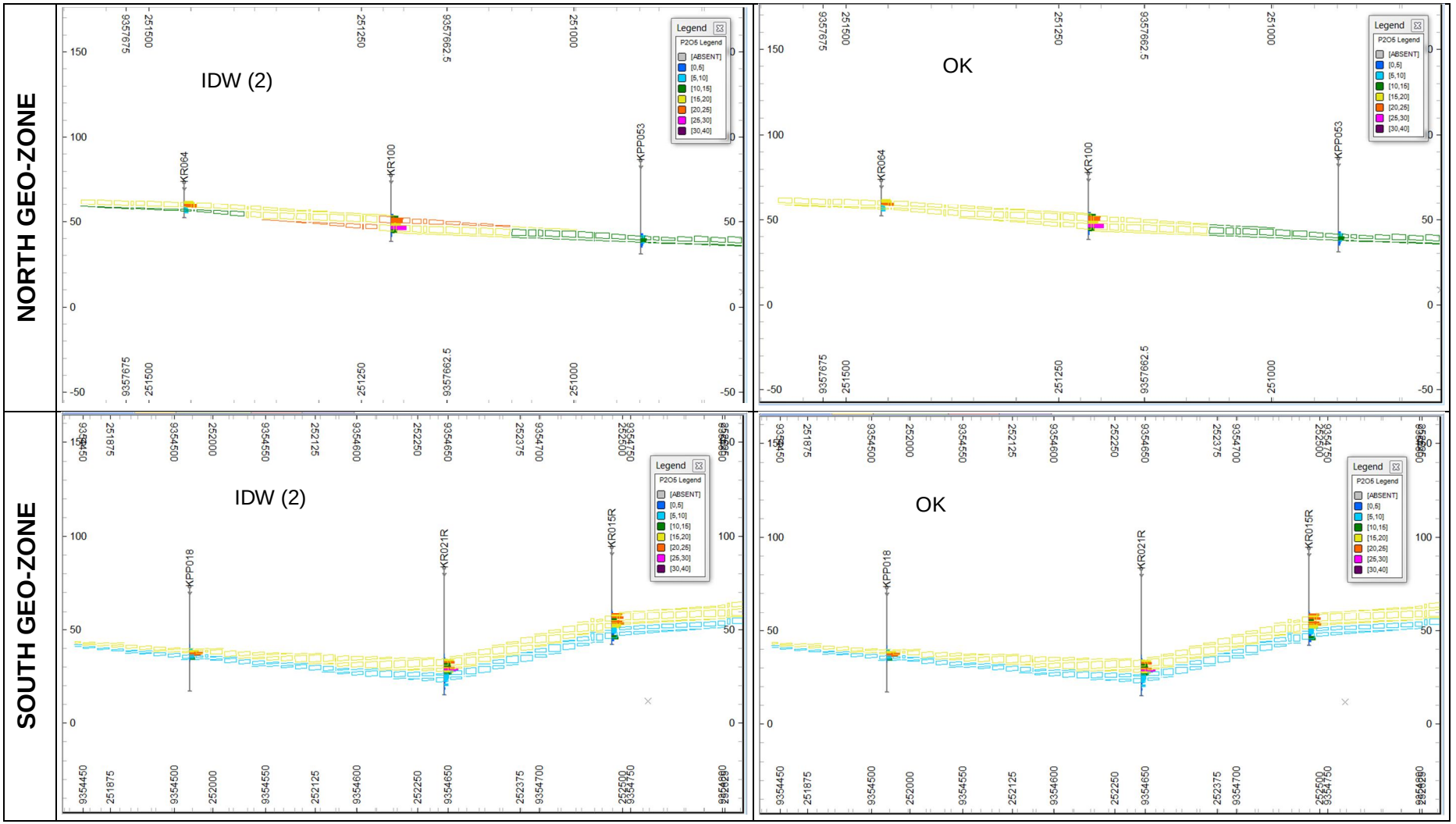


Figure 6.4.2_1: Comparison of IDW(2) and OK.

6.4.3 Grade Tonnage Analysis

An understanding of grade and tonnage relationship in mining industry is crucial. The grades and tonnage contribute to the value of the mineral's project. The grade tonnage curves are one of the most used tools in economic and financial analysis of a mining/exploration project. They are used in determining the volume and grade based on the variations of cut-off grades (Silva & Soares, 2013). Mine plans are mostly based on the grade tonnage curves. The grade tonnage curves for different domains are presented on Figure 6.4.3_1.

BL

The grade tonnage curve for the BL shows that the OK and IDW2 produced different results at higher grades. At lower grade the results of OK and IDW2 are almost identical. The shapes of the graphs for OK and IDW2 are identical. The OK slightly underestimated the higher grade. The grade tonnage curve produced by the IDW2 technique is better than the one produced by OK method. The IDW method defined both the lower and higher grades.

ML

The results of the IDW and OK are comparable. The tonnages and grades above the cut-off for both OK and IDW2 methods defined both the lower and the higher grades. The ML had more data than other layers and population distribution is symmetrical. The estimation results are better for ML than for the TL and BL.

TL

The OK provided better grade tonnage curve than the IDW method. The smoothing effect is high. This is because the population is not complete.

North Geo-Zone

The IDW method produced better results than the OK method. The OK methods did not pick the higher and lower grade. It smoothed them. The grade tonnage curve produced by IDW can be used for mine planning purposes and valuation of the project. The grade tonnage curve is identical to that of the ML. This supports that the ML and the North Geo-Zone are one domain.

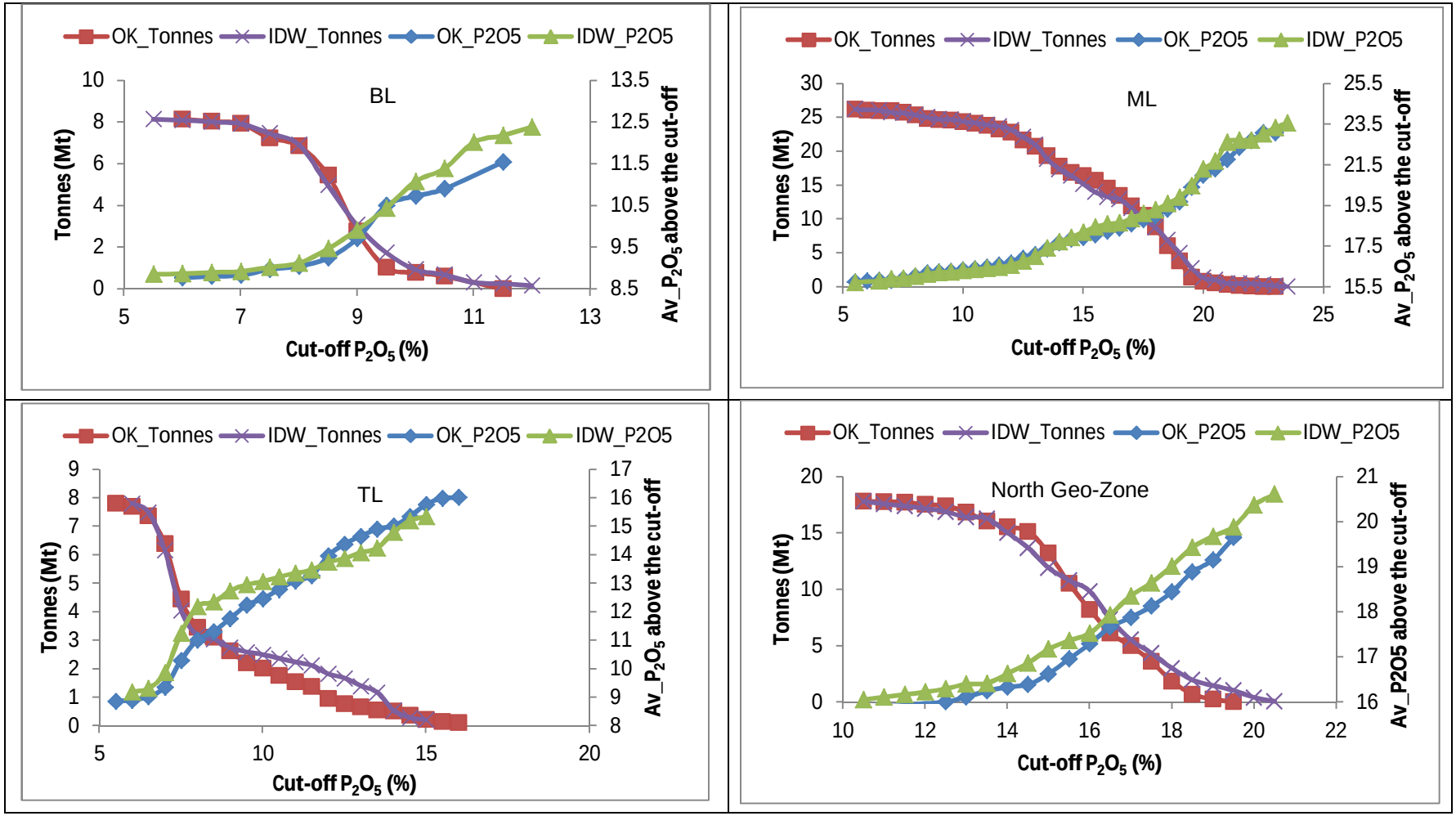


Figure 6.4.3_1: The Grade Tonnage Curves for the different domains.

6.5 Summary Findings on Linear Estimation Methods

The application of IDW (2) and OK techniques were studied. The methods are basic and easy to understand and apply. The problem with the methods is that they produce smoothed estimates and the detail is lost. In the case of Kanzi the detail in the grade distribution is more important than the average grade. Thus, the grade variability is more important.

IDW

- The issue raised about the IDW is the criteria used in selecting the appropriate exponent. The higher the exponent the more the results resemble the nearest neighbour estimates.
- The continuity of spatial relationship is not 'fully' honoured. The inverse type of relationship is applied.
- When appropriate search volume and estimation parameters are selected the estimation results are better and comparable to advanced methods such as OK.
- The IDW (2) like other linear methods provides the smoothed results and the detail is lost.
- For bulk mining purpose like mining of phosphates the IDW (2) is suitable.

OK

- In theory, the OK method provides the best linear unbiased estimates provided
  - The populations are well defined and normally distributed
  - The variograms are well-defined and second order stationarity is honoured.
  - The search volume and estimation parameters are well-set.
- Kanzi phosphate deposit was sub-divided into geo-zones based on geology and grades. There seemed to be spatially integrated populations in the geo-zones.
- The variograms models were used in the estimation. The performance of OK was identical to that of IDW (2). This is due to the fact that the same parameters were used and populations are moderately mixed in the domains. The second order of stationarity was not 'fully' honoured.
- OK provided the estimates that lack the detail and are affected by smoothing effect. The local variability was lost. The histograms of OK estimates show narrow range, low standard deviation and well defined populations.

The local variability is crucial for the Kanzi Phosphate Project. Understanding of local variability will help mine planning in terms of blending strategies and selective mining. As Kanzi phosphates upgrade differently, the understanding of grade variations is critical in processing design. The IDW and OK methods failed to define the local variability. The non-linear methods were then used to better define the local grade variability.

The drawback of OK is that it requires more data points (than IDW) to define populations, variograms and honour second order of stationarity. In mineral industry, these conditions are rarely met at the exploration stage due to the costs of collecting data. On the other hand IDW provided better estimates using few samples when properly set. The IDW degrades the estimates according to the distance from the samples.

The linear estimation methods showed that the estimates are over-smoothed. The detail is lost and the mining companies are exposed to risks due to smoothing effect. The uncertainty cannot be studied in detail. The linear methods works well when the domains are properly defined and domains are well-informed with data. Advanced methods that can better handle the data without following the linear relationships are needed. The non-linear methods will be tested in the next chapter and the results will be compared to the linear methods.

7 NON-LINEAR GEOSTATISTICAL MODELLING

7.1 Introduction

In mathematical terms linear methods are best explained using linear regression relationship with is a straight line defined by:

$$y = mx + c$$

The relationship between two variables (y and x) is linear. Using this relationship to estimate values between the two variables, the results will be values along the straight line honouring the linear relationship. For example; if a mineral deposit has a higher grade variable at location h and a low grade variable at location g, to estimate a variable between locations h and g using linear estimators, the estimates in between the known geological information will follow the linear relationship (Journel & Huijbregts, 1978).

Linear estimation techniques such as Inverse Distance Weighting (IDW), Ordinary Kriging (OK) and Simple Kriging (SK) are the mostly used geostatistical methods in mineral resources estimation. This is due to their simplicity, not necessarily their robustness. Non-linear estimation techniques are more accurate methods than linear estimators (Deraisme, et al., 2004; Vann & Guibal, 1998; Clark, 2000; Chilès & Delfiner, 1999). Though they are better techniques, non-linear methods are not appealing to mining industry due the fact that they are difficult to interpret and there is a shortage of skills in applying the advanced geostatistical concepts.

Linear geostatistical techniques also estimate the variance between the true and estimated values; and small variance means a better estimation (Clark, 2000; Deraisme, et al., 2004; Coombes, 1994). Ordinary Kriging (OK) is the most widely used geostatistical technique in Mineral Resource estimation and evaluation. However, the OK variance does not recognise local data variability. When estimating highly variable mineral deposits, local data variability is crucial. Variogram provides the link between kriging variance and data values. This link is rather global than local in its definition.

There are many variants of non-linear regression and the simplest form of non –linear relationship according to Journel and Huijbregts, 1978 is:

$$y = ax^2 + b$$

The relationship described by the formula above is parabolic or quadratic. It can be explained that the relationship between variables (y and x) is dependent on variable x (Journel & Huijbregts, 1978). This type of non-linear estimator uses the weight of the variable rather than being dependent on a sample position only.

Non-linear methods do not depend on the assumption of the distribution of the mineral deposits and they are simply non parametric (Vann & Guibal, 1998; Deraisme, et al., 2004).

It has been shown that estimation of ore tonnage conducted using OK under-estimates when the cut-off is below the mean and over-estimates when cut-off is above the mean; this is because of smoothing effect of linear regression (Deraisme, et al., 2004).

7.2 Non-Linear Geostatistical Techniques

Non-linear geostatistical methods are mostly used in estimating recoverable mineral resources, both local and global. The main advantage of these methods is their swiftness but more importantly, they give a much more detailed description of the variability of the deposit.

Non-linear techniques approximate a conditional distribution and expectation of mineral content at a specific location. This can be described by the following expression:

$$\Pr[Z(x_0)|Z(x_i)]$$

This expression describes the probability of grade Z at location x_0 given the grade information at specific location, $Z(x_i)$. This is a conditional expectation and the probability will yield a conditional distribution; consequently the grade tonnage curves can be constructed easily and cut off studies can be conducted (Journel & Huijbregts, 1978).

Non-linear techniques estimate the recovered ores based on the volumes on which ore and waste are determined. Insufficient information causes the misclassification of locations as being above or below a threshold; resulting in loss of efficiency in the operations. In the case of selective mining techniques, a block selected based on estimate Z will yield inferior economic results compared to the block selected based on true values. To overcome this problem, modelling of the joint distribution of true and estimated values is necessary (Deraisme, et al., 2004; Chilès & Delfiner, 1999).

There are number of non-linear techniques and the following are mostly used in the mineral industry using linear regression as an interpolator within:

- Indicator estimation
- Lognormal Kriging (LK)
- Multi-Gaussian Kriging (MK)
- Uniform Conditional (UC)

Most of the non-linear methods are used in the mine planning stage to conduct local estimation of the recoverable resources (SMU). Kanzi is still at an exploration stage and global estimation of the recoverable resource is important for mine planning and designing beneficiation test-work. This research project focussed on indicator estimation.

7.2.1 Indicator Estimation

Indicator estimation is a non-linear geostatistical estimation technique introduced by Andre Journel in 1983 and is known as distribution free method. It does not consider

population distribution when estimating, thus it is non-parametric. It was mostly used for categorical variables such rock types, facies and other discrete descriptions. Its application has been extended to continuous variables such as grade by considering a series of increasing thresholds that discretise the range of variability in the continuous variable. Indicator formalism provides a means to determine a nonparametric conditional distribution which constructs local distributions of uncertainty.

For each point estimate, SK or OK of a set of indicator-transformed values determines a resultant value between 0 and 1. This is in effect an estimate of the proportion of the values in the neighbourhood which are greater than the indicator or threshold value.

The indicator estimation produces a conditional cumulative distribution function (ccdf). The ccdf is built at each point based on the correlation structure and behaviour of the indicator transformed points in the neighbourhood.

It has gained popularity and acceptance by the geostatistical community as, if correctly set up, it is resistant to over/under estimation effects of statistical outliers. It is built on the knowledge that different portions of the mineralisation can have different spatial characteristics.

The indicator estimation is an estimation method developed in the 1980s to deal with the issues of how to weight outliers in skewed distributions. It was developed to reduce the bias in estimation especially estimation of the precious metals. The estimation results in the distribution of grades within a block. The OK or SK gives the average grade (Snowden, 1989).

Indicator kriging can best described by

$$I_C^*(u) = \sum_{i=1}^{n} \lambda_i I_c(u)$$

$$= estimator\ for\ probability\ of\ u \in C$$

It is a robust method because

- It is based on kriging of the indicator transformed values defined as series of cut-off grades, and
- Different distributions are assumed based on the kriged indicators

Therefore indicator estimation provides probability (of grade above cut –off), proportion (of blocks above cut off on data support) and helps in structural analysis determining average dimensions of mineralised pods at different cut-offs. The indicators are crucial in studying the spatial variability of variables.

Indicator Kriging as defined by Bárdossyg (2000) assigns binomial coding of the $Z(x)$ into 1 or 0 based on the relationship of the categorical classes according to the following formula

$$I(x;k) = \begin{cases} 1, & if\ Z(x) \in k \\ 0, & else \end{cases}$$

The probability that x prevails at k can be expressed as

$$E\{I(x;k|(n))\} = Prob\{(x;k) = 1|(n)\} = f(x;k|(n))$$

With (n) consisting of n neighbouring data values $Z(u_\propto)$, wherein $\propto = 1, \ldots, n$. Continuous variable can also be transformed into indicators. The indicators are defined by exceeding certain thresholds according to:

$$I_x(u) = \begin{cases} 1\ if\ Z(x) \leq \propto \\ 0\ if\ Z(x) > \propto \end{cases}$$

When the kriging algorithm is applied to the indicator data the least squares estimates of its conditional expectation is found.

The benefit of indicators is that the estimated value is within the expected range as

$$[minZ(u_i); maxZ(u_i)]$$

The advantages of indicator estimation according to Vann & Guibal, 1998, Deraisme et al., 2004 and Bárdossy, 2000 are:

- It considers the structure of each indicator; Prior assumptions on the shape of distributions are not necessary in the IK.
- It is less prone to smoothing effects and conditional biases
- It produces a variance of the estimation;
- It has capability to estimate recoverable resources inclusive of dilution and ore loss .
- Unlike other methods, IK requires local stationarity, not global stationarity.

Drawbacks of IK according to Deraisme, et al., 2004 are

- A number of variograms are modelled;
- It is tedious to set-up.

The IK allows the resource estimates to be conducted as

- E-type estimates (the average block grade) and
- The recovered tonnes and grade defined by selective mining unit.

Indicator Variograms

The indicator variogram can be represented by

$$\gamma(h) = \frac{1}{2N(h)} \sum_{u_i - u_j = h} (I_\alpha(u_i) - I_\alpha(u_j))^2$$

Which is identical to:

$$\gamma(x - y) = \frac{1}{2}[P\{x \in X, y \notin X\} + P\{x \notin X, y \in X\}]$$

The $N(h)$ represents the number of pairs of locations of samples separated by the vector h. The mean of the indicator variable is equal to the probability of occurrence of the corresponding property and the variance of the variable is defined by

$$v = x(1 - x)$$

When mixed populations are spatially integrated, indicator variograms become more useful and robust. For sequential indicator simulations, indicator variograms are useful.

There are variants of the indicator variograms depending on the estimation method used. The multiple indicator variograms are used in the Multiple IK and median indicator variograms are used in the Median IK.

For Multiple IK variograms for different cut-offs are calculated. The selection of cut-offs are based on the deciles (10^{th}, 20^{th}, 30^{th}, 40^{th}, 50^{th}, 60^{th}, 70^{th}, 80^{th} and 90^{th} percentiles of the data distribution), inflection point in the distribution, mine plan cut-offs or some relevant factor. For multiple indicator variograms, all the indicators are modelled. The indicator variograms are not modelled independently.

The median IK is easier than multiple IK because only one variogram is modelled. The assumption is that all indicators have same variogram models. The variogram of the median value or indicator is selected and modelled.

Median IK

The median used in the variogram should be for the declustered distributions. For this project the declustering is not necessary as the drillholes are well-spread. The median indicators of different domains were determined using 100 cut-offs from 0% P_2O_5 by a step of 0.5% P_2O_5. The chosen median indicators are shown in the Table 7.2.1_1. These indicators are almost equal to the median from the data distribution.

Table 7.2.1_1: P_2O_5 Median Indicators for the different domains

Median Type	BL	ML	TL	North Geo-Zone
Raw Data	8.85	17.14	8.14	16.49
Indicator Cut-off	8.75	17.25	8.25	16.50

Nugget Effect Determination

There are enough samples to conduct the downhole spatial studies. Downhole variograms for the indicator medians for different domains are presented in Figure 7.2.1_1. The downhole variograms are for the median indicators presented in Table 7.2.1_1. The nugget effects are low showing high spatial relationship for samples at closer ranges.

The downhole variograms show that there are still some issues with the vertical domaining. The trends are noted and could not be resolved as there is no enough data. These trends are not material for now as they could not highly influence the outcomes. The trends are inherent in the deposit and closer sampling interval will not resolve them.

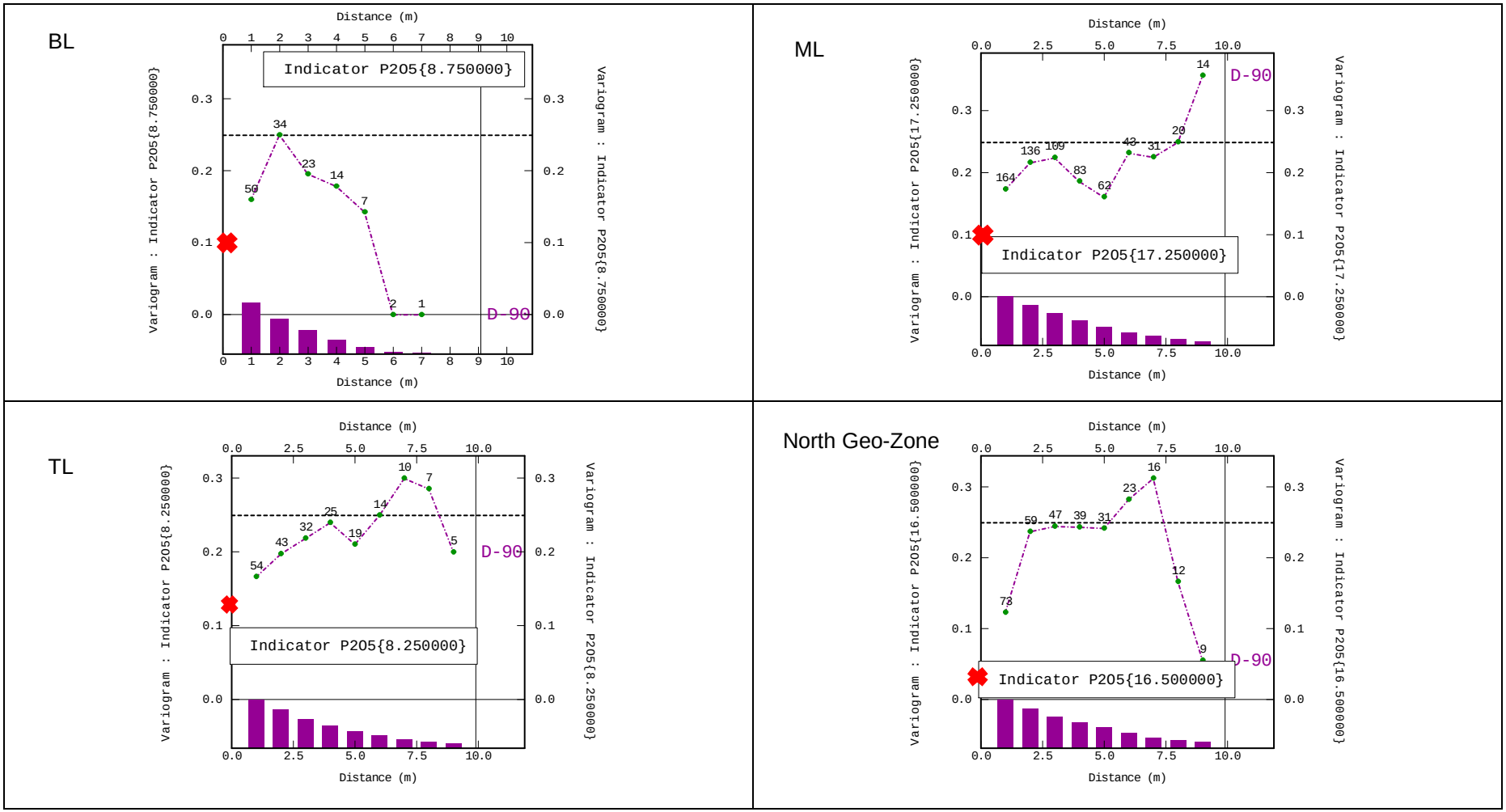


Figure 7.2.1_1: Median Indicator Downhole Variogram Models for P_2O_5.

Table 7.2.1_2: Median Indicator Variogram Model Parameters

Domain	Nugget	C1 Range (m)	C1 Sill	C1 Model type	C2 Range (m)	C2 Sill	C2 Model type
BL	0.080	79.87	0.089	Spherical	347.95	0.080	Spherical
ML	0.097	275.39	0.096	Spherical	880.73	0.056	Spherical
TL	0.110	353.28	0.139	Spherical	-	-	-
North Geo-Zone	0.025	264.81	0.158	Spherical	602.15	0.067	Spherical

Median Indicator Variogram Modelling

The variogram model parameters are presented in Table 7.2.1_2. The modelled median indicator variograms for the different domains are shown in Figure 7.2.1_2. All the variograms are omni-directional as there was no specific directional continuity noted. This might be due to paucity of data and/or mineralization style. The nugget effects were taken from the respective downhole variograms presented in Figure 7.2.1_1.

Variogram models for TL, ML and North Geo-Zone have two structures. All the variogram models are spherical. The ML has the highest spatial continuity and BL have the shortest range.

The data that informs the variograms is not enough and the structures are not well-defined. ML variogram is better defined as this domain has more data than other domains. Geological knowledge and understanding of data helped in modeling the variograms.

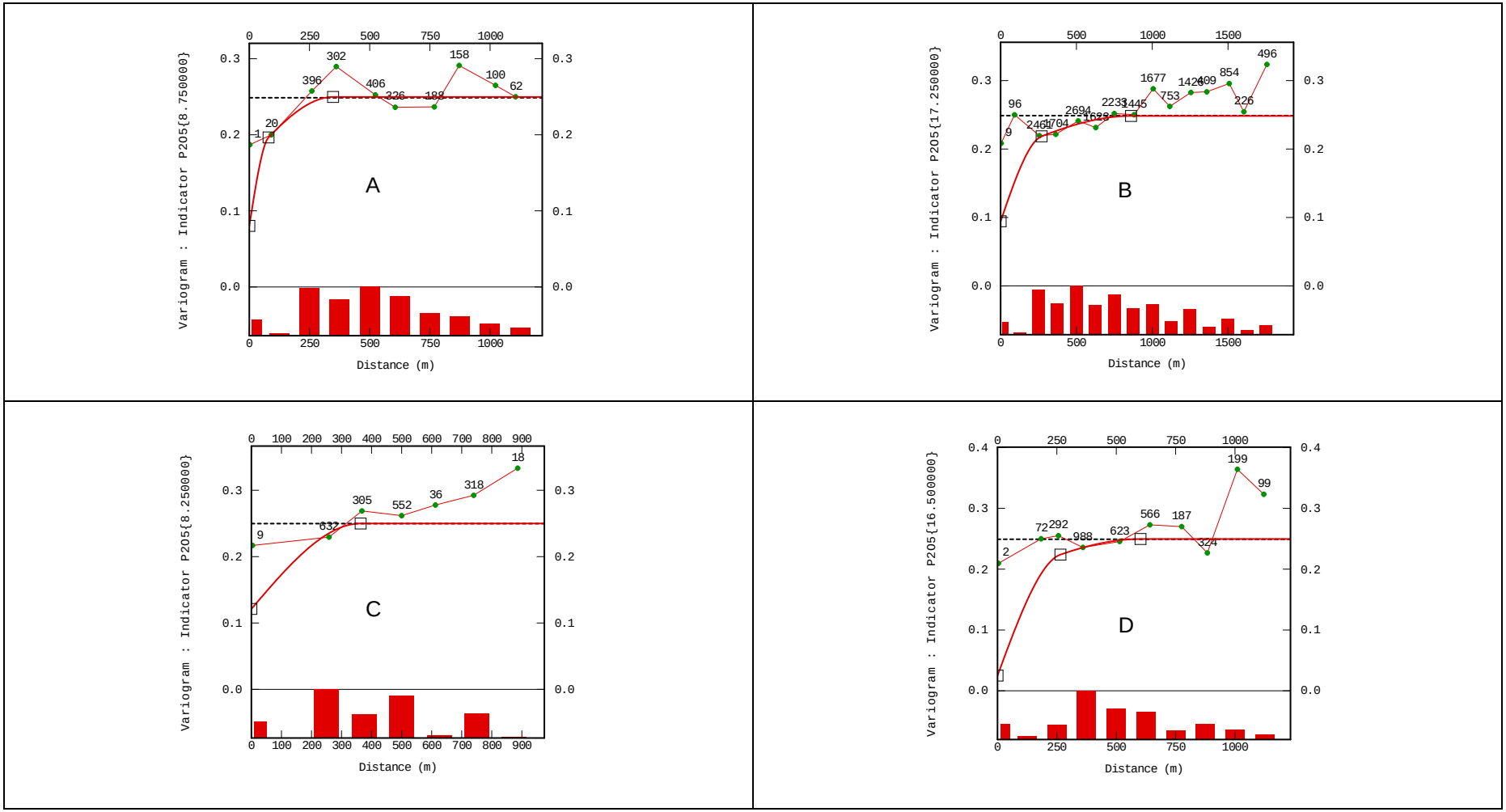


Figure 7.2.1_2: Median Indicator Variogram Models for different zones. Variograms A, B, C and D are for the bottom, middle, top and North geo-zones respectively.

The Estimation Methodology

The estimation of the indicators is mostly conducted using Multiple IK and Median IK. These methods use either OK or SK. The only difference between the Multiple IK and Median IK lies in the use of indicator variograms. Multiple Indicator estimation technique uses all defined cut-off interval variograms and Median IK assumes that all indicator variograms are identical and the median variogram model is used in the estimation of all indicators.

The OK systems will be used in the median IK. The SK systems cannot be used as the mean of the population is not confidently known.

The IK can be performed in either 2D or 3D environment. For this project, estimation will be done into the 3D geological model defined in section 5. This will allow a better comparison of the results from the linear methods studied in section 6 and indicator estimates.

The IK uses the hard boundary between the indicators as transformed indicator data points as coded as either 0 or 1. The indicator data that are undefined or missing are ignored (Deutsch & Journel, 1992).

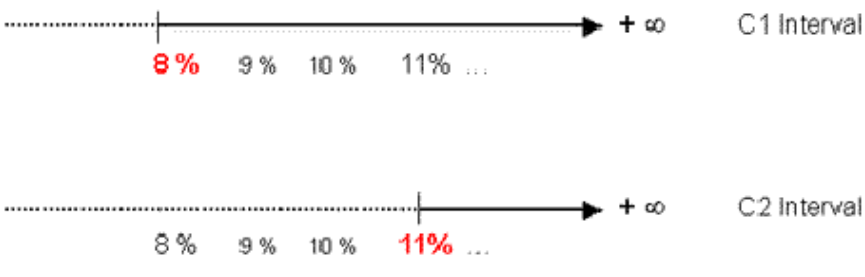
The IK as a probabilistic method defines distribution of grades of samples within each search window. The IK involves pre and post processing:

Pre-processing

The cut-offs are defined and data is transformed into 0s and 1s. The statistics can be conducted for each cut-off interval should there be enough data. The cut-offs are generally defined as shown in Figure 7.2.1_1 and by the formula presented below when the boundary is not known. For Kanzi phosphate, the cut-off are known.

Cut-offs: C1 = [8,+Inf[C2=[11,+Inf[

where C1 and C2 are the cut-offs



This figure was taken from (Deraisme, et al., 2004)

Figure 7.2.1_1: Examples of cut-off determined.

For continuous variables, selection of the cut-offs should be done carefully as selecting too many cut-offs makes the process tedious and the outcomes too detail. On the other

hand selecting too few cut-offs makes the detail of the distribution to be lost (Deutsch & Journel, 1992).

The processing characteristics of the Kanzi phosphates were considered when selecting the cut-offs. The processing study conducted for the Kanzi phosphate found that the phosphate behaves differently at the different cut-offs. The processing study shows that a 12.5%, 17.5%, 22.5% P_2O_5 upgrade differently. These cut-offs have been used in the IK. These cut-offs show that there is a physical break of differences in the phosphate characteristics.

The following considerations were made when selecting the appropriate cut-offs for Kanzi Phosphate project:

- The cut-offs should be able to guide the potential of the mining project. The lowest cut-off should be 7.5% P_2O_5 as anything below that is un-economic.
- The cut-offs from a processing study: 12.5%, 17.5%, 22.5% P_2O_5 have been used.
- A step of 5 from 7.5% up to 27.5% P_2O_5 seems reasonable and practical for this project as at these cut-offs phosphate behaves differently. These cut-offs may allow good mine planning as blending and selective mining can be done according to processing requirements.

Post-processing

- The post processing is done to so that probability maps may be created. The probability of exceeding threshold (cut-off) and the mean of the cdf are estimated.
- The mean of the cdf is estimated using

$$[z(u)]_E^* = \int_{-\infty}^{+\infty} z\, dF(u; z|(n)$$

$$\approx \sum_{k=1}^{k+1} z_k' \left[F\left(u; z|(n)\right) - F(u; z_{k-1}|(n))\right]$$

  where z_k, $k = 1, \ldots K$ are the cut-offs retained and $z_0 = z_{min}$, $z_{k+1} = z_{max}$ are the minimum and the maximum of the z range.

- The probability for the continuous variables is determined by

$$Prob\{Z(u) \leq z|(n)\} = F(u; z|(n) \in [0,1]$$

and

$$F(u; z_{k'}|(n)) \geq F(u; z_k|(n), \forall z_{k'} > z_k$$

- Correcting Order of Relation

Order of relation (OR) is problematic in the IK. OR problems caused by negative IK weights and lack of data in some classes. For this project the assessment of negative

weights were done and none were found; thus the negative weights did not have any effects. The lack of data in the upper classes was noted in domains as expected. Where there is lack of data in the classes, no estimation was carried out and probability was set to 0.

7.2.2 Results of the IK

The average P_2O_5 and proportions above the defined cut-offs are presented in Figure 7.2.2_1 to 4. The global recoverable grades and selective mining strategies can be assessed.

Average P_2O_5

The average P_2O_5 for different domains are drawn against the drillhole data. The IK produced results that are not highly smoothed. There is a good correlation between raw data and modelled data.

Mean Grades per Different Cut-offs

For each cut-off, the average grades above the cut-off were determined for each block. The average grades increase with the cut-off until the grade cease to exist. The higher cut offs result in lower probabilities in place.

Probability Maps

The probability ranges from 0% to 100% and these are represented as proportion (minimum = 0 and maximum = 1). The probability maps can be used to assess the risk during mining. For the probability to be considered good for planning purpose, the proportion should be at least 0.5. Less than that proportion, the risk for mining such blocks is high. The blocks can be assessed individually. This project focussed on global recoverable estimation.

North Geo-Zone

The probability maps are presented in Figure7.2.2_1. There is high proportion of mineralized material above the first two cut-offs (7.5 and 12.5% P_2O_5) in North Geo-Zone. There is a high probability of getting at least 7.5% P_2O_5 and there is low probability of getting above 17.5% P_2O_5.

BL

The BL is the low grade layer and the probability map is presented in Figure 7.2.2_2. The higher probability is seen on the lowest cut-off interval. A second cut-off show sporadic higher probabilities on the north-west side. The last three cut-off intervals show 0 to 25% probability.

ML

The first three cut-off intervals show some potential as shown in Figure 7.2.2_3. This layer is richer in the south than in the North. The maps of the proportions of material

above certain cut-off grade can be correlated to the average P_2O_5 grades. The last two cut-off intervals (state them) map show very low probabilities of getting high grades.

TL

The probability maps for TL are presented on Figure 7.2.2_4. More than half of the TL area has high probability of being greater 7.5% P_2O_5. At 12.5%, less than a quarter has higher probability of being above the cut off. This layer is a low grade one. The last three cut-offs have very low probability of being attainable.

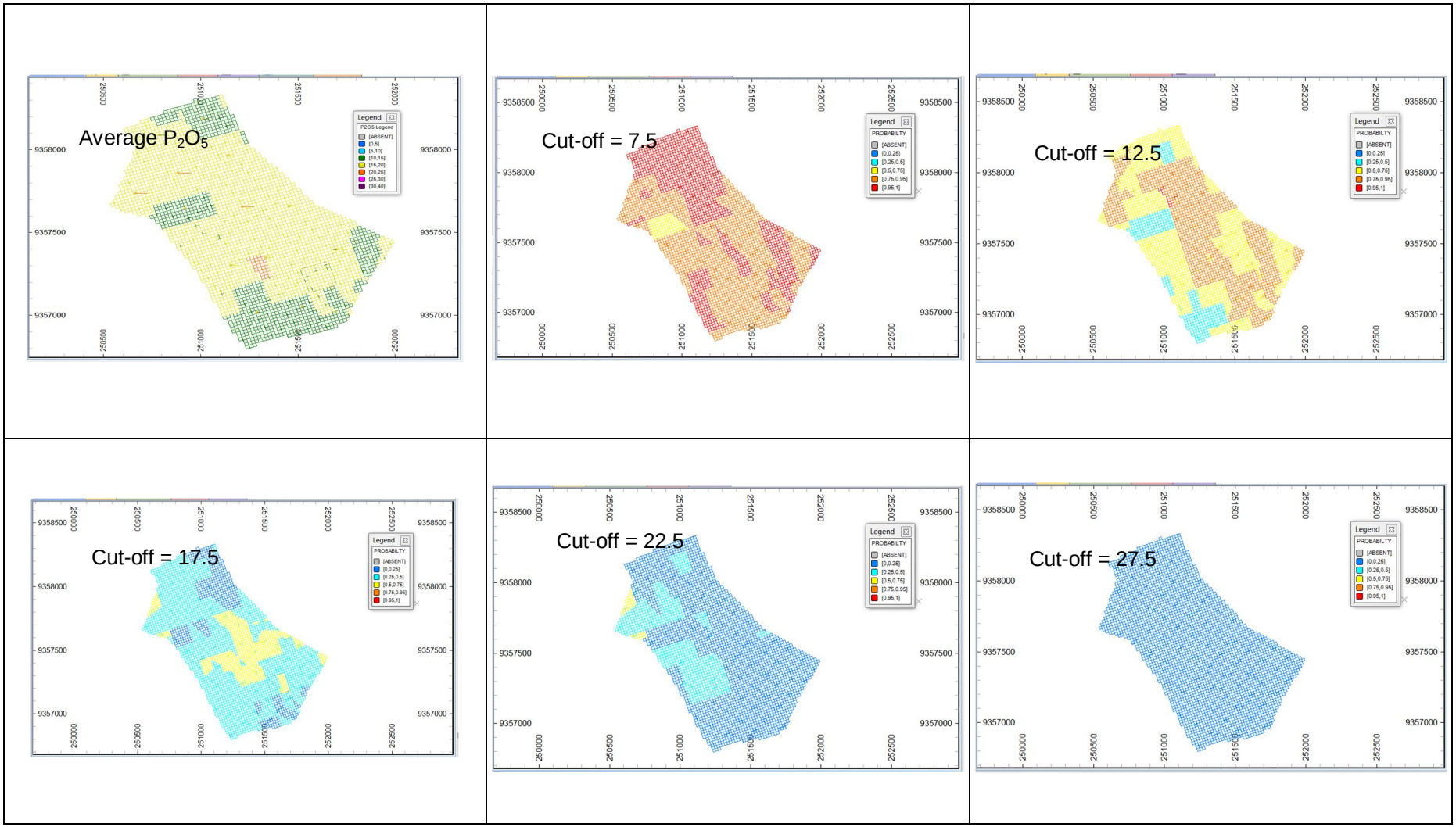


Figure 7.2.2_1: The maps of North Geo-Zone showing the average P_2O_5 grade and proportions of materials above the cut-off.

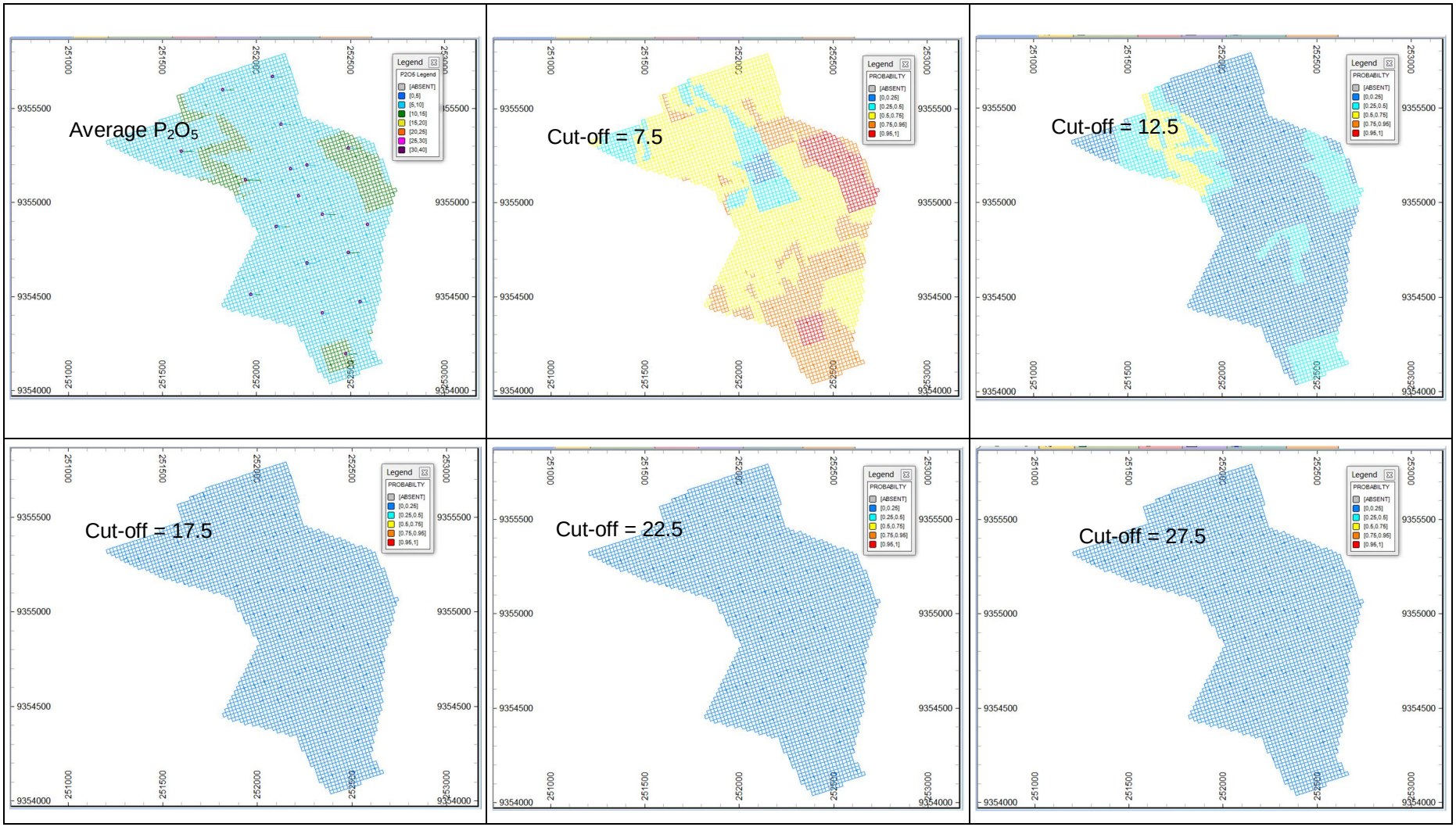


Figure 7.2.2_2: The maps of BL showing the average P_2O_5 grade and proportions of materials above the cut-off.

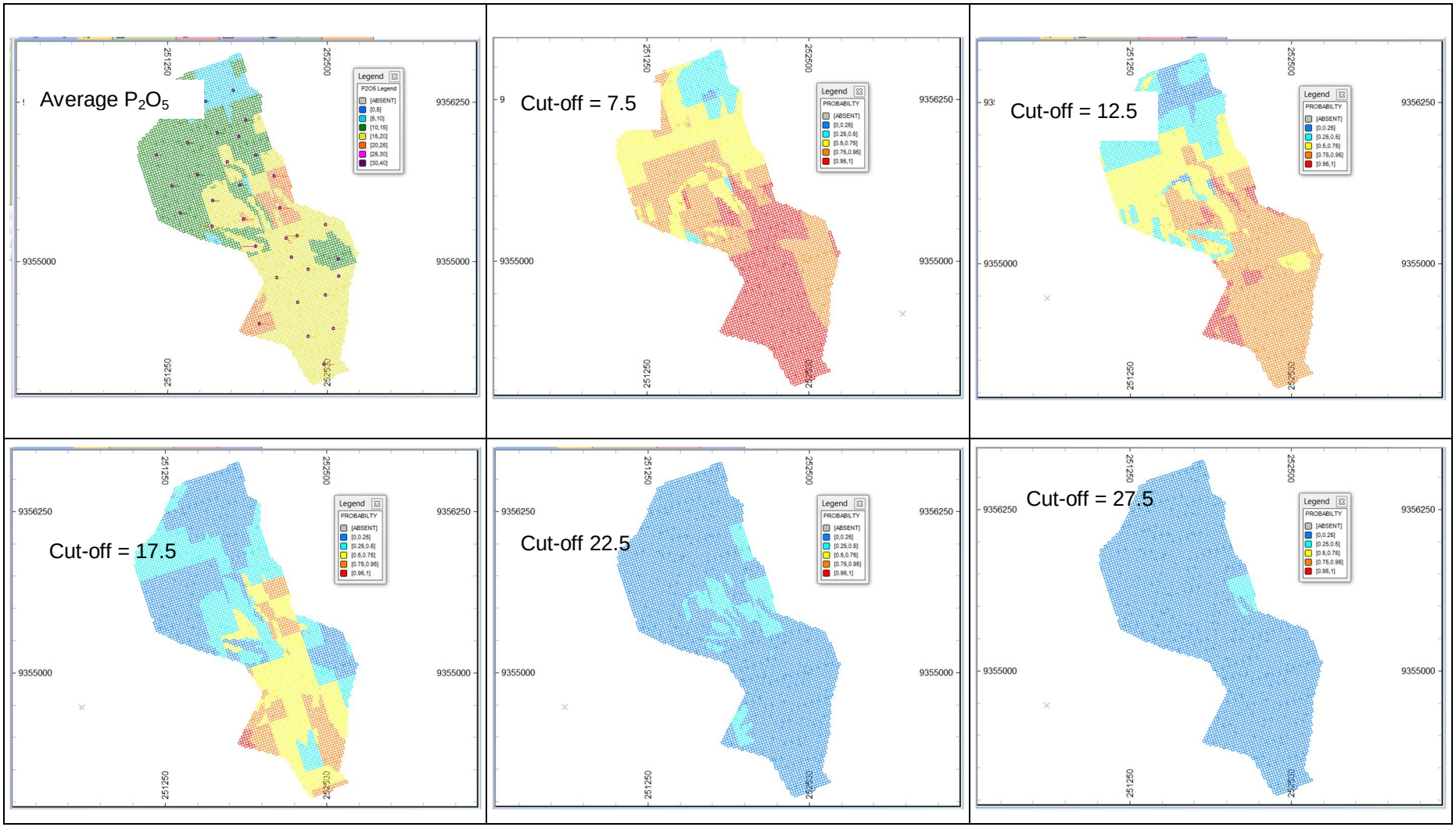


Figure 7.2.2_3: The maps of ML showing the average P_2O_5 grade and proportions of materials above the cut-off.

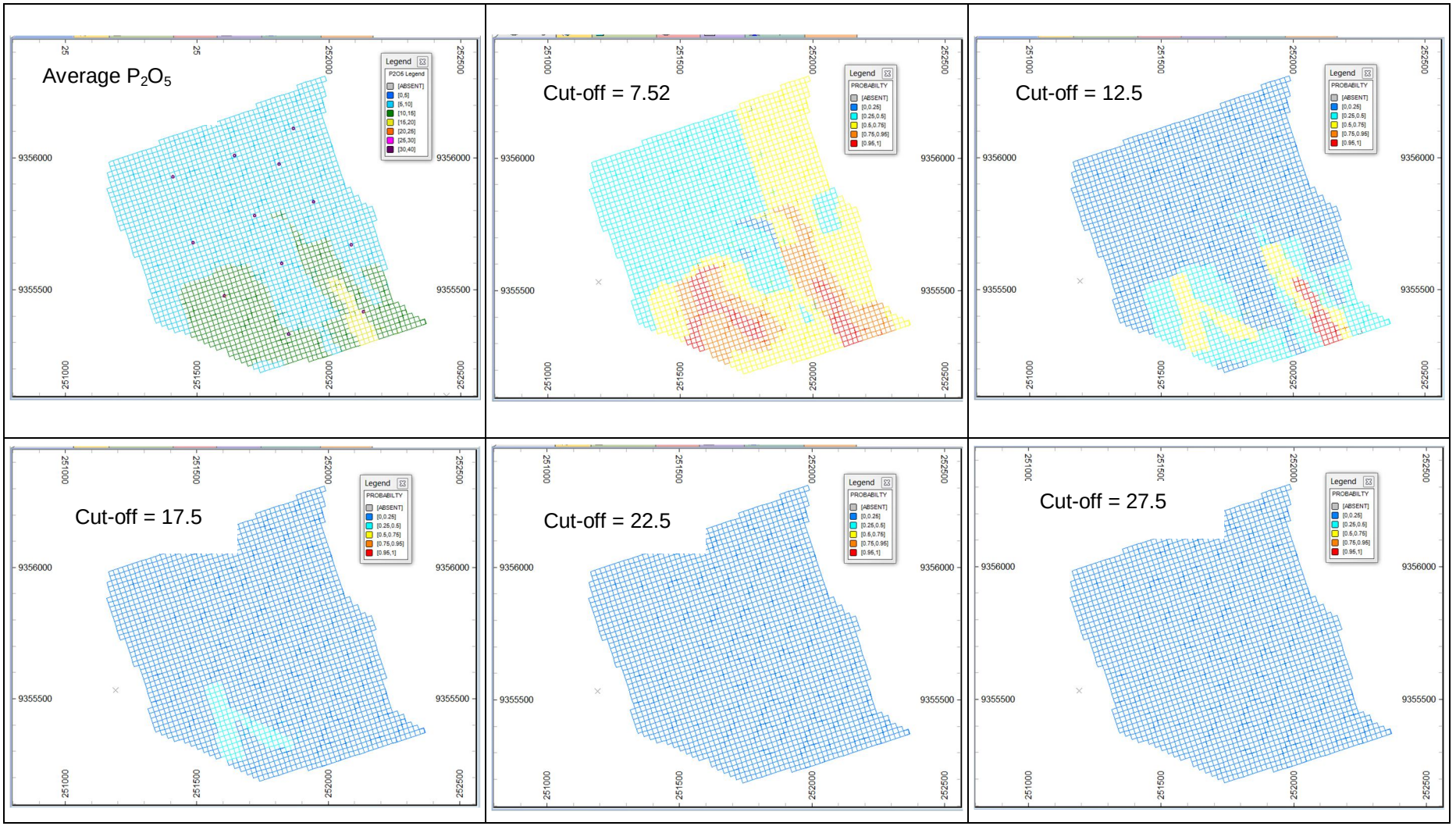


Figure 7.2.2_4: The maps of TL showing the average P_2O_5 grade and proportions of materials above the cut-off.

Grade Tonnage Curves

The IK has the advantage of producing different variations of grade tonnage curves. Unlike the OK and IDW that produced only single grade tonnage curves, the IK produced the traditional grade tonnage curves and grade tonnage curves for all indicator cut-offs (Figure 7.2.2_5 to 7.2.2_7).

Traditional grade tonnage curves

The total tonnages of the grade above the cut-off can be calculated by using the

$$Total\ Tonnage\ above\ the\ cut-off\ =\ total\ block\ tonnage\ X\ proportion\ above\ the\ cut-off$$

All the traditional grade tonnage curves derived from the IK technique defined all ranges of the grades (Figure 7.2.2.5). The results are easily interpreted and the mine planning, processing or mineral resource studies can be conducted on both the curves. There are good definitions of the grades and tonnages. More tonnages at higher grade can be mined from the ML and North Geo-Zone.

Because of the use of indicator intervals, the smoothing effect was minimized. The higher and lower grades were well estimated. This showed that the IK is a good method in dealing with the tails or outliers.

The grade tonnage curves for different indicator cut-offs

At an indicator cut-off of 7.5%, all the domains had defined the grades and tonnages above the cut-off (Figure 7.2.2_6). When the cut-off is raised to 12.5%, only ML and North Geo-Zone described the grade and tonnage better than the TL and BL (Figure 7.2.2_7). This meant that by raising the cut-off to 12.5%, only ML and North Geo-Zone could be mined economically. The other higher cut-offs (17.5, 22.5 and 27.5) could not produce grade tonnage curves as there were not enough tonnages above these cut-offs.

Total Tonnage above Cut-off

BL

There was a higher proportion of the tonnage reported when a cut-off of 7.5% is applied. The proportion of tonnages decreased rapidly when higher cut-offs was used. This was expected as BL is a low grade layer.

ML

There were high proportions of tonnages when the first three cut-offs were used. This is because the ML has high P_2O_5 grade. The last two cut-offs had low proportion of tonnage above the cut-off.

TL

The proportion of the tonnage above cut-off was low for both the cut-offs. This layer has the lowest proportions of tonnage above cut-off. The TL is a lower grade layer than ML.

North Geo-Zone

This domain is a high grade layer. The proportion of the tonnage above the cut-off was high for the first two cut-offs and moderate for the third cut-off. The last two cut-offs had low proportions of tonnages above cut-off. The grade tonnage curve for the North Geo-Zone is identical to that of the ML supporting that the two domains are the same.

The proportion of tonnage above the cut-off curves for different domains were simplified and presented in Figure 7.2.2_8.

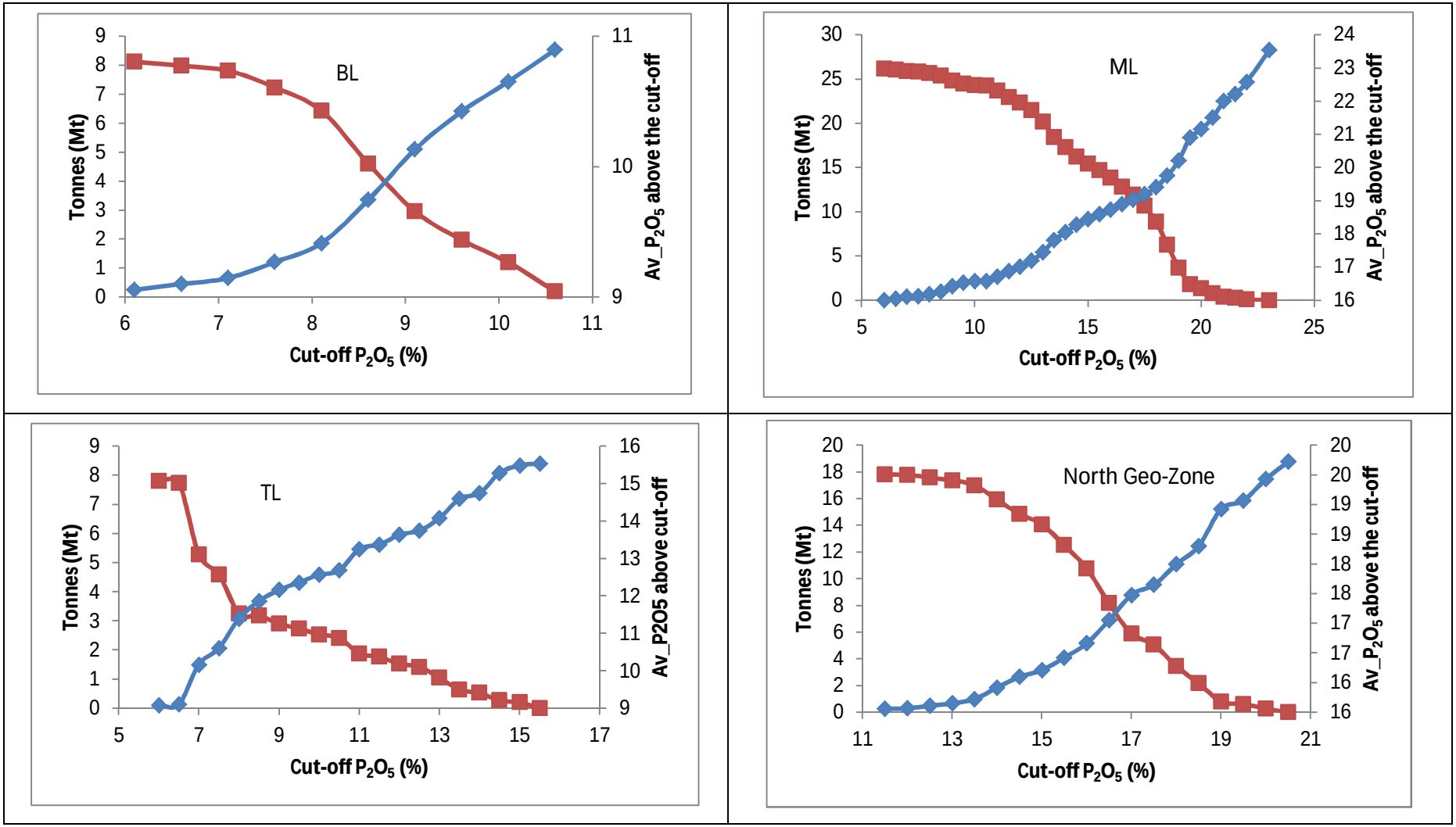


Figure 7 2.2_5: The grade tonnage curves modelled from IK.

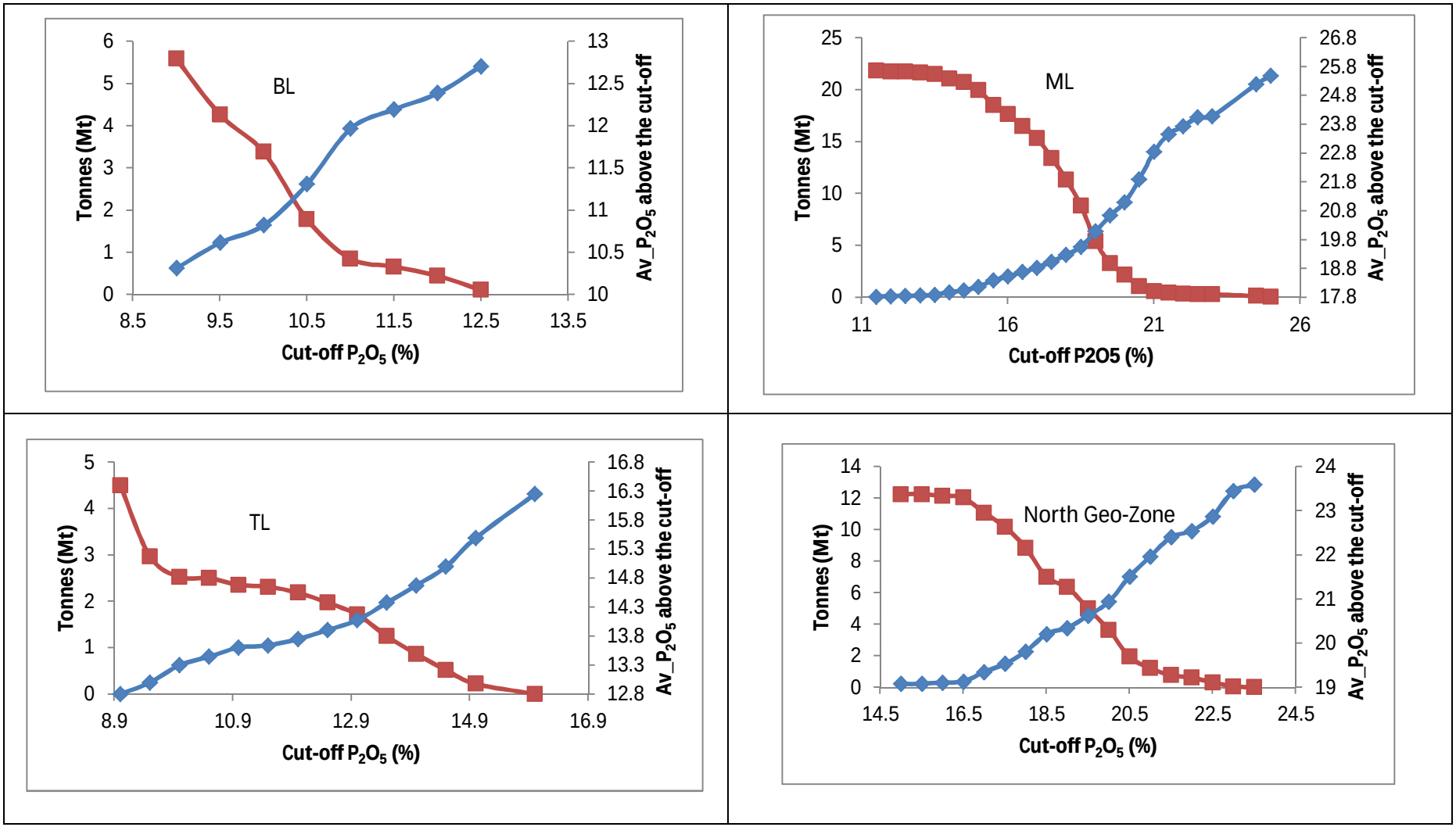


Figure 7 2.2_6: The grade tonnage curves modelled from 7.5% P_2O_5 indicator cut-off.

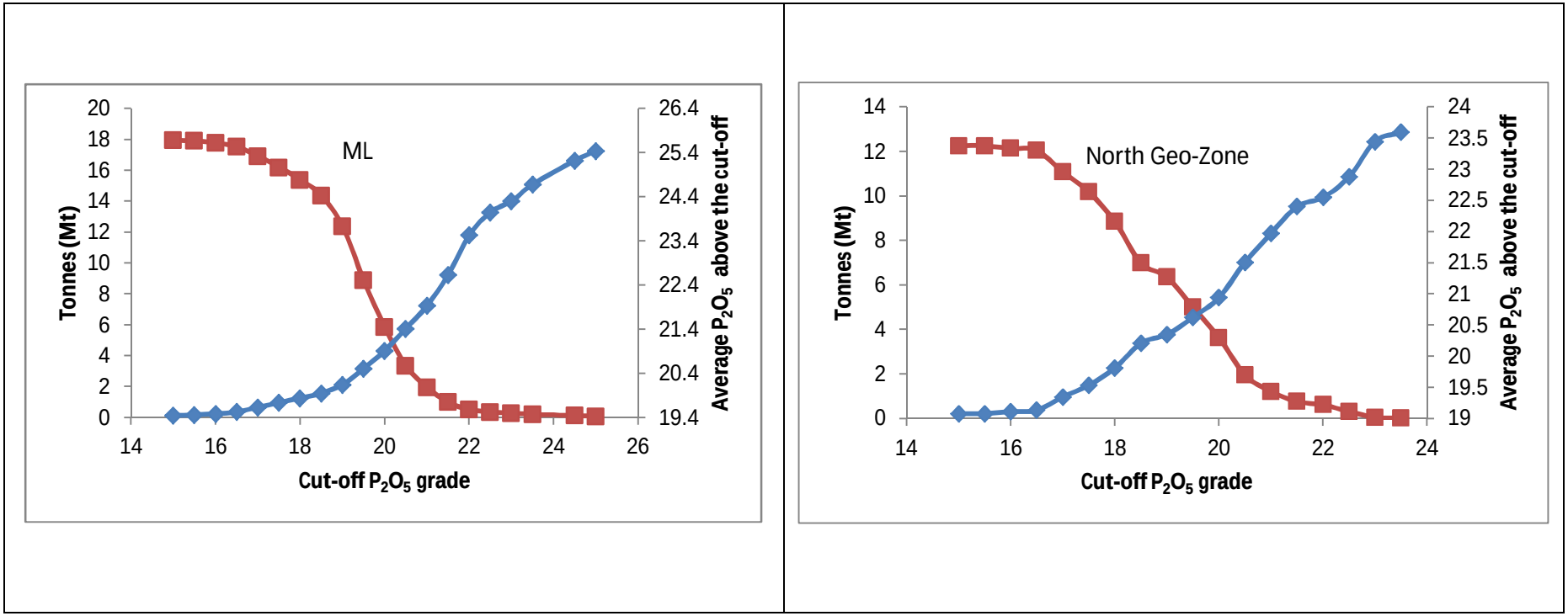


Figure 7 2.2_7: The grade tonnage curves modelled from 12.5% P_2O_5 indicator cut-off.

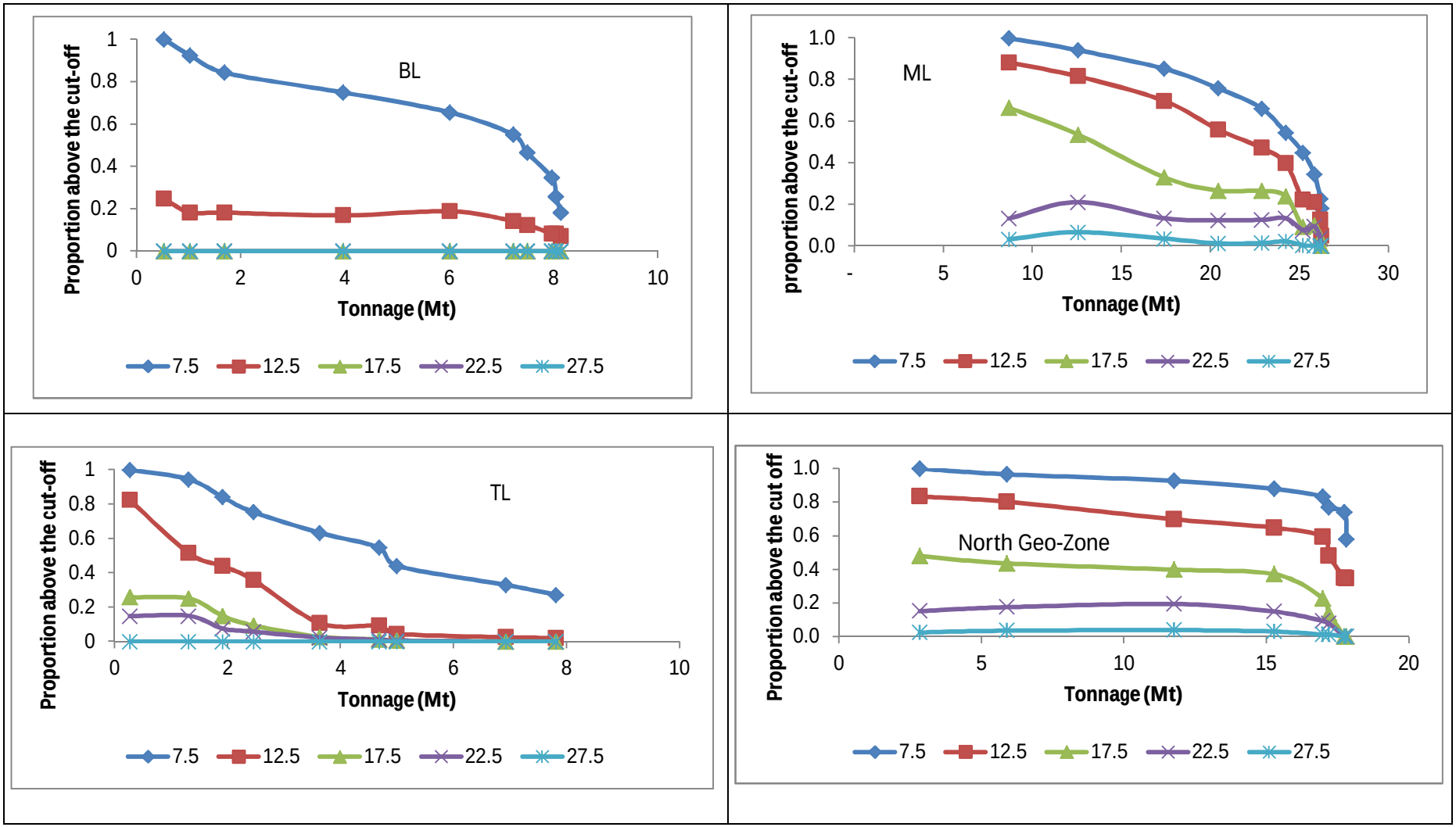


Figure 7 2.2_8: Proportion and Tonnage above the cut-off curves.

7.3 Summary Findings on the IK

The IK is a non-linear geostatistical technique that uses the indicator transformed data points. Different cut off intervals were defined. The coding of 0 and 1 was used to define if the data should be included in the defined cut-off intervals.

The median IK was used because of its simplicity and paucity of data. The median IK assumed that all variograms of the indicator transformed cut-off intervals were identical and the median variogram was used in the estimation. All but one layer has two structure variograms. All variogram models were spherical.

The nugget effect was determined using the downhole variograms of the defined median. Kanzi phosphate project has low nugget effect as shown by the downhole variograms.

The determination of the cut off was motivated by processing and mining factors other than using deciles or quartiles. These cut-off intervals were practical and relevant to the study. The selected cut-offs were 7.5%, 12.5%, 17.5%, 22.5% and 27.5%. These cut offs were used in all the domains.

The estimation was carried out in the geological model defined in section 5. This was done so that the results of the IK may be compared to the results of the linear methods. No negative weights were identified.

The average P_2O_5 grade, proportion above the cut-off and average grade above the cut off were studied. The IK as a non-parametric method, produced results that correlated well with the raw data. The smoothing effect was very low.

The probability maps for different domains were analysed. The probability of getting grade above first cut-off (7.5%) was high for both domains. The probability of getting grade above the second cut off (12.5%) was high for North Geo-Zone and ML. The BL and TL have low probabilities of getting the grades above the second cut-off. All domains except ML had low to zero probability of achieving grade above the third (17.5%) cut-offs. ML had high probability in the south and low probability in the north. All domains had low probability of achieving grade above the fourth (22.5%) and fifth (27.5%) cut-offs.

The proportion and tonnage above the cut-off curves for all domains were constructed. The curves showed that when higher cut-offs are applied, the proportion of the tonnage above the cut-off is reduced. These curves can be used to select an appropriate cut-off for mining and processing methods.

8 INTERPRETATION AND DISCUSSION OF RESULTS

8.1 Introduction

The linear (OK and IDW2) and non-linear (IK) methods were used in the global resource estimation of Kanzi Phosphate project. This chapter presents a comparative analysis and discussion of the methods used. The comparison is based on the average grade estimated, risk assessment of the estimated grades/tonnages, grade tonnage curves and practical application to mining projects. A ranking summary is given at the end of this chapter.

8.2 Comparison of the estimated P_2O_5 grades

The average grades estimated using linear methods are highly smoothed. The grade distribution has a narrow spread indicating that the estimated grades have a low variability. The average grades from the IK were not highly smoothed and the grade distributions for different domains were fairly reproduced. The variability of the estimates produced by the IK method was higher than the variability of the estimates produced by the IDW and OK methods. This is because the IK used indicator transformed data points to conduct estimation.

The linear methods estimated average P_2O_5 grade only and the IK estimated both the average grades and average grades above the defined cut-offs. This made IK more useful than the linear methods as the IK outcomes could be used for different studies to enhance understanding of the mineralization and viability of the ore body.

8.3 Risk Assessment

The IDW had no reasonable measure of uncertainty in the estimated grade. However the estimated grades were validated using cross-validation, mean-to-mean comparison and swath plots if there is enough data. Kriging has as an advantage a measure of uncertainty through the kriging variance. The problem with the kriging variance is that it is more dependent on the configuration of data than the actual values. The kriging variance did not solve the issue of uncertainty in the accuracy of estimates.

As a probabilistic method, the IK provided proportions above the cut-offs. This allowed the probability maps to be drawn and analysed. This is a good measure of uncertainty for a mining project especially for selective mining. Many mining companies would like to generate more cash in the early stages of extraction. Probability maps could help in planning for selective mining.

8.4 Grade Tonnage Curve Analyses

8.4.1 Traditional Grade Tonnage Curves

The traditional grade tonnage curves produced by the OK, IDW and IK methods are presented in Figure 8.4.1_1. In general the grades reported by the IK methods lies between those reported by the OK and IDW methods.

BL

The grade tonnage curves produced by the IDW and IK methods are identical. These grade tonnage curves defined all ranges of the grades and could be used in defining the Mineral Resources better. The OK method produced a grade tonnage curve that is not well developed.

ML

The grade tonnage curves from both methods are identical. The minor difference is at the high grade values. All the grade tonnages can be used for Mineral Resource reporting.

TL

The grade tonnage curves produced by the IDW, OK and IK for the TL do not define the grade ranges well. This domain has very few data points. The confidence on the estimation results is low.

North Geo-Zone

The tonnages and grades reported by the OK and IK methods are identical with IK method reporting slightly higher grades than OK grades. The IDW reported higher grades than the grades produced by the OK and IK methods.

8.4.2 Grade Tonnage Curves from different cut-offs

The IK estimated the global recoverable tonnages for different cut-offs. The proportion of the tonnages above the defined cut-offs were studied in detail. The linear method estimated the total global resources and an assessment could be done on the recoverability based on different cut-offs through the kriging variance.

The grade tonnage curves from the linear methods are affected by smoothing effect. This smoothing effect was inherited from the estimation methods used. Because of the use of indicators, smoothing effect was minimized when the IK was used.

The grade tonnage curves from OK and IDW consider all blocks above the cut-off mineable or accessible. The curves assume that the blocks are in one continuous area. These curves cannot be used in selective mining strategies. The IK method give the proportion of the SMU distributions within a block and this is valuable for mining studies.

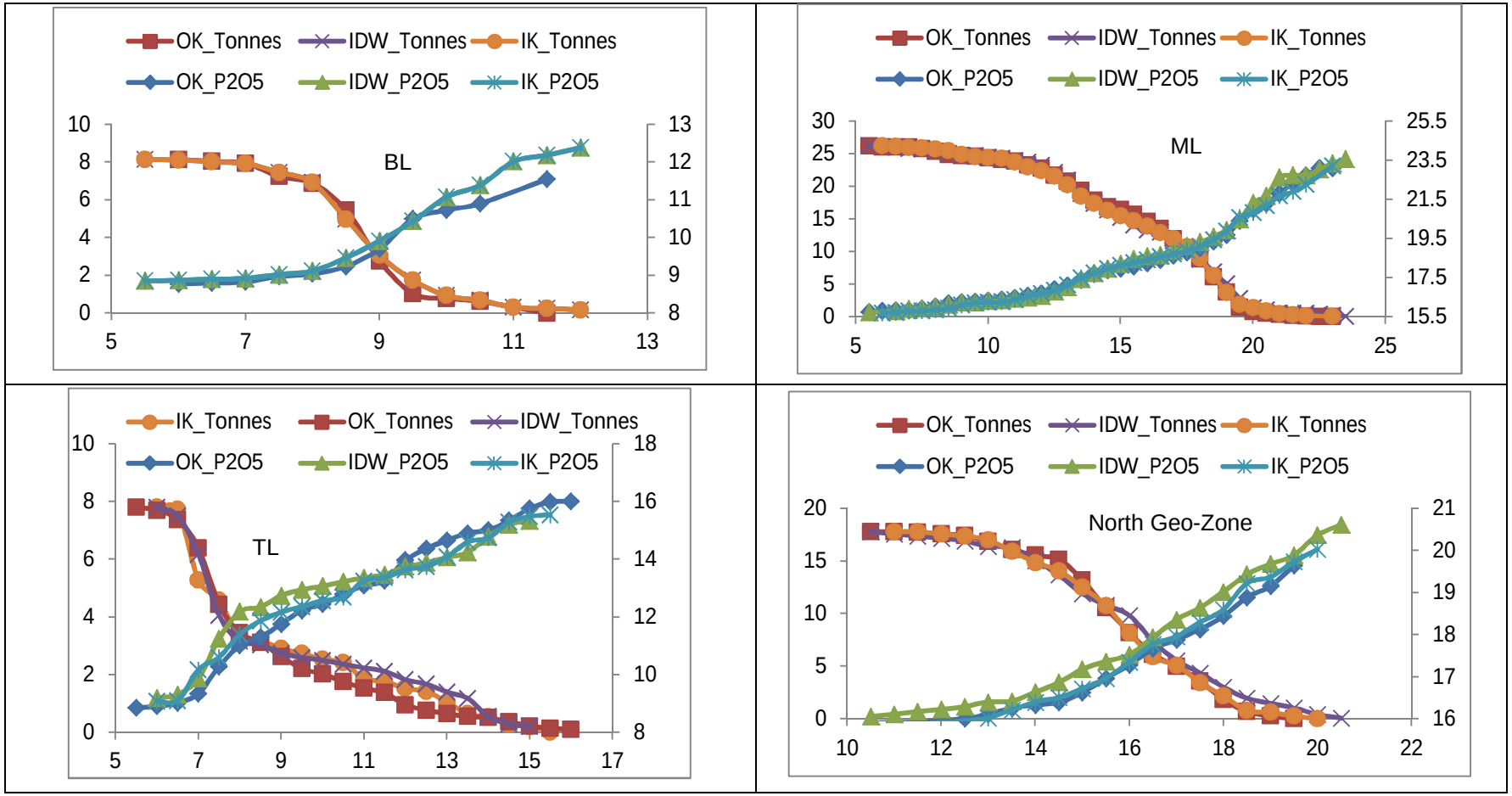


Figure 8.4.1_1: The Traditional Grade Tonnage Curves produced by the OK, IDW and IK methods with left Y, right Y and X axes representing tonnages (Mt), average grade above cut-off (%) and cut-off grade (%) respectively.

8.5 Practical Application to Mining Projects

Both linear and non-linear methods are relevant to mining projects. Linear methods (OK and IDW) were easy to use. The non-linear method (IK) was more advanced than linear methods and provided advanced solutions that can be used to minimize the risks in mining investment. The pre and post processing of the IK is tedious.

The OK and IDW methods helped in defining the global mineral resource. The IK estimated the recoverable global resources and gave good measure of uncertainty in the Mineral Resource. The IK methods produced probability maps that can aid in assessing uncertainty.

For Kanzi Phosphate Project, the local variability of the grades is more important than the mean grade. As Kanzi phosphates upgrades differently based on the grade, local variability will help in process designs and blending strategies. The IK method defined the local variability better than the IDW and OK methods.

8.6 Ranking of the estimation techniques used

The three methods were used in the estimation of the mineral resource for Kanzi phosphate project. These methods produced different results because they use different algorithms. The following ranking specifically to the estimation of Kanzi phosphate resource is based on the overall performance of the methods:

1. IK

2. Ordinary Kriging and Inverse Distance Weighting

The IK produced better results than OK and IDW because it used the cut-off intervals and indicators to estimate. It did not assume the population distribution. The smoothing effect was minimized and probability maps were produced.

For Kanzi Phosphate Project, OK and IDW produced identical results. They are ranked the same. The OK method performs better when there is enough data and domains are well defined whereas IDW2 as a non geostatistical method works better when there is less data. When same estimation parameters and search volumes are used the OK and IDW methods produce identical result.

8.7 Estimation of other crucial variables

The linear regression was used to determine the SiO_2, Al_2O_3, and CaO. The TiO_2 was determined using the correlation matrix. The confidence on TiO_2 values is low. Table 8.7_1 shows the formulae used to estimate the values for major variables

Assumption made was that the relationship was constant throughout the domains.

Table 8.7_1: The formulae used to estimate SiO_2, CaO, Al_2O_3 and TiO_2

	BL	ML	TL	North Geo-Zone
SiO_2	$-0.3738P_2O_5+34.08$	$-1.3418CaO+70.75$	$-1.346CaO+67.24$	$-1.4667CaO+76.14$
CaO	$1.3655P_2O_5+0.16$	$1.3154P_2O_5+1.94$	$1.2565P_2O_5+1.44$	$1.4406P_2O_5-1.96$
Al_2O_3	$-0.0938CaO+4.86$	$-0.1974CaO+10.17$	$-0.2291CaO+11.62$	$-0.1207CaO+7.85$
TiO_2	$0.40\ Al_2O_3$	$0.89\ Al_2O_3$	$0.92\ Al_2O_3$	$0.72\ Al_2O_3$

9 CONCLUSION AND RECOMMENDATIONS

9.1 Introduction

This chapter presents the conclusion and recommendations for future work on Kanzi Phosphate Project to advance the geostatistical understanding of the phosphates and minimize the risks during mining and processing stages.

9.2 Conclusion

9.2.1 Methods and their outcomes

The understanding of geology and mineralization style of the Kanzi Phosphate Project helped in mapping and domaining the different layers. Four different layers were identified based on geology and geo-chemistry. The phosphates in Kanzi are of apatite origin with some dolomite and clay matrix in places. This formed the foundation upon which the evaluation of the Mineral Resource could be done.

The domain populations are nearly normally distributed. There are some spatially integrated sub-domains. The Kanzi phosphate samples have no identifiable outliers. The variability of grades is not very high.

The linear methods are easy to use. They provided a good global resource estimation. As the distribution of grades in the mineral deposits is never purely symmetrical, the linear methods should be used as a starting point to understand the Mineral Resource behaviour and non-linear methods should be used to study the probabilistic nature and grade-tonnage distribution of the mineral resources.

The mineral extraction industry is a high risk business. The risks are exaggerated by low availability of data as the cost of acquiring data is high. The advanced mineral resource estimation techniques are needed to quantify risk. The probabilistic methods are sophisticated to use but they can help in defining the recoverable resources and an assessment of uncertainty.

The Table 9.2_1 presents the concluding remarks on the three methods studied.

Table 9.2_1: The performance measure of the three techniques on the Kanzi Phosphate Project

Aspect	IDW2	OK	IK
1. Easiness of the method	The IDW method was the easiest.	The OK method was easy to use but construction of variography took time.	The IK method is tedious as pre-and post-processing takes time. The method is very advanced. Many variograms are modelled.
2. Data amount requirements	The IDW method worked well with less data as it did not assume the spatial relationship. The inverse distance relationship was assumed.	More data is required as assumptions about stationarity need to be met.	Moderate amount of data is required. The method is non-parametric. There is no need for assumptions about the stationarity
3. Global Resource Estimation	The IDW method produced estimates that are good for global resources.	The OK method produced results comparable to IDW.	The IK produced results identical to IDW and OK for the global resources.
4. Smoothing Effect	The smoothing effect was moderate.	The smoothing effect was moderate.	The smoothing effect was very minimal.
5. Recoverable Resources	There was no good decisive measure of recoverable resources.	There was no good decisive measure of recoverable resources. Kriging variance is not enough.	The use of processing cut-offs allows for a better understanding of the recoverable resources.
6. Grade Tonnage Curves	The IDW method produced grade tonnage curves that could be used in stating the global mineral resources.	The OK method produced grade tonnage curves that could be used in stating the global mineral resources.	The IK produced grade tonnage curves that could be used in assessing both the global and the recoverable mineral resources.
7. Risk Assessment	Risk assessment could not be conducted with high confidence. The block variance could be used to understand and measure uncertainty.	The kriging variance produced by OK could not be used with high confidence to assess the risk.	The probability maps produced by IK for each cut-off could be used with high confidence to assess the risk associated with mine planning.

9.2.2 Implications of applying IDW, OK or IK in Mineral Resources studies

Confidence on the Mineral Resources estimation

The Mineral Resource derived from both the IDW, OK and IK methods are acceptable. The use of IK in the estimation of Kanzi Phosphate project increases the confidence on the grades and tonnages. Unlike the IDW and OK, the IK minimizes the smoothing of the grades.

Value-add

The technical understanding increased when the IK was applied. Because the IK outcomes can be post-processed; many technical variables such as probability data can be derived.

The use of Mineral Resource data derived from three techniques in the feasibility study or mining

The results of IDW, OK and IK methods could be used in the feasibility study or mining. The IK method provided more information that could be of great help in accessing the uncertainty and provides opportunity to mine selectively and improve on the processing. The financial model could be based on the Mineral Resources from IK as it produced more useful results overall.

9.3 Recommendations

This study recommended the following so that the understanding of Kanzi Phosphate deposit can be enhanced and consequently reduce the risks involved:

9.3.1 Conduct Conditional Simulation Studies

Simulation of the deposit identifies the real variability of the characteristics of the resources and reserves. It produces a histogram and a variogram of a random function (Journel & Huijbregts, 1978). Due to its robustness in re-producing true variability, simulation can be used in risk and sensitivity analyses and evaluation of results under constraints (Deraisme, et al., 2004). Simulation models can also offer an opportunity to measure the range of impact of the grade variability over several equally likely models.

Simulation offers an advantage over kriging. Because kriging is based on a local average of the data, it produced smoothed output. Simulation, on the other hand, can produce better representations of the local variability because it retains the local variability that is lost in kriging.

9.3.2 Twining using diamond drilling technique

Twining of 10% of the drillholes by the diamond drilling technique will help in gaining confidence on the mineralization in terms of layering and grades. Density measurements could be taken from core samples. This may increase confidence in the reported tonnage.

9.3.3 Variography

The Aircore drillholes that were recently done on the South-western portion for grade control purpose should be assayed and analysed for variography. This drillholes have 50m X 50m drillholes spacing and could provide structural information at short range that may be used in other less drilled areas.

9.3.4 Estimation of other variables

The overall quality of the phosphate deposit does not depend on P_2O_5 content only. All other crucial variables (CaO, SiO_2, Al_2O_3, and TiO_2) should be estimated using geostatistical methods. These will help in reducing the conditional bias introduced by estimating the CaO, Al_2O_3, TiO_2 and SiO_2 from P_2O_5 using linear regression relationship. These elements are crucial in processing, environmental or marketing issues. The estimation technique can be co-kriging or other techniques. This will give confidence on the quality of the mineral resource.

9.3.5 The processing studies of the phosphate mineralization

More studies on the processing or beneficiation of the Kanzi phosphate are recommended. The samples for process studies should be taken from all the different layers. This will help in characterizing all four domains.

10 REFERENCES

Armstrong, M., 1998. *Basic Linear Geostatistics.* Paris: Springer.

Bárdossy, A., 2000. *Introduction to Geostatistics,* London: University of Stuttgart.

Barnes, R., 2013. *Golden Software Inc.* [Online]
Available at:
http://www.google.com.au/url?sa=t&rct=j&q=&esrc=s&frm=1&source=web&cd=5&ved=0CEcQFjAE&url=http%3A%2F%2Fwww.goldensoftware.com%2FvariogramTutorial.pdf&ei=45pyUvPwO4vMswbosYCgBg&usg=AFQjCNHTehwv0kUdI3Py3Q3Hi1kZ8kZlXQ&bvm=bv.55819444,d.Yms
[Accessed 31 October 2013].

Body, K., 2013. *Mineral Resource Updates for Cabinda Phosphate Project, Angola,* s.l.: Unpublished.

Chilès, J. -P. & Delfiner, P., 1999. *Geostatistics: Modelling Spatial Uncertainity.* New York: Wiley.

Clark, I., 2000. *Practical Geostatistics.* London: Applied Science Publishers.

Coombes, J., 1994. *The art and science of resource evaluation.* Perth: Oxford.

Coombes, J., 1997. Handy hints for variography. *AusIMM Ironmaking Resources and Reserve Estimation,* pp. 127-130.

David, M., 1977. *Geostatistical Ore Reserve Estimation.* Amsterdam: Elsevier.

Deraisme, J. et al., 2004. *Isatis Software Manual,.* Paris: Geovariance and Ecole des Mines.

Deutsch, C. V. & Journel, A. G., 1992. *Geostatistical Software Library and User's Guide.* New York: Oxford University Press.

Diggle, J. P. & Ribeiro, P. J., 2007. *Model-based Geostatistics.* London: Springer.

Dohm, C., 2010. *Notes for Statistical and Geostatistical Methods in evaluation.* Johannesburg: University of the Witwatersrand.

Dominy, S., Noppe', M. & Annels, A., 2002. Errors and Uncertainty in Mineral Resource and Ore Reserve Estimation: The Importance of Getting it Right. *Exploration and Mining Geology,* 11(1), pp. 77-98.

Goovaerts, P., 1997. *Geostatistics for Natural Resources Evaluation.* New York: Oxford University Press.

Hohn, M., 1988. *Geostatistics and Petroleum Geology.* New York: Van Nostrand.

Isaaks, E. H. & Srivastava, R. M., 1989. *An Introduction to Applied Geostatistics.* New York: Oxford University press.

Journel, A. G. & Huijbregts, C. J., 1978. *Mining Geostatistics.* New York: Academic Press.

Juang, K.-W., Chen, Y.-S. & Lee, D.-Y., 2004. Using sequential indicator simulation to assess the uncertainty of delineating heavy-metal contaminated soils. *ScienceDirect,* Volume 127, pp. 229-238.

Leuangthong, O., Khan, D. & Deutsch, C., 2008. *Solved Problems in Geostatistics.* New Jersey: John Wiley & Sons.

Matheron, G., 1963. Principles of geostatistics. *Economic Geology,* Volume 58, pp. 1246-1266.

Minbos, 2013. [Online]
Available at:
http://www.minbos.com/assets/documents/asx/2013/minbosannualreportfortheyearended30june2013.pdf
[Accessed 25 October 2013].

Mudau, M., 2013. *Mineral Resource Updates for Kanzi phosphate project, DRC,* Johannesburg: Internal Report.

Olea, R., 1999. *Geostatistics for Engineers and Earth Scientists.* Boston: Kluwer Academic Publishers.

Penn, 2013. *Universtity of Pennsylvania.* [Online]
Available at: http://www.seas.upenn.edu/~ese502/NOTEBOOK/Part_II/4_Variograms.pdf
[Accessed 31 October 2013].

Rendu, J. -M., 1978. *An Introduction to Geostatistical methods of Mineral Evaluation.* Johannesburg: SAIM.

Rivoirard, J., 1994. *Introduction to disjunctive kriging and non-linear geostatistics.* New York: Oxford University Press.

Sama, A., 2011. *Quantitative Risk Analysis of Estimated Resources: An Overview ,* s.l.: s.n.

Silva, F. & Soares, A., 2013. [Online]
Available at: http://www.kgs.ku.edu/Conferences/IAMG//Sessions/D/Papers/silva.pdf
[Accessed 31 October 2013].

Snowden, V., 1989. Estimating Recoverable Reserves - Developments in Applied Geostatistics. *AIG Seminar*, November, pp. 4-7.

Thwaites, A. & Deraisme, J., 1998. *On the use of non-linear geostatistical techniques for recoverable reserves estimation: A practical case study.* s.l., s.n.

University of Edinburgh, 2013. [Online]
Available at: http://www.geos.ed.ac.uk/homes/s0198247/variograms.html
[Accessed 31 October 2013].

Vann, J., 2007. *Applied Geostatistics for Geologists & Mining Engineers,* Fremantle: Quantitative Group.

Vann, J. & Guibal, D., 1998. *An overview of non-linear estimation.* Perth, Geostatistical Association of Australasia.

Verly, G., David, M., Journel, A. & Marechal, A., 1984. *Geostatistics for Natural Resources Characterization.* 2 ed. Dordrecht: D. Reidel Publishing Co..

Wackernagel, H., 1998. *Multivariate Geostatistics.* 2nd ed. Paris: Springer.

Webster, R. & Oliver, A. M., 2007. *Geostatistics for Environmental Scientists.* 2nd ed. London: John Wiley & Sons Ltd.

Wikipedia, 2013. *Wikipedia.* [Online]
Available at: http://en.wikipedia.org/wiki/Coefficient_of_variation
[Accessed 25 October 2013].

Zanon, S. & Leyangthong, O., 2004. *Implementation Aspects of Sequential Simulation.* Dordrecht, Springer, pp. 543-548.

Appendix A

Maps and Cross-Sections

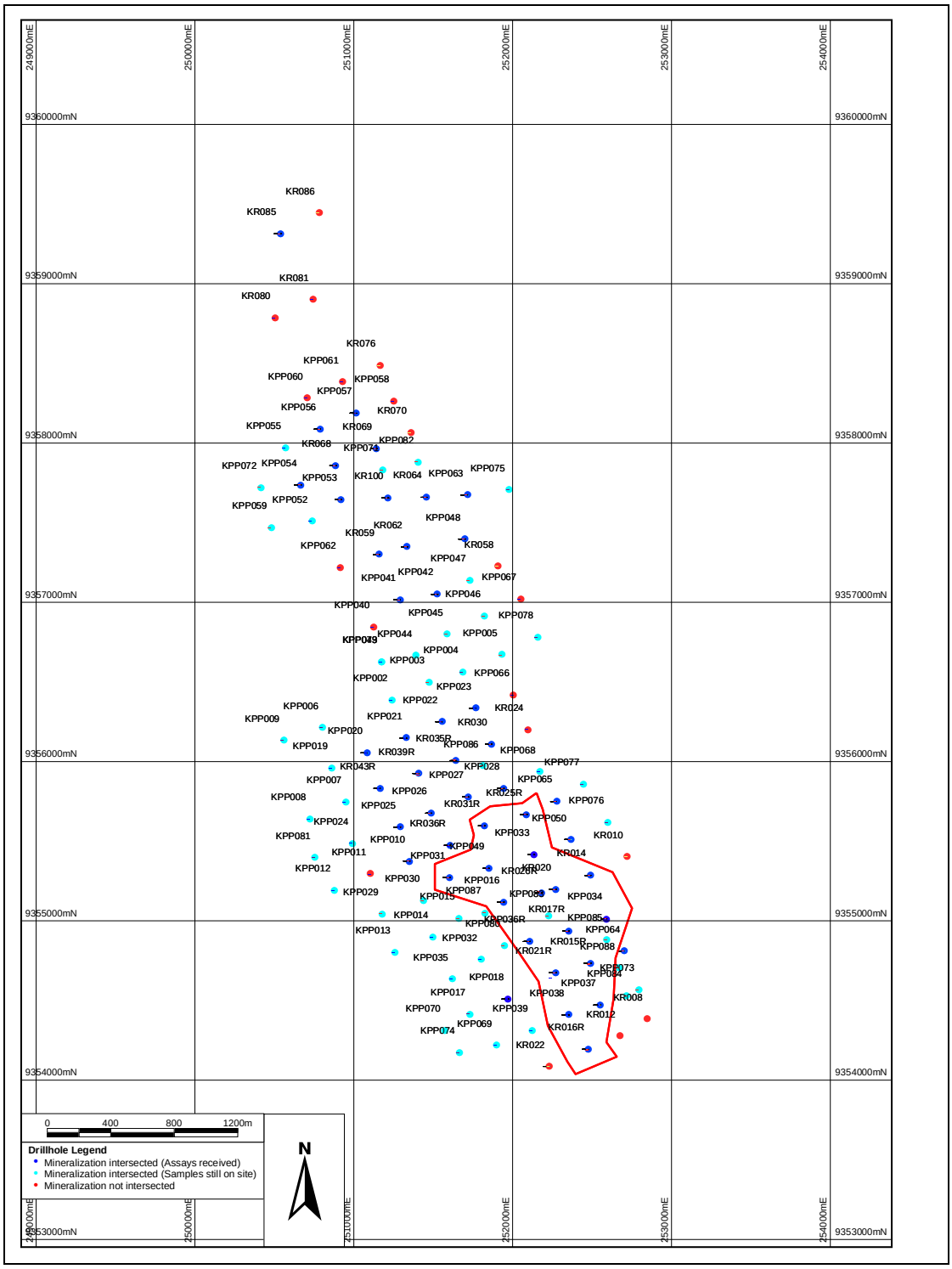


Figure A_1: Outline of the BL of the South geo-zone.

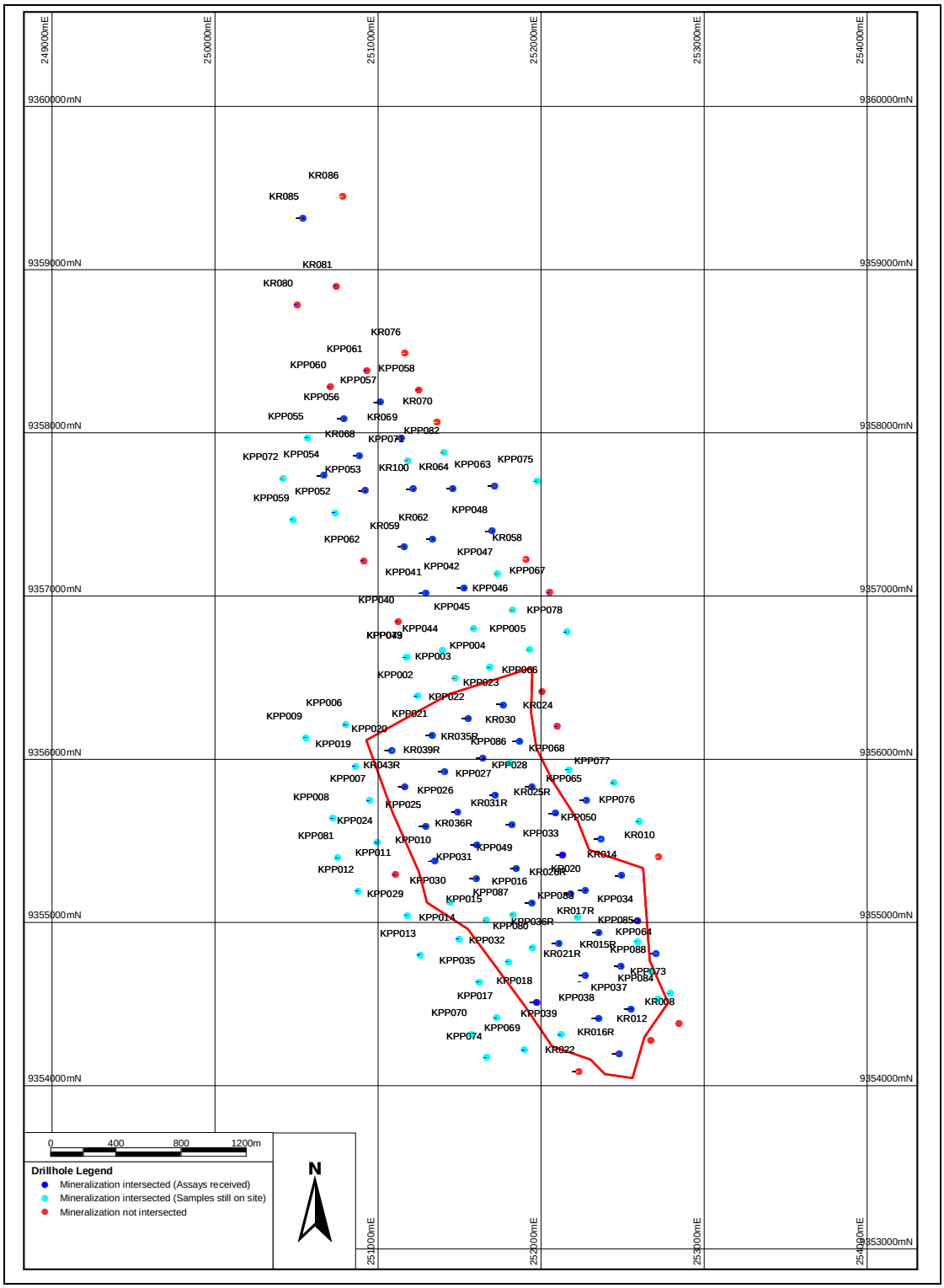


Figure A_2: Outline of the ML of the South geo-zone.

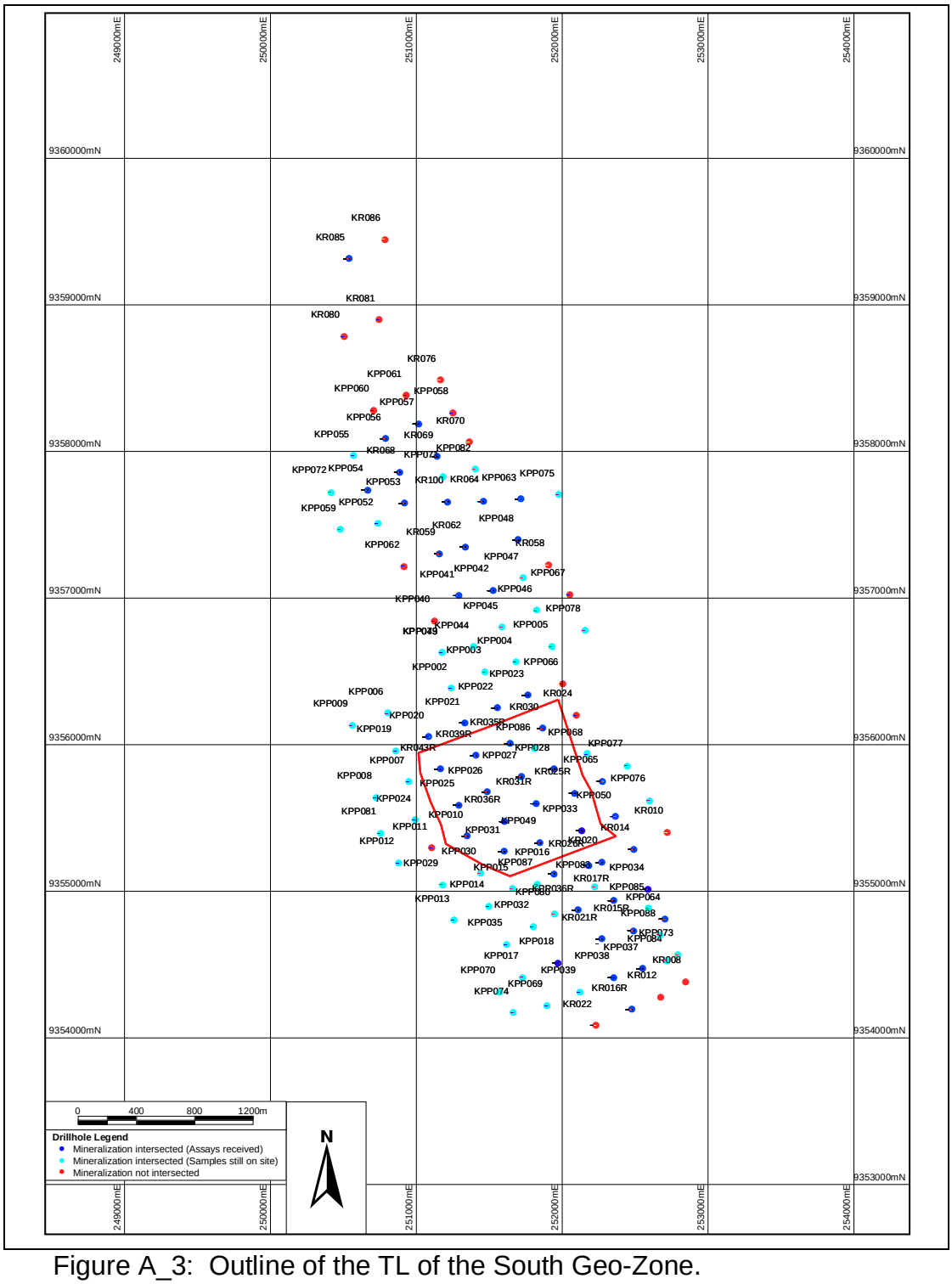


Figure A_3: Outline of the TL of the South Geo-Zone.

Appendix B

Histograms, descriptive statistics and correlation matrix

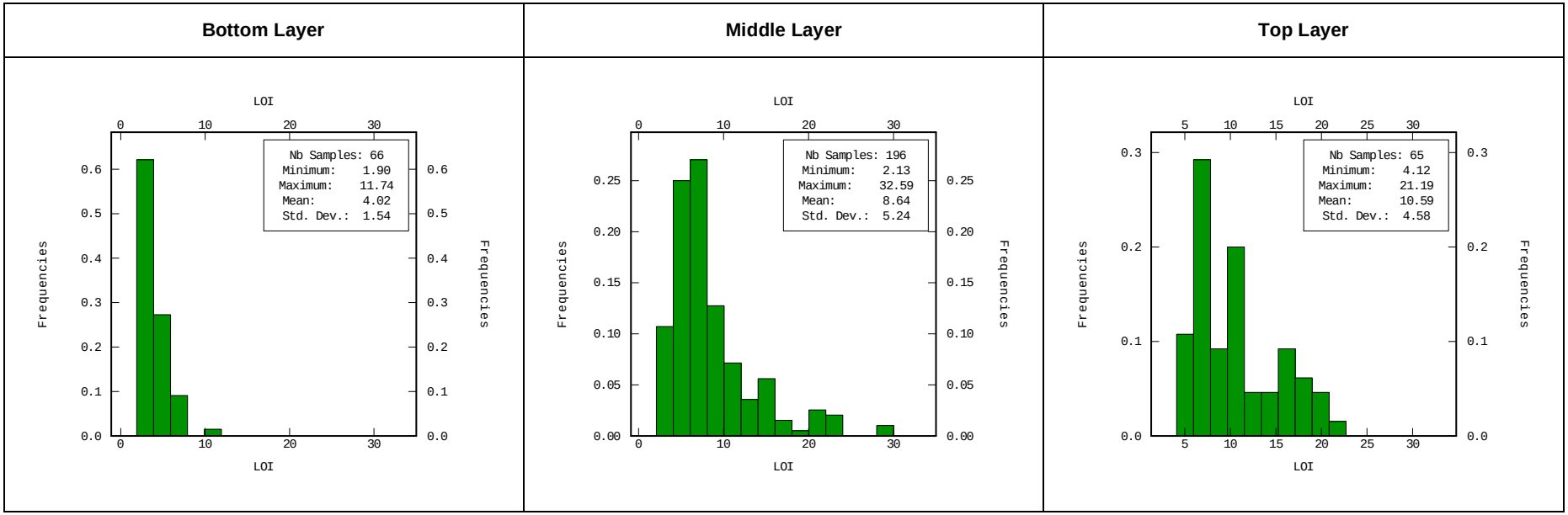


Figure B _1: Histograms for the layers in the South Geo-Zone showing the distribution of LOI.

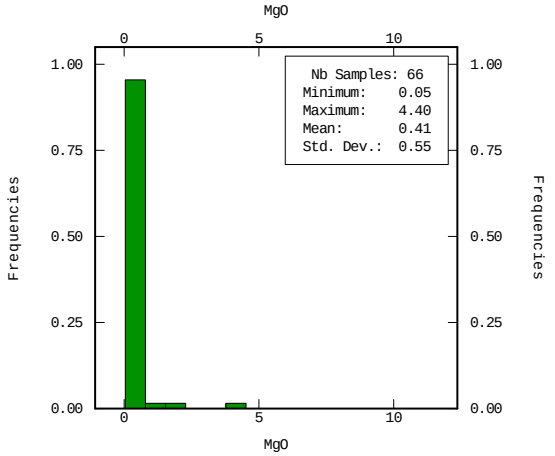
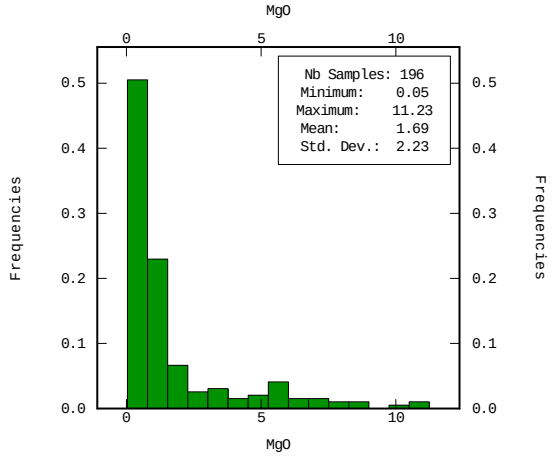
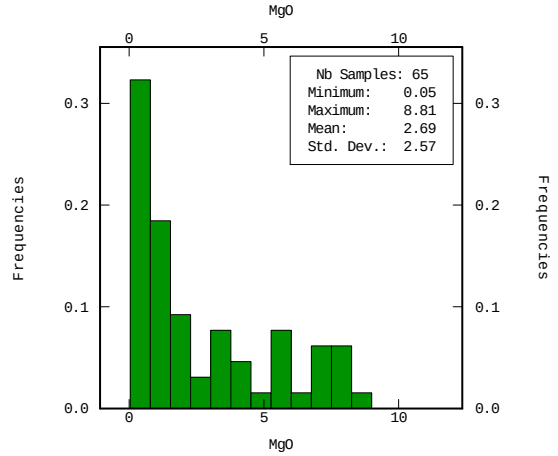
Bottom Layer	Middle Layer	Top Layer
		

Figure B _2: Histograms for the layers in the South Geo-Zone showing the distribution of MgO.

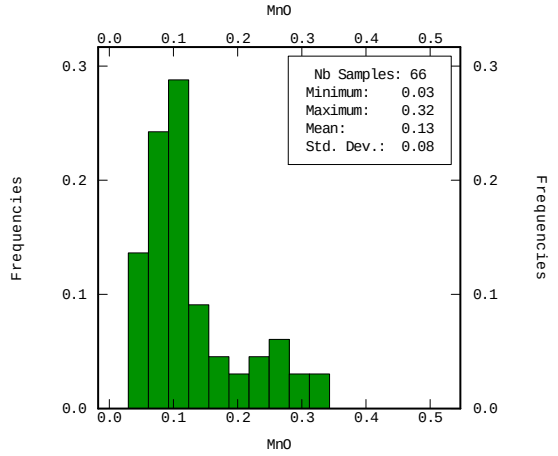
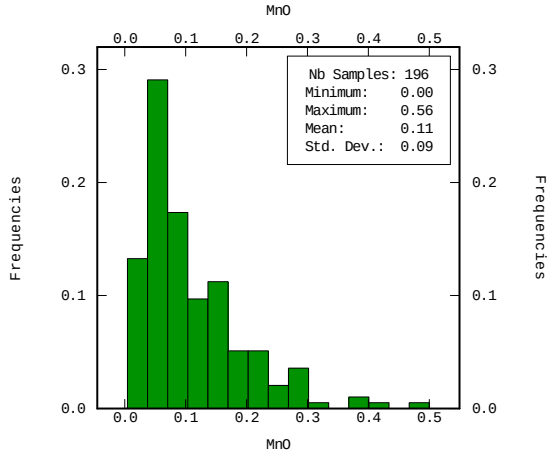
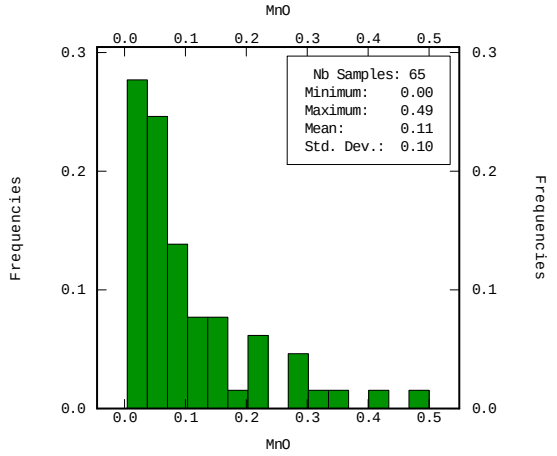
Bottom Layer	Middle Layer	Top Layer
		

Figure B _3: Histograms for the layers in the South Geo-Zone showing the distribution of MnO.

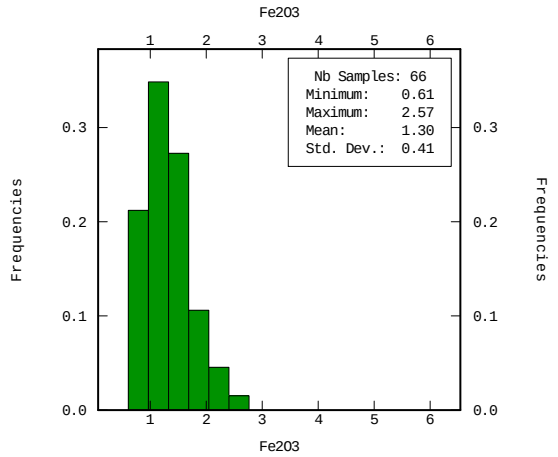
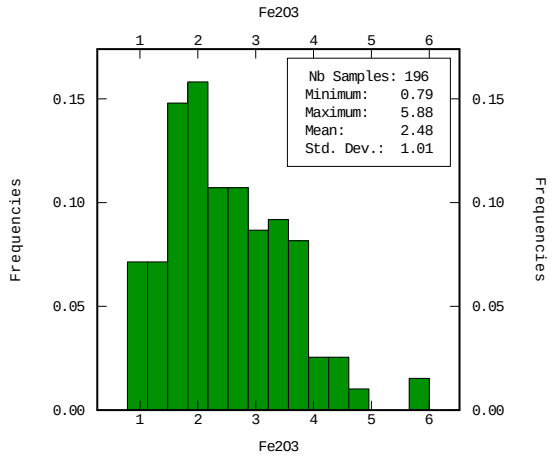
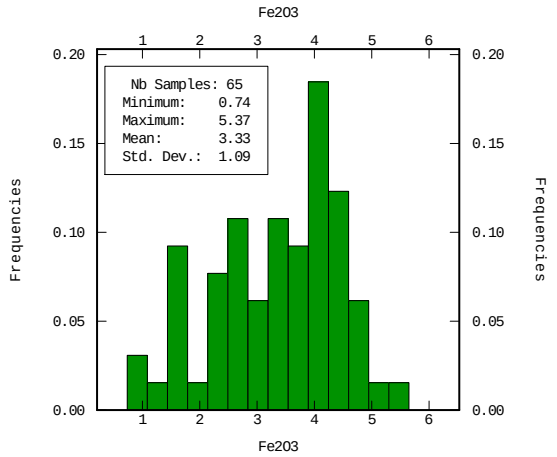
Bottom Layer	Middle Layer	Top Layer
		

Figure B _4: Histograms for the layers in the South Geo-Zone showing the distribution of Fe_2O_3.

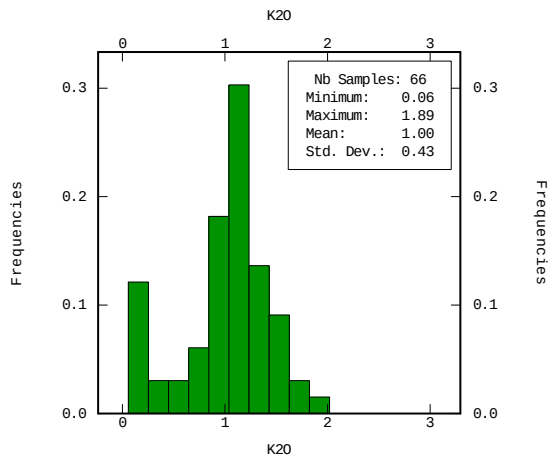
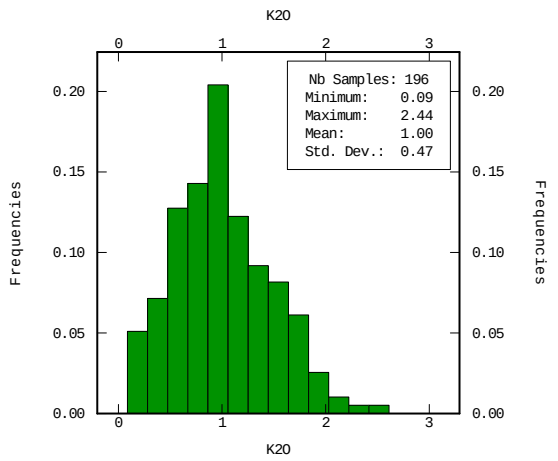
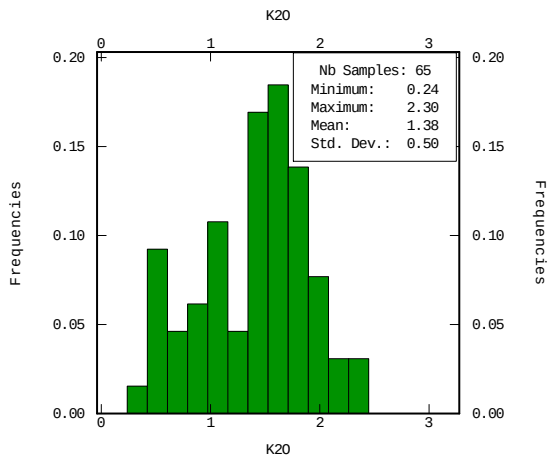
Bottom Layer	Middle Layer	Top Layer
		

Figure B _5: Histograms for the layers in the South Geo-Zone showing the distribution of K_2O.

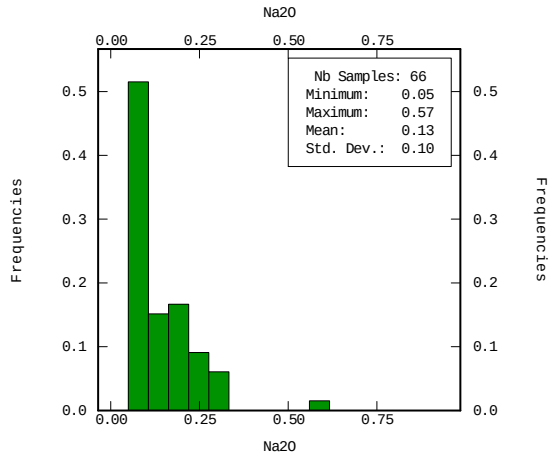
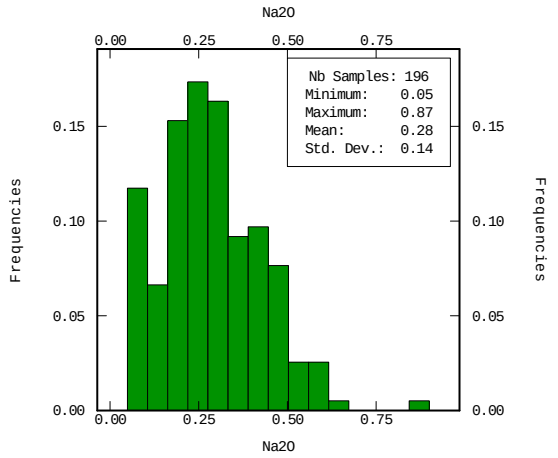
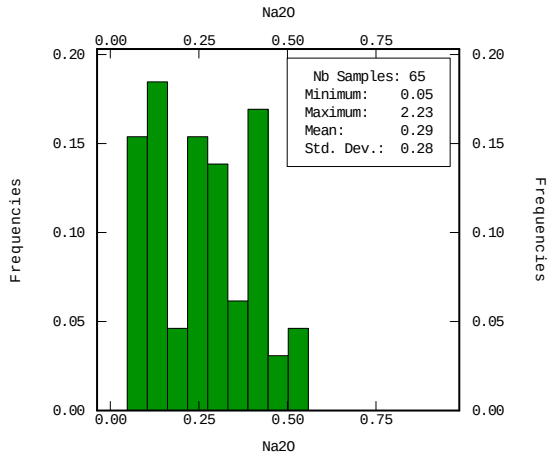
Bottom Layer	Middle Layer	Top Layer
		

Figure B _6: Histograms for the layers in the South Geo-Zone showing the distribution of Na_2O.

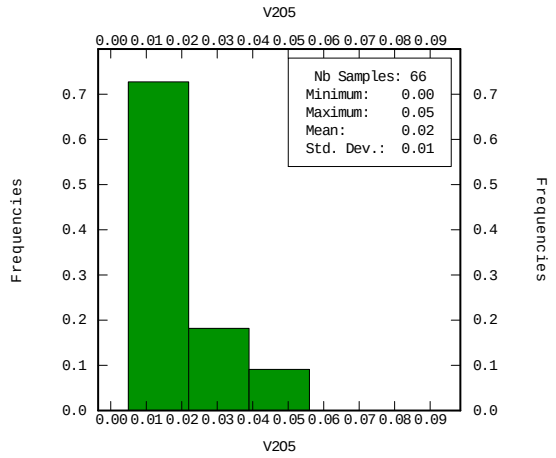
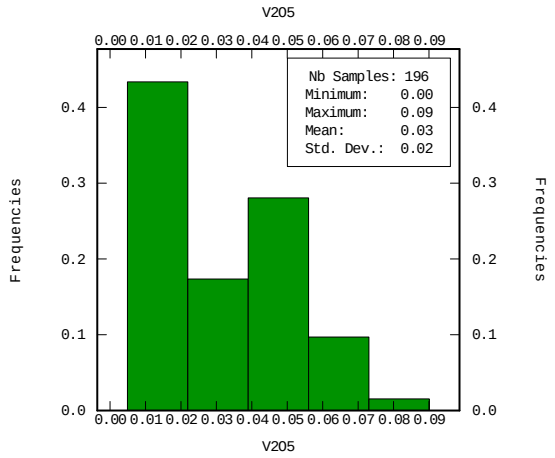
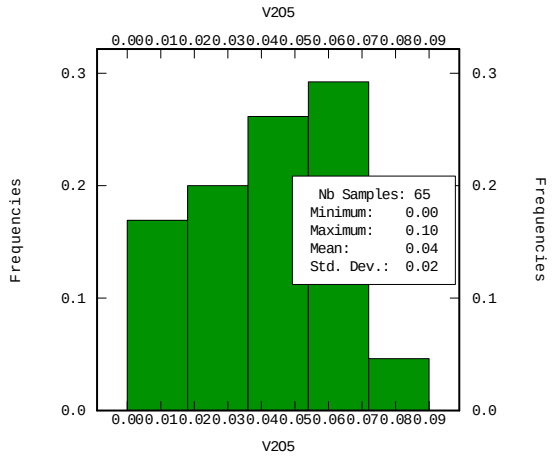
Bottom Layer	Middle Layer	Top Layer
		

Figure B _7: Histograms for the layers in the South Geo-Zone showing the distribution of V_2O_5.

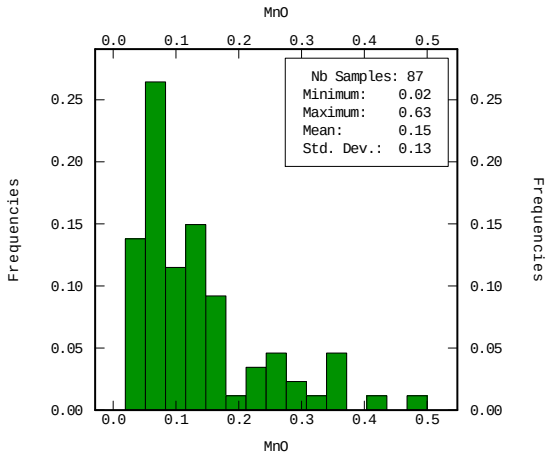
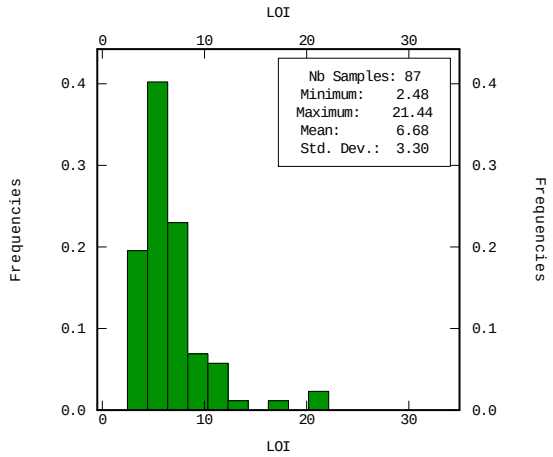
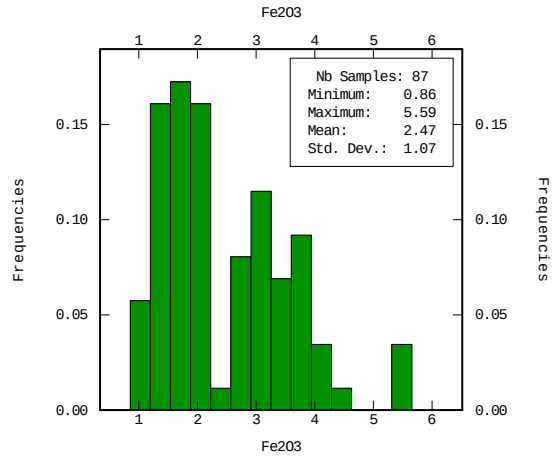
MnO	LOI	Fe_2O_3
		

Figure B _8: Histograms for North Geo-Zone showing the distribution of MnO, LOI and Fe_2O_3.

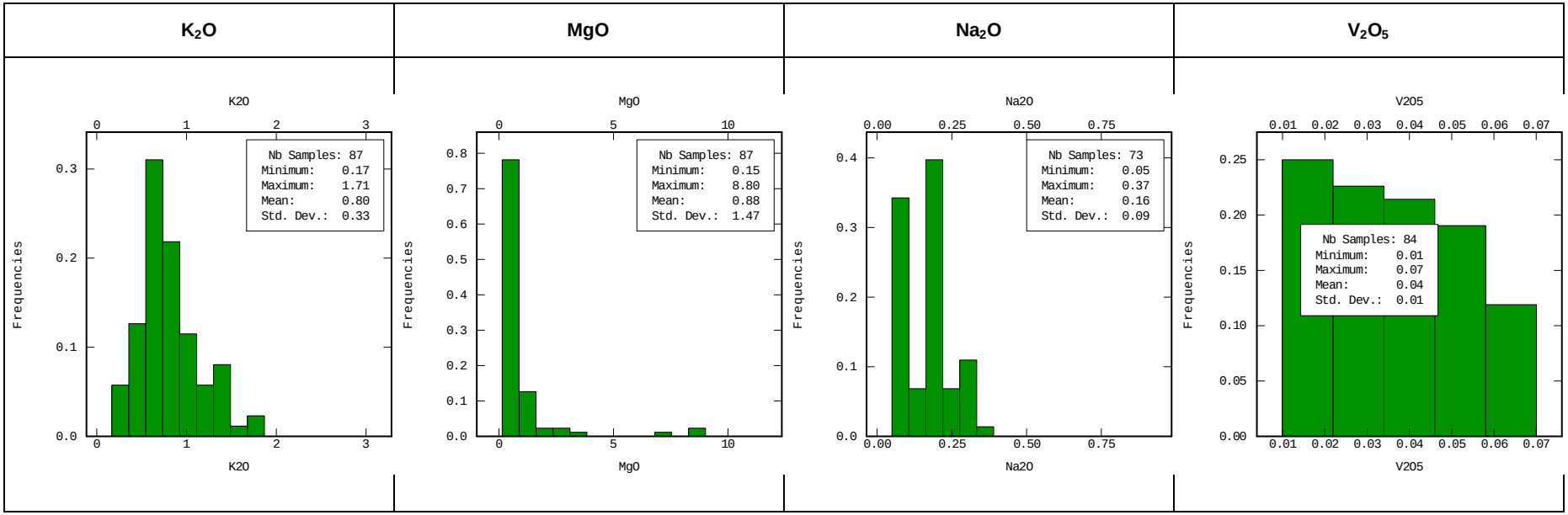


Figure B _9: Histograms for North Geo-Zone showing the distribution of different oxides.

Table B_10: Descriptive Statistics – South Geo-Zone

(Bottom layer)													
Element	Fe_2O_3	MnO	Cr_2O_3	V_2O_5	TiO_2	CaO	K_2O	P_2O_5	SiO_2	AL_2O_3	MgO	Na_2O	LOI
Mean	1.30	0.13	0.03	0.02	0.36	11.16	1.00	8.75	67.77	3.81	0.41	0.13	4.02
Standard Error	0.05	0.01	0.00	0.00	0.01	0.57	0.05	0.38	0.90	0.09	0.07	0.01	0.19
Median	1.27	0.10	0.03	0.02	0.36	11.15	1.08	8.85	68.57	3.65	0.31	0.05	3.71
Mode	1.37	0.10	0.03	0.01	0.29	6.40	1.01	5.62	59.90	5.29	0.30	0.05	2.66
Standard Deviation	0.41	0.08	0.02	0.01	0.08	4.64	0.44	3.06	7.33	0.74	0.55	0.10	1.55
Sample Variance	0.17	0.01	0.00	0.00	0.01	21.51	0.19	9.39	53.73	0.55	0.31	0.01	2.40
Kurtosis	0.57	0.57	7.31	0.16	0.49	-0.40	0.26	-0.10	-0.36	-0.38	42.80	4.41	8.74
Skewness	0.79	1.19	1.86	0.88	0.72	-0.03	-0.80	-0.07	-0.09	0.63	6.07	1.69	2.42
Range	1.96	0.29	0.12	0.05	0.38	19.56	1.83	14.15	31.70	2.81	4.35	0.52	9.84
Minimum	0.61	0.03	0.01	0.01	0.21	2.00	0.06	1.19	51.89	2.48	0.05	0.05	1.90
Maximum	2.57	0.32	0.12	0.05	0.59	21.56	1.89	15.34	83.59	5.29	4.40	0.57	11.74
Count	66	66	66	66	66	66	66	66	66	66	66	66	66
CoV	0.31	0.59	0.57	0.67	0.22	0.42	0.44	0.35	0.11	0.19	1.34	0.80	0.39

Table B_11 Descriptive Statistics – South Geo-Zone

(Middle layer)													
Element	Fe_2O_3	MnO	Cr_2O_3	V_2O_5	TiO_2	CaO	K_2O	P_2O_5	SiO_2	AL_2O_3	MgO	Na_2O	LOI
Mean	2.48	0.11	0.03	0.03	0.35	23.39	1.00	16.30	39.36	5.55	1.69	0.28	8.64
Standard Error	0.07	0.01	0.00	0.00	0.01	0.72	0.03	0.49	1.10	0.21	0.16	0.01	0.38
Median	2.36	0.09	0.03	0.03	0.35	24.07	0.96	17.14	38.43	4.88	0.77	0.27	7.01
Mode	1.89	0.07	0.03	0.02	0.32	24.07	1.09	18.72	44.16	2.90	0.40	0.05	6.22
Standard Deviation	1.01	0.09	0.02	0.02	0.15	10.08	0.47	6.89	15.46	2.98	2.23	0.14	5.25
Sample Variance	1.02	0.01	0.00	0.00	0.02	101.61	0.22	47.42	238.98	8.90	4.99	0.02	27.60
Kurtosis	0.40	5.13	36.31	-0.12	0.52	-0.06	-0.22	-0.28	1.32	0.99	4.59	0.62	4.21
Skewness	0.67	1.95	4.50	0.51	0.30	-0.08	0.37	-0.06	0.69	0.95	2.21	0.50	1.91
Range	5.09	0.56	0.25	0.09	0.85	48.08	2.35	33.56	85.73	15.43	11.18	0.82	30.46
Minimum	0.79	0.01	0.01	0.01	0.01	0.34	0.09	0.68	5.56	0.99	0.05	0.05	2.13
Maximum	5.88	0.56	0.25	0.09	0.85	48.42	2.44	34.24	91.29	16.42	11.23	0.87	32.59
Count	196	196	196	196	196	196	196	196	196	196	196	196	196
CoV	0.41	0.83	0.67	0.58	0.42	0.43	0.47	0.42	0.39	0.54	1.33	0.51	0.61

Table B_12: Descriptive Statistics – South Geo-Zone

(Top layer)													
Element	Fe_2O_3	MnO	Cr_2O_3	V_2O_5	TiO_2	CaO	K_2O	P_2O_5	SiO_2	AL_2O_3	MgO	Na_2O	LOI
Mean	3.33	0.11	0.04	0.04	0.49	13.39	1.38	9.50	49.23	8.55	2.69	0.29	10.59
Standard Error	0.14	0.01	0.00	0.00	0.02	1.01	0.06	0.59	1.52	0.30	0.32	0.03	0.57
Median	3.50	0.07	0.04	0.05	0.51	13.22	1.45	8.14	48.40	8.90	1.50	0.25	9.89
Mode	4.22	0.03	0.04	0.06	0.54	14.38	1.56	10.47	48.40	5.06	0.55	0.05	6.39
Standard Deviation	1.10	0.11	0.02	0.02	0.16	8.12	0.51	4.73	12.22	2.46	2.59	0.28	4.61
Sample Variance	1.21	0.01	0.00	0.00	0.02	65.92	0.26	22.35	149.42	6.03	6.70	0.08	21.29
Kurtosis	-0.58	3.02	2.14	-0.86	-0.76	-0.36	-0.58	1.72	-0.93	-0.49	-0.60	35.70	-0.49
Skewness	-0.45	1.76	1.12	0.02	-0.39	0.13	-0.39	1.43	0.23	-0.18	0.91	5.20	0.75
Range	4.63	0.49	0.08	0.10	0.62	32.65	2.06	20.28	43.66	11.08	8.76	2.18	17.07
Minimum	0.74	0.01	0.01	0.01	0.14	0.24	0.24	3.77	27.98	2.86	0.05	0.05	4.12
Maximum	5.37	0.49	0.09	0.10	0.76	32.89	2.30	24.05	71.64	13.94	8.81	2.23	21.19
Count	65	65	65	65	65	65	65	65	65	65	65	65	65
CoV	0.33	1.00	0.43	0.56	0.32	0.61	0.37	0.50	0.25	0.29	0.96	0.98	0.44

Table B_13: Descriptive Statistics – North Geo-Zone

North Geo-Zone													
Element	Fe_2O_3	MnO	Cr_2O_3	V_2O_5	TiO2	CaO	K_2O	P_2O_5	SiO_2	AL_2O_3	MgO	Na_2O	LOI
Mean	2.47	0.15	0.02	0.04	0.35	21.49	0.80	16.32	44.62	5.26	0.88	0.16	6.68
Standard Error	0.12	0.01	0.00	0.00	0.02	1.07	0.04	0.70	1.72	0.24	0.16	0.01	0.36
Median	2.17	0.11	0.02	0.04	0.35	21.36	0.75	16.49	44.03	4.77	0.40	0.20	5.80
Mode	1.33	0.08	0.01	0.03	0.32	15.33	0.81	17.11	60.50	4.40	0.40	0.20	6.04
Standard Deviation	1.08	0.13	0.01	0.02	0.14	10.02	0.33	6.49	16.04	2.24	1.48	0.09	3.32
Sample Variance	1.17	0.02	0.00	0.00	0.02	100.40	0.11	42.18	257.43	5.04	2.18	0.01	11.01
Kurtosis	0.19	2.90	0.46	-0.72	-0.60	-0.34	0.16	-0.52	-0.57	0.43	19.52	-0.89	8.11
Skewness	0.75	1.79	0.98	0.12	-0.06	0.24	0.71	0.32	0.15	0.88	4.34	0.12	2.50
Range	4.73	0.61	0.05	0.06	0.64	46.26	1.54	29.26	75.03	10.71	8.65	0.32	18.96
Minimum	0.86	0.02	0.01	0.01	0.06	0.21	0.17	3.82	7.45	1.97	0.15	0.05	2.48
Maximum	5.59	0.63	0.06	0.07	0.70	46.47	1.71	33.08	82.48	12.68	8.80	0.37	21.44
Count	87	87	87	84	87	87	87	87	87	87	87	73	87
CoV	0.44	0.86	0.61	0.41	0.41	0.47	0.41	0.40	0.36	0.43	1.69	0.54	0.50

Bottom Layer: Normal	Bottom Layer: Log normal
	

Figure B_10: The Probability Plots for the Bottom layer.

Top Layer: Normal	Top Layer: Log normal
	

Figure B_11: The Probability Plots for the Top layer.

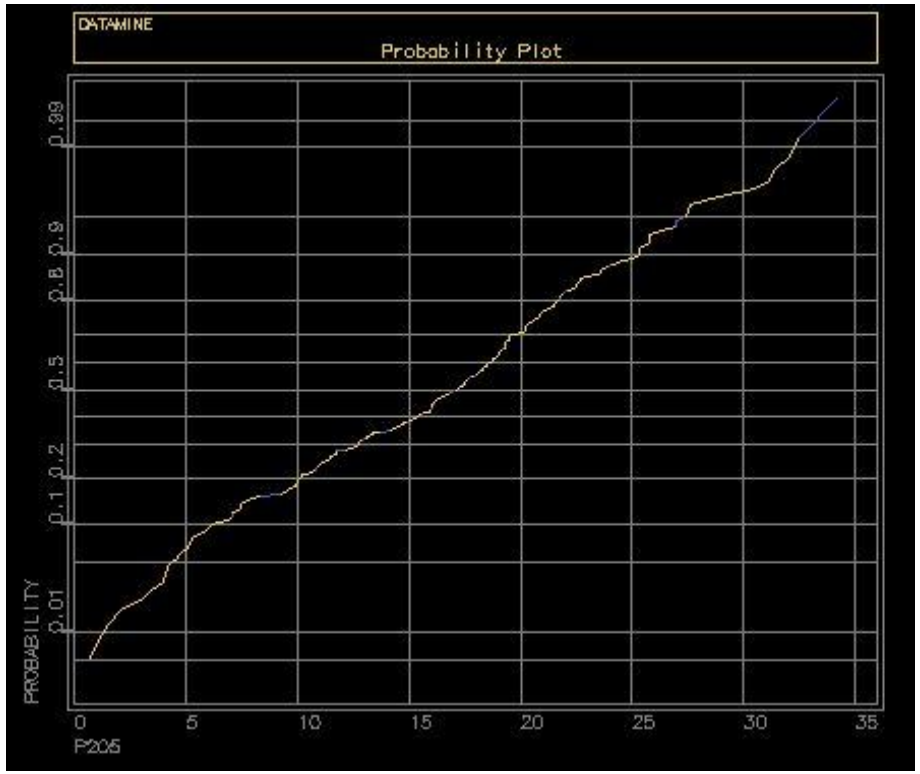
Middle Layer	North Geo-Zone
	

Figure B_12: The Probability Plots for the Middle and North layers.

Appendix C

Variography

Models with a sill or transition models

- Spherical
- Exponential
- Gaussian, a sill is reached asymptotically

Models without sill

- Logarithmic
- Parabolic
- Linear
- Models in $|h|^{\theta}$, with θ]0,2[

Variogram Parameters

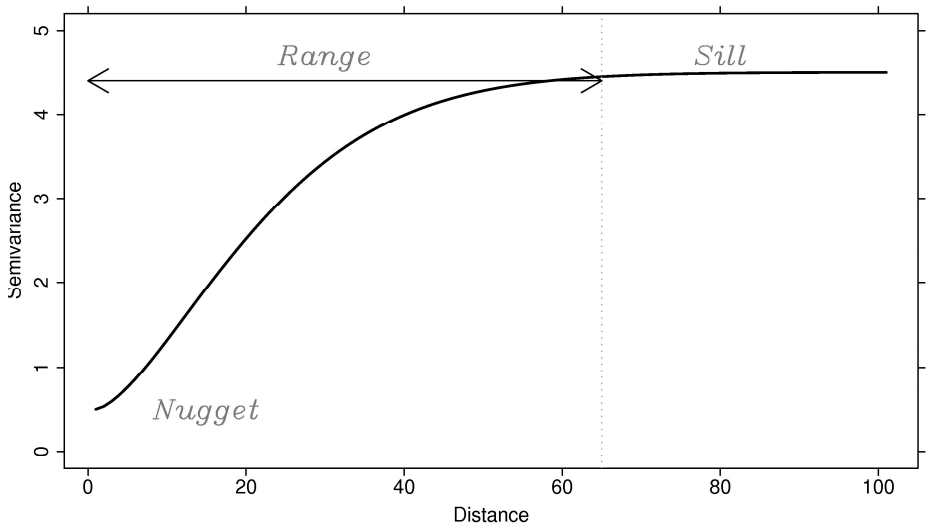


Figure C_1: The picture of variogram taken from University of Edinburgh website, 2013.

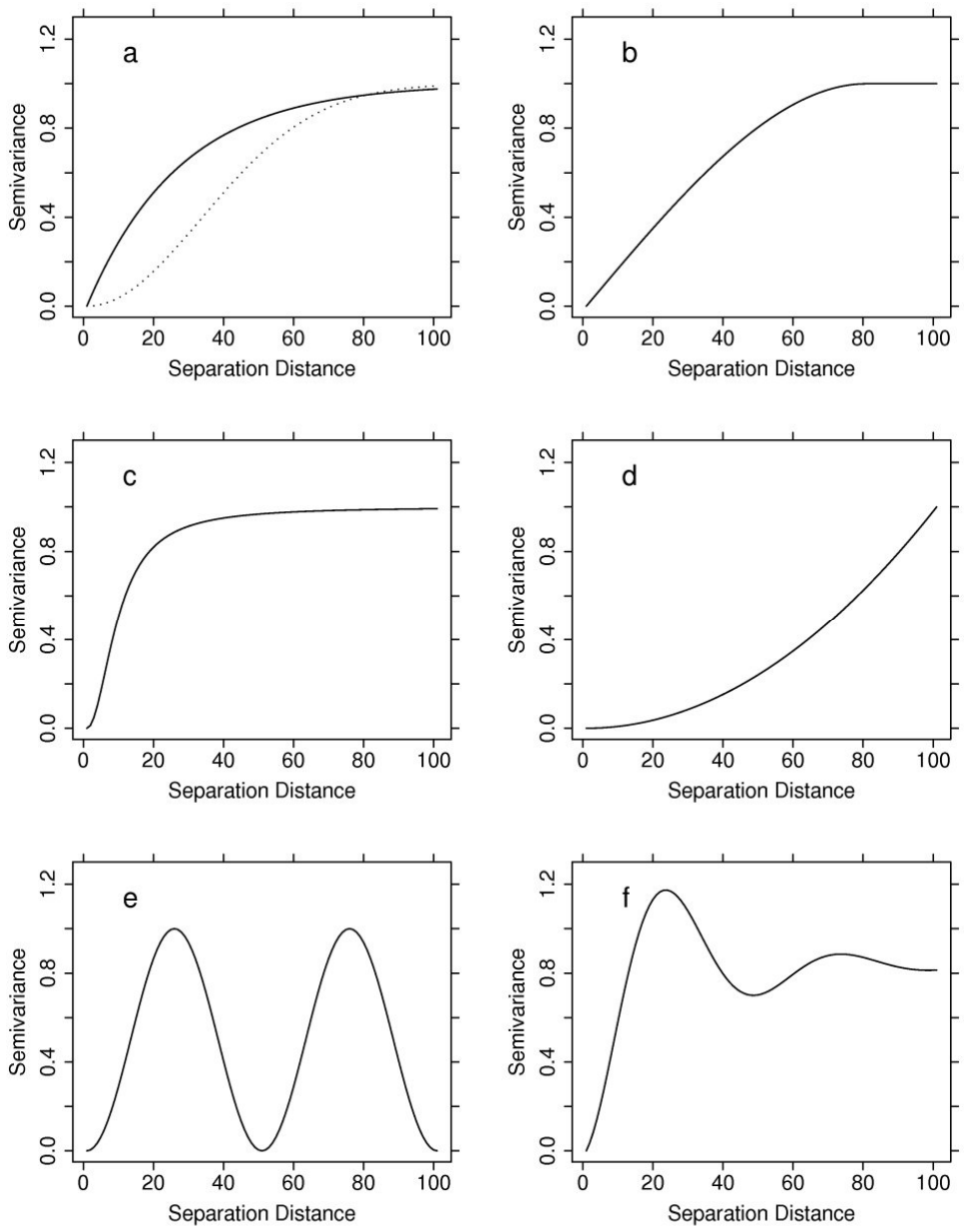


Figure C_2: Variogram models with (A) Powered Exponential model (i) Broken line with power (ω)=2, equivalent to a Gaussian model. (ii) Solid line with ω=1. (B) Spherical model. (C) Rational Quadratic model. (D) Power model. (E) Cosine (hole effect) model. (F) Dampened Hole model (University of Edinburgh, 2013).

Appendix D

Block Size Test-Work

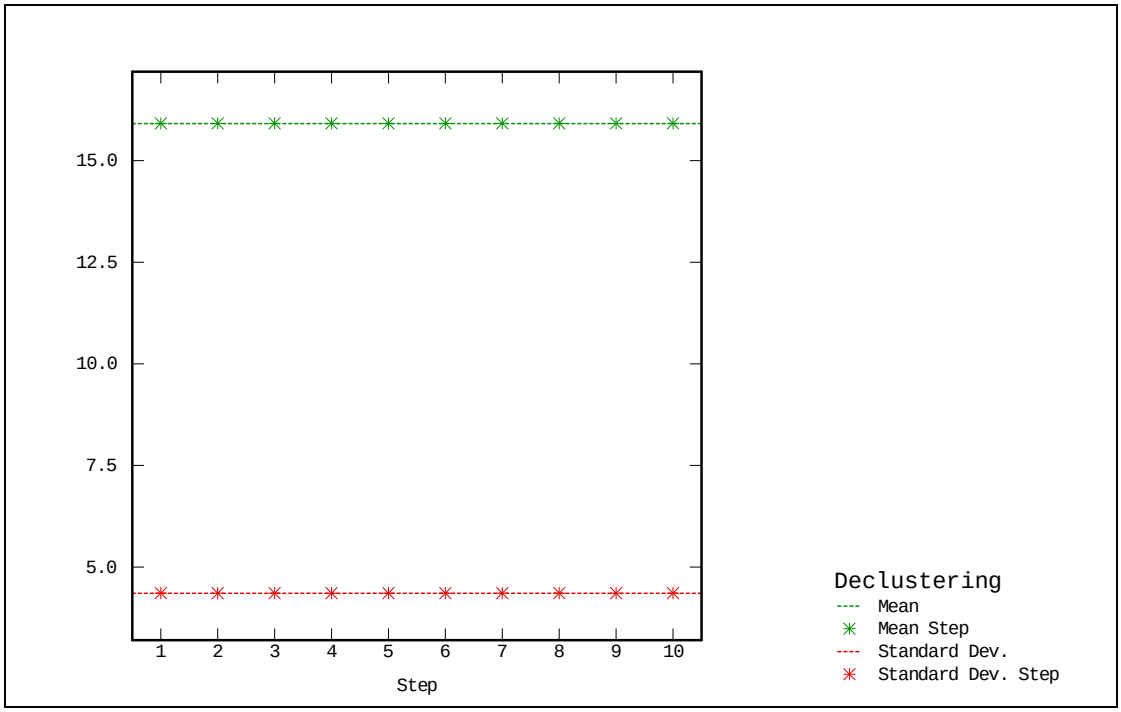


Figure D_1: Test on the thickness of the block cells. The cells are not sensitive to the thickness.

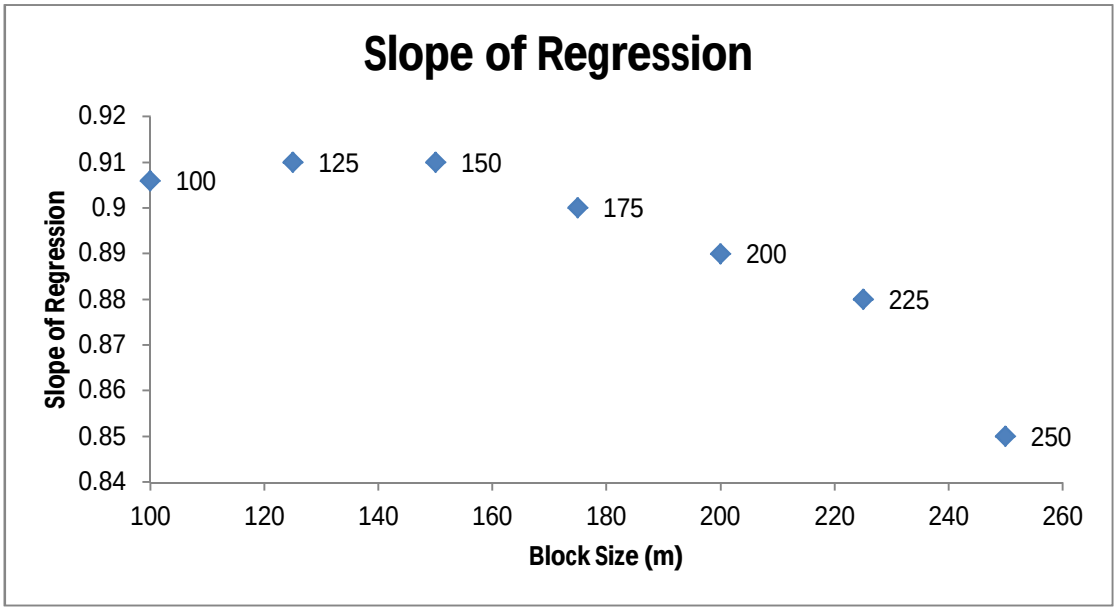


Figure D_2: Test on the block sizes: Slope of Regression.

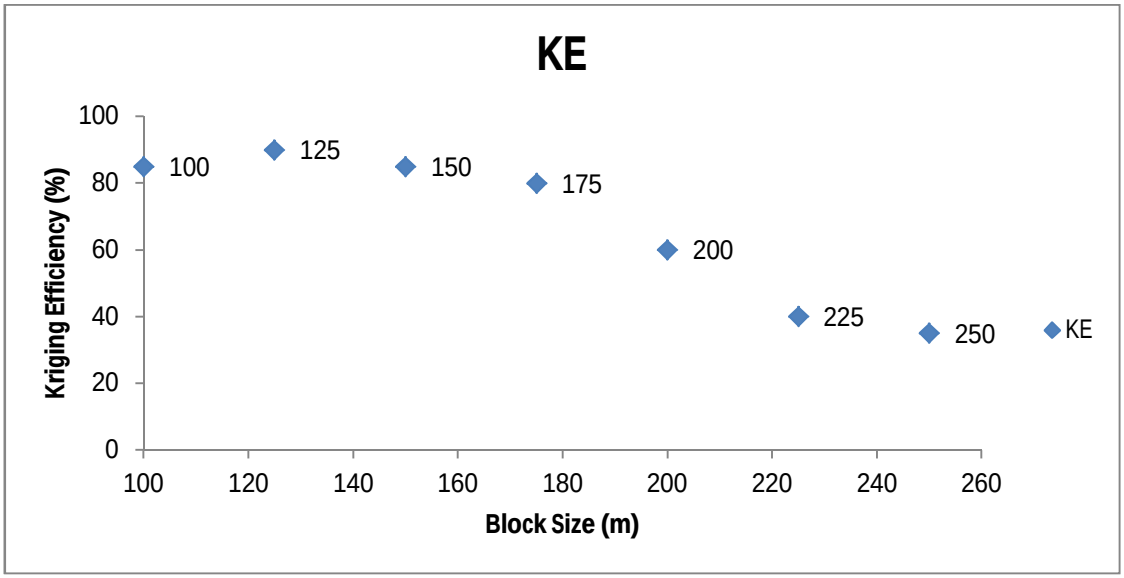


Figure D_3: Test on the block sizes: Kriging Efficiency.

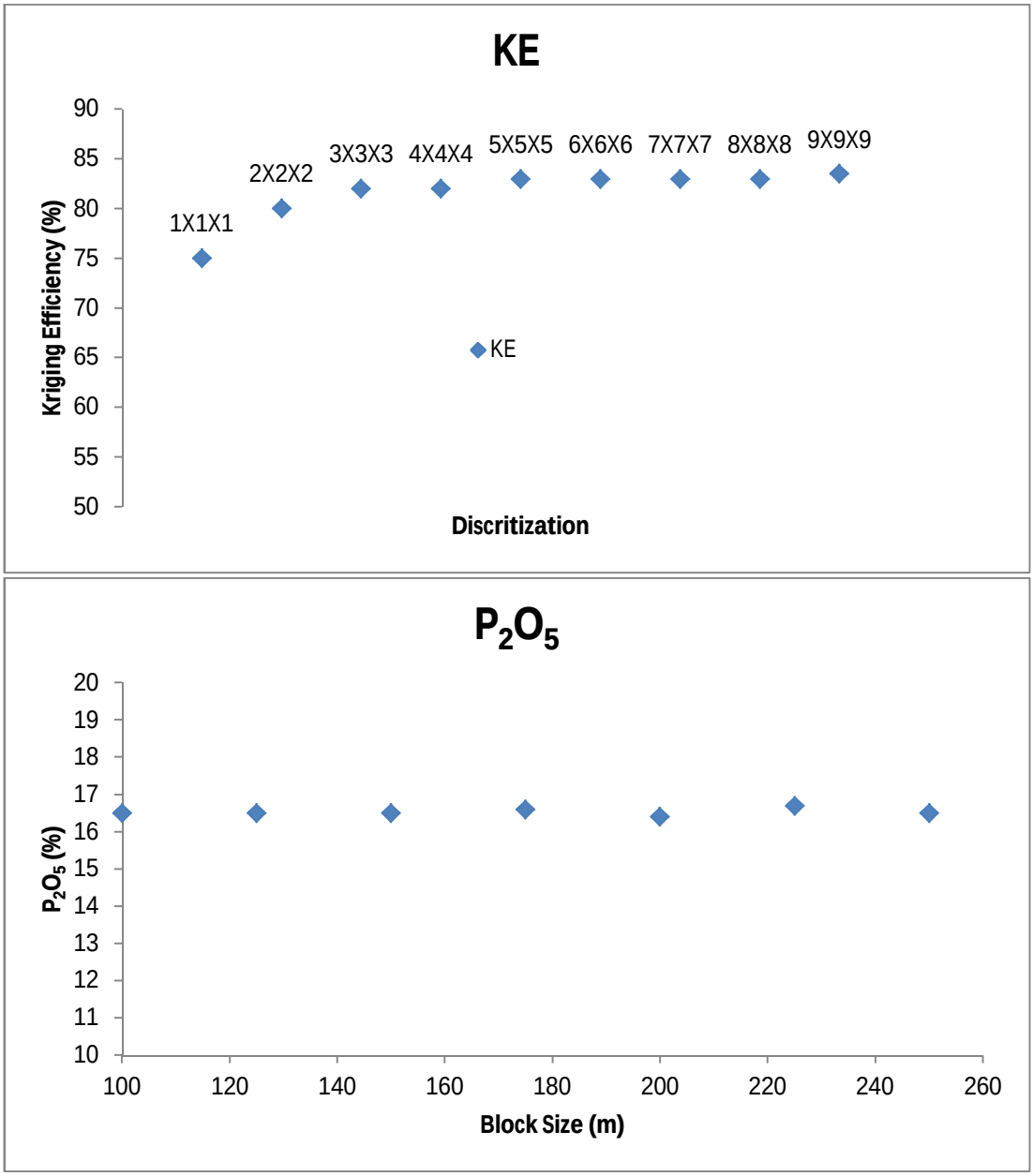


Figure D_4: Test on the block sizes: Slope of Regression, Discretization and average P_2O_5 grade.

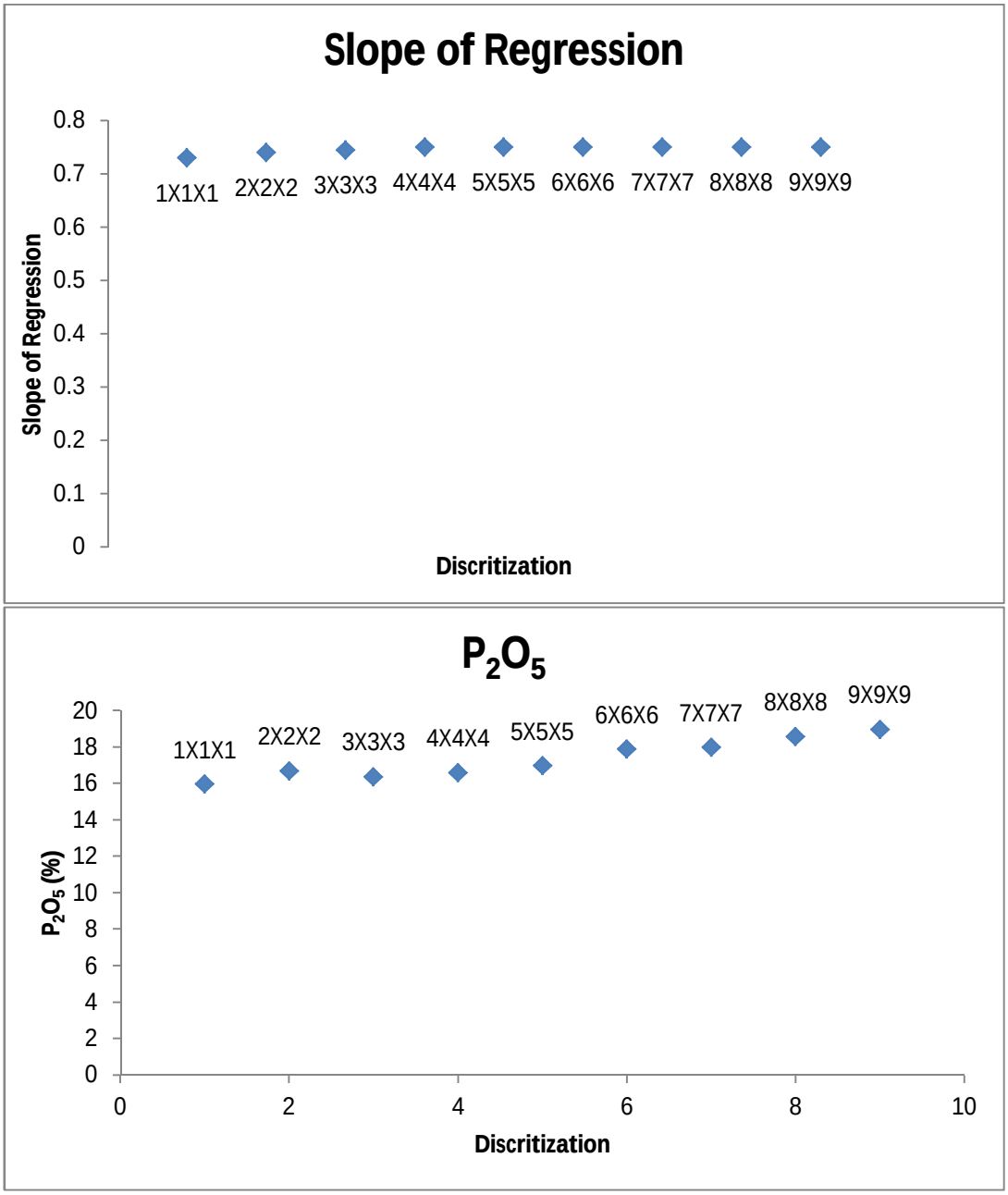


Figure D_5: Test on the block sizes: Slope of Regression, Discretization and average P_2O_5 grade.